

Initiation of Vertebrate Limb Development

Martin J. Cohn

Thesis submitted for the degree of Ph. D.

**Department of Anatomy and Developmental Biology
University College London
University of London
1997**

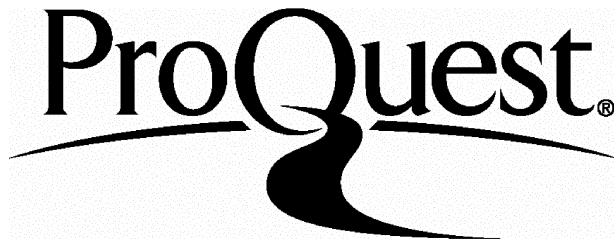
ProQuest Number: 10045536

All rights reserved

INFORMATION TO ALL USERS

The quality of this reproduction is dependent upon the quality of the copy submitted.

In the unlikely event that the author did not send a complete manuscript and there are missing pages, these will be noted. Also, if material had to be removed, a note will indicate the deletion.



ProQuest 10045536

Published by ProQuest LLC(2016). Copyright of the Dissertation is held by the Author.

All rights reserved.

This work is protected against unauthorized copying under Title 17, United States Code.
Microform Edition © ProQuest LLC.

ProQuest LLC
789 East Eisenhower Parkway
P.O. Box 1346
Ann Arbor, MI 48106-1346

ABSTRACT

Development of paired appendages at appropriate levels along the body axis characterizes the jawed vertebrate body plan. Molecular networks that operate within limb buds have received much attention, although very little is known about how limb budding is initiated. Here I show that beads soaked in Fibroblast growth factors (FGFs) and placed in prospective flank of chick embryos induce formation of ectopic limb buds, which contain their own signaling regions and develop into complete limbs. Application of FGF to anterior flank induces ectopic wings, and FGF applied to posterior flank induces ectopic legs. *Hox* genes are good candidates for encoding position in lateral plate mesoderm along the body axis, and thus determining where limbs form. If particular combinations of *Hox* gene expression determine where wings and legs develop, then formation of additional limbs from flank should involve changes in *Hox* gene expression which reflect the type of limb induced. Here I show that the same population of flank cells can be induced to form wing or leg. Induction of ectopic limbs is accompanied by specific changes in expression of 3 *Hox* genes in lateral plate mesoderm which reproduce, in the flank, expression patterns found at normal limb levels. Together, these results suggest that local production of FGF may initiate limb development, and that *Hox* gene expression may specify limb position.

Pythons lack forelimbs, have vestigial hindlimbs, and regional specialization of the axial skeleton has been lost. I have examined patterns of *Hox* gene expression in python embryos, and show that the uniform pattern of vertebrae is associated with uniform *Hox* gene expression. Transplantation experiments and analysis of gene expression in python hindlimbs suggest that limb development is arrested due to failed apical

ridge formation. Absence of a ridge in pythons may result from failure of limb ectoderm to respond to mesenchymal signals.

ACKNOWLEDGEMENTS

I would like to thank Professor Cheryll Tickle, my supervisor, for accepting me as her student and taking me under her extra wing. I am grateful to Cheryll for teaching, inspiring and encouraging me during my Ph.D. in her laboratory. I would also like to thank Professor Lewis Wolpert for many stimulating discussions and enthusiastic support for the project. Many thanks to Dr. Ketan Patel for being an excellent collaborator, teacher and friend. I am grateful to Dr. Ronald Nittenberg for tremendous friendship, for translating papers, and for many great discussions.

I would also like to thank Prof. John Heath, Dr. Helen Abud, Dr. Juan Carlos Izpisúa-Belmonte, Dr. Jon Clarke, Dr. Robb Krumlauf and Dr. David Wilkinson, with whom I collaborated on various aspects of this project. I am grateful to Dr. Mike Coates for sharing his wealth of knowledge, for a terrific and what I hope will be a long-lasting collaboration, and for many "Dead" discussions. Thanks to Dr. Susan Evans for sharing her knowledge of reptiles. Many thanks to Esther Wenman of London Zoo, John Foden of Drayton Manor Zoo, Nick Jackson of The Welsh Mountain Zoo, and Miranda Stevenson of Edinburgh Zoo for generously providing me with fertile python eggs. Thanks also to past and present members of the lab, for creating a wonderful working environment.

I would like to thank Prof. Owen Lovejoy for continuous encouragement, support and friendship. I would also like to thank Adam Levine, the Cosmic Charlies, the Levine family and the Bright family for making London feel like home.

Special thanks to my parents and brothers for their endless support and encouragement. Finally, I thank Philippa for supporting and tolerating me.

This work was supported by the BBSRC and Action Research.

CONTENTS

| | |
|-----------------|----------|
| ABSTRACT | 1 |
|-----------------|----------|

| | |
|-------------------------|----------|
| ACKNOWLEDGEMENTS | 3 |
|-------------------------|----------|

CHAPTER ONE: General Introduction

| | |
|---|------------|
| 1. Structure of the limb | 1 0 |
| 2. Patterning the anteroposterior axis of the limb | 1 1 |
| 2.1 Polarizing activity in urodele amphibians | 1 8 |
| 2.2 Molecular basis of polarizing activity | 2 0 |
| 2.2.1 Retinoic acid | 2 0 |
| 2.2.2 <i>Sonic hedgehog</i> | 2 1 |
| 2.2.3 <i>Hox</i> genes in limbs | 2 4 |
| 3. Proximodistal outgrowth and patterning | 2 8 |
| 3.1 The apical ectodermal ridge | 2 8 |
| 3.2 Molecular basis of ridge signaling | 3 2 |
| 3.2.1 Fibroblast growth factors | 3 2 |
| 3.3 The progress zone | 3 4 |
| 3.4 Candidate molecules expressed in the progress zone | 3 4 |
| 4. Dorsoventral polarity | 3 5 |
| 5. Evolutionary conservation of signaling networks | 3 8 |
| 6. Patterning the primary body axis | 4 0 |
| 6.1 <i>Hox</i> genes | 4 0 |
| 6.2. <i>Hox</i> genes and axial patterning. | 4 4 |
| 6.3 Retinoids, limbs and the body plan | 4 5 |
| 7. How are limbs induced? | 4 6 |
| 7.1 Ectopic limb development | 4 9 |
| 7.2 Initiation of limb budding | 4 9 |

CHAPTER TWO: Materials and Methods

| | |
|---|------------|
| 1. Application of FGF beads to chick embryos | 5 2 |
| 2. Application of SHH beads to chick embryos | 5 2 |
| 3. Application of retinoic acid beads to chick embryos | 5 3 |

| | | |
|------|--|------------|
| 4. | Whole-mount skeletal preparations: | |
| | Alcian green staining | 5 3 |
| 5. | Whole-mount skeletal preparations: | |
| | Alcian blue and Alizarin red staining | 5 4 |
| 6. | Scanning Electron Microscopy | 5 4 |
| 7. | Whole-mount <i>in situ</i> hybridization | 5 5 |
| 8. | Tissue transplantations | 5 5 |
| 9. | Iontophoretic application of Dil and DiAsp | 5 6 |
| 10. | Dig-FGF2 | 5 7 |
| 11. | Microinjection of Dig-FGF2 | 5 7 |
| 12. | Antibody staining | 5 8 |
| 12a. | Whole-mount antibody staining | 5 8 |
| 12b. | Antibody staining frozen sections | 6 0 |
| 13. | Nile Blue Sulphate staining | 6 1 |

CHAPTER THREE: FGF and Limb Initiation

| | | |
|-----------|---|------------|
| 1. | Background | 6 2 |
| 2. | Results | 6 3 |
| 2.1 | FGF beads induce additional limbs in chick embryos | 6 3 |
| 2.2 | Identity and morphological pattern of additional limbs | 6 4 |
| 2.3 | Early development of additional buds | 7 0 |
| 2.4 | FGF acts within two hours | 7 3 |
| 2.5 | Molecular polarity of early buds | 7 7 |
| 2.6 | Competence of flank cells to express <i>Shh</i> | 8 0 |
| 2.7 | Application of SHH to the flank | 8 4 |
| 2.8 | Application of FGF2 and SHH to the flank | 8 5 |
| 3. | Discussion | 9 2 |
| 3.1 | Initiation of a Limb by Application of FGF | 9 2 |
| 3.2 | Reversed Polarity of the Additional Limbs | 9 3 |
| 3.3 | Establishment of the polarizing region | 9 4 |
| 3.4 | Which FGF member initiates limb development in the normal embryo? | 9 7 |
| 3.5 | Control of limb position | 9 9 |
| 3.6 | Molecular basis of limb induction | 9 9 |

CHAPTER FOUR: *Hox* Genes and Specification Of Limbs

| | |
|--|------------|
| 1. Background | 101 |
| 2. Results | 102 |
| 2.1 Cell lineage in ectopic wings and legs | 102 |
| 2.2 Dynamics of <i>Hoxb9</i> expression in lateral plate mesoderm | 106 |
| 2.3 Comparative analysis of <i>Hoxb9</i> , <i>Hoxc9</i> and <i>Hoxd9</i> in lateral plate mesoderm | 107 |
| 2.4 <i>Hox9</i> gene expression and induction of ectopic limbs | 108 |
| 2.5 Application of FGF to paraxial mesoderm | 117 |
| 2.6 Effects of retinoic acid on <i>Hoxb9</i> expression at wing level | 121 |
| 2.7 <i>Hoxb9</i> boundaries and cell lineage in the wing bud | 121 |
| 2.8 Loss of <i>Hoxb9</i> expression in posterior limb buds | 125 |
| 3. Discussion | 129 |
| 3.1 <i>Hox</i> gene expression specifies limb position | 129 |
| 3.2 The polarizing region pathway is independent of <i>Hoxb9</i> | 130 |
| 3.3 <i>Hoxb9</i> is reduced by local signals in the limb bud | 130 |
| 3.4 <i>Hox</i> genes and the evolution of paired appendages | 131 |

CHAPTER FIVE: Developmental Analysis of Limblessness and Axial Patterning in Python Embryos

| | |
|--|------------|
| 1. Background | 133 |
| 2. Results | 135 |
| 2.1 Segmental identity in the python axial skeleton | 136 |
| 2.2 Morphology of python limbs | 142 |
| 2.3 Early development of the python hindlimb bud | 145 |
| 2.4 Gene expression in the python limb ectoderm | 151 |
| 2.5 Polarizing activity in python limbs and flank | 155 |
| 2.6 Python SHH expression can be rescued by a chick apical ridge | 156 |

| | | |
|--|--|-----|
| 2.7 | Failure of apical ridge formation in python limb buds | 160 |
| 3. | Discussion | |
| 3.1 | <i>Hox</i> gene expression and regionalization of the python body axis | 164 |
| 3.2 | Dorsoventral position of the hindlimb | 166 |
| 3.3 | Failure of hindlimb development | 166 |
| 3.4 | Rescuing snake limb development | 169 |
| 3.5 | Evolution of the snake body plan | 170 |
| CHAPTER SIX: General Discussion | | |
| 1. | FGF as limb initiation signal | 174 |
| 2. | Positioning FGF along the body axis | 174 |
| 3. | Reprogramming <i>Hox</i> expression in the flank | 176 |
| 4. | Implications for co-ordinating axial patterning | 177 |
| 5. | Evolution of body plans | 178 |
| References | | 180 |

LIST OF FIGURES AND TABLES

CHAPTER ONE

| | | |
|------------------|--|------------|
| Figure 1. | The Zone of Polarizing Activity (ZPA) patterns the anteroposterior axis of the limb | 1 7 |
| Figure 2. | The Apical Ectodermal Ridge (AER) maintains proximodistal outgrowth of the limb | 3 1 |
| Figure 3. | Hox gene cluster diversity and evolution | 4 3 |

CHAPTER THREE

| | | |
|-------------------|---|------------|
| Table 1. | Effects of beads soaked in FGF2 and implanted into the lateral plate mesoderm of chick embryos | 6 7 |
| Figure 4. | Additional limbs produced by application of FGF2 beads to the flank | 6 9 |
| Figure 5. | Scanning electron micrograph of embryo with ectopic limb bud 48 hours after bead implantation | 7 2 |
| Figure 6. | Distribution of Digoxigenin-tagged FGF2 after application to the chick flank | 7 6 |
| Figure 7: | <i>Sonic hedgehog</i> and <i>Hoxd13</i> are expressed in additional limb buds | 7 9 |
| Figure 8. | Activation of <i>Shh</i> in flank cells transplanted under the apical ridge | 8 3 |
| Table 2. | Effects of mSHH198 beads applied to lateral plate mesoderm of chick embryos | 8 7 |
| Figure 9. | Skeletal malformations induced by application of SHH protein to the flank | 8 9 |
| Figure 10. | Application of SHH beads to posterior flank alters patterning of the leg | 9 1 |

CHAPTER FOUR

| | |
|---|------------|
| Figure 11. FGF induces bidirectional transformations in flank cell fate to induce ectopic wings and legs | 105 |
| Figure 12. <i>Hoxb9</i> expression during normal chick development | 112 |
| Figure 13. Expression of <i>Hox</i> group 9 paralogues in lateral plate mesoderm of normal chick embryos | 114 |
| Figure 14. Expression of <i>Hox</i> group 9 paralogues in chick embryos treated with FGF to induce ectopic limbs | 116 |
| Figure 15. <i>Hoxb9</i> expression in chick embryo 48 hours after application of FGF to paraxial mesoderm | 119 |
| Table 3. Effects of FGF on <i>Hox</i> gene expression in lateral plate mesoderm of the chick | 120 |
| Figure 16. Analysis of cell lineage and <i>Hoxb9</i> expression in the posterior wing bud. | 124 |
| Figure 17. Regulation of <i>Hoxb9</i> in the chick leg bud and flank | 128 |

CHAPTER FIVE

| | |
|---|------------|
| Figure 18. Morphological pattern in the python axial skeleton | 139 |
| Figure 19. Comparative <i>Hox</i> gene expression in python and chick embryos. | 141 |
| Figure 20. Morphological pattern in python limbs | 144 |
| Figure 21. Scanning electron micrographs of python limb buds | 148 |
| Figure 22. Cell death in python limb buds | 150 |
| Figure 23. Gene expression in limb bud ectoderm | 154 |
| Figure 24. Polarizing activity in python limb buds | 159 |
| Figure 25. Dorsoventral polarity in python limb buds | 163 |
| Figure 26. Developmental model for evolution of the snake body plan | 173 |

CHAPTER ONE: General Introduction

In virtually all vertebrates, two pairs of limb buds form from lateral plate mesoderm at particular axial levels and grow out to form the limbs. Once limb buds have formed, tissue interactions within them lead to morphogenesis and patterning, and the buds develop almost autonomously into limbs. Considerable progress has been made in understanding the cellular and molecular basis of limb pattern formation, but the problem of how limb buds are initiated has remained poorly understood. The focus of this thesis is the cellular and molecular interactions in the chick embryo that initiate the process of limb development. The main problems to be addressed are: How are limbs induced? What controls the position at which budding is initiated? How is limb identity determined? What controls the number of limbs that develop?

This thesis is also directed towards understanding the developmental mechanisms that underlie the limbless condition in snakes. Pythons fail to initiate forelimb development, yet well-developed hindlimb buds are induced adjacent to the cloaca. These buds give rise to rudimentary hindlimbs because subsequent outgrowth is not maintained. These changes are associated with major changes to the body plan during snake evolution. Here I explore limb development and patterning of the axial skeleton, and their relationship to one another in python embryonic development.

1. Structure of the limb

A defining characteristic of tetrapod body plan is the presence of paired limbs at two positions along the primary body (head to tail) axis. Each limb is made-up of three segments, the *zeugopod* (humerus in the forelimb [f], femur in the hindlimb [h]), the *stylopod* (ulna and radius [f], tibia and

fibula [h]) and *autopod* (carpals, metacarpals and phalanges [f], tarsals, metatarsals and phalanges [h]). These structures are organized and patterned along three axes. For example, in the forelimb, the proximal to distal axis extends from the humerus to the digits, the anterior to posterior axis extends from thumb and radial side of the limb to the small finger and ulnar side of the limb, and the dorsal to ventral axis extends from the back (extensor) surface of the hand to the palmar (flexor) surface of the hand. During embryonic development, the limb skeleton and tendons are derived from lateral plate mesoderm which emerges from a body wall as a bud of undifferentiated mesenchyme cells surrounded by a layer of ectoderm. Limb muscle forms from paraxial mesoderm cells which migrate into the limb bud, and the limb is innervated by axons that migrate from the spinal cord at approximately the same anteroposterior level as the limb bud. Cellular interactions involving both long-range and short-range signaling are involved in organizing cells in the limb bud mesenchyme into structures that form an integrated and functional anatomical system. The following sections will introduce the cellular and molecular nature of the interactions that occur within the limb bud after it emerges from the body wall. The second part of this introduction will cover the earlier events of induction and initiation of limb budding.

2. Patterning the anteroposterior axis of the limb

Patterning of the limb is organized by specialized signaling centers that communicate with other cells to inform them of their position or otherwise influence their behavior. Signaling regions act by secreting signaling molecules over long or short distances, and these signals are interpreted by responding cells. Wolpert formulated the French flag problem to demonstrate how cells located at different positions within a morphogen gradient can respond differentially to morphogen concentration (Wolpert,

1969) According to the model, cells receiving a high dose of morphogen have their position specified and interpret this to differentiate into blue cells, a lower dose induces white cells and an even lower dose induces red cells, so that the population of cells is programmed to make a French flag pattern by responding differentially to a single chemical. Similarly, cells within the limb must be informed of their position and interpret this information to differentiate into the appropriate structures, so that a thumb develops anteriorly and a small finger develops posteriorly. The region of cells with the ability to polarize the anteroposterior axis is called the zone of polarizing activity (ZPA) or polarizing region. Saunders and Gasseling demonstrated that this group of cells, located at the posterior edge of the chick wing bud, could induce a mirror-image duplicated pattern of digits when transplanted to the anterior edge of the bud (Fig. 1) (Saunders and Gasseling, 1968). The normal pattern of digits in the chick wing is 2-3-4, reading from anterior to posterior (digits 1 and 5 have been lost during evolution of the avian wing) (Hinchliffe, 1985). Transplantation of posterior limb cells to the anterior results in a pattern of digits reading 4-3-2-2-3-4 from anterior to posterior.

Tickle *et al.* suggested that the polarizing region is a source of a diffusible morphogen which patterns the limb in a concentration-dependent manner (Tickle, Summerbell, and Wolpert, 1975). According to the model, the concentration of morphogen, which decreases with distance from the polarizing region, determines the positional address of the cell, such that cells adjacent to the polarizing region receive a high dose of morphogen and acquire a posterior positional value. This value will ultimately be translated into a differentiation program that results in formation of a digit with a posterior identity. This model implies that cells can respond differentially to threshold levels of morphogen. Cells situated further from the

polarizing region are exposed to a lower dose of morphogen due to diffusion, and thus, lower threshold responses are activated resulting in more anterior positional values. This model also explains the effects of a polarizing region graft; when an additional polarizing region is grafted anteriorly, the new polarizing region acts as a new source of morphogen which is distributed in a gradient opposite that which is normally present. Under these experimental conditions, cells at the anterior and posterior extremes of the limb would be exposed to high concentrations of morphogen and form posterior digits, and as the gradients decrease towards the apex of the limb bud, more anterior digits would be specified. Thus, the concentration of morphogen along the anterior to posterior axis of the limb bud would be high-medium-low-low-medium-high, corresponding to a morphological pattern of 4-3-2-2-3-4. This explanation is consistent with the pattern of digit duplication being affected by changing the position of the polarizing region graft. When the grafted polarizing region is moved closer to the apex of the bud (shortening the distance between the two polarizing regions), the gradients of morphogen intersect before either drops below the level needed to induce anterior digits, and thus anterior digits are eliminated from the pattern (Tickle, Summerbell, and Wolpert, 1975). Cells respond to duration of exposure as well as concentration of morphogen. Smith showed that removal of the polarizing region at different time points affected the extent of duplication; longer exposure to the signal resulted in induction of more posterior digits (Smith, 1980). Thus, the polarizing region appears to influence anteroposterior patterning of the limb by a mechanism involving dose and time of exposure to a morphogen secreted by this specialized group of cells.

Polarizing activity can be defined quantitatively according to the strength of the polarizing signal. Tickle quantified the number of cells

required to polarize the limb and found that as few as 9 cells could induce an additional digit 2 (Tickle, 1981). Induction of an additional digit 4 requires approximately twice the number of polarizing cells needed to induce a digit 3, which requires approximately twice the number of cells needed for induction of digit 2. The observation that number of polarizing region cells is related to identity of the digits induced suggested that a quantitative relationship between a polarizing signal and specification of digits may control pattern in the limb (Tickle, 1981).

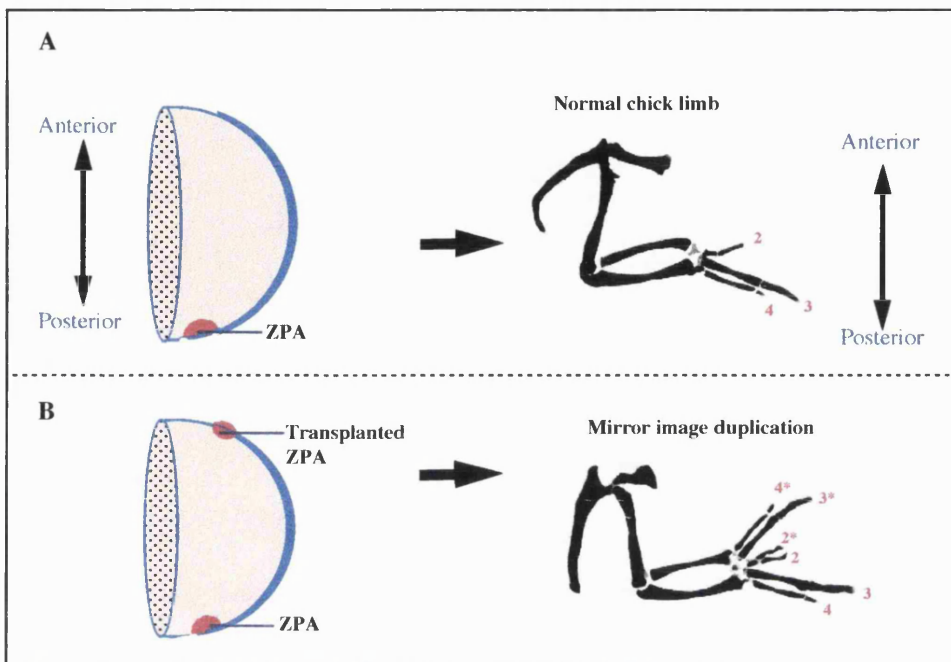
The distribution of polarizing activity in the wing was mapped by MacCabe *et al.* (1973) and by Honig and Summerbell (1985), who showed that the strength of the signal was not evenly distributed, but was highest in the posterior wing bud and decreased in a gradient extending proximally in the bud and posteriorly into the flank (MacCabe, Gasseling, and Saunders, 1973); (Honig and Summerbell, 1985). Subsequent work on chick embryos at pre-limb stages showed that as early as stage 10, cells located at the posterior margin of the prospective wing, and flank cells posterior to the prospective wing level could induce duplications when transplanted to a host wing bud (Hornbruch and Wolpert, 1991). Prior to limb budding, the strongest polarizing potential is detected in posterior prospective limb and in anterior flank. Signaling activity decreases posteriorly along the flank such that flank cells just anterior to the prospective leg bud do not have polarizing activity. Although the same polarizing signal operates in forelimb and hindlimb development (Tickle *et al.*, 1976), the distribution of polarizing potential is not continuous between the posterior wing and posterior leg. The polarizing region of the leg is derived from a separate population of cells extending from the posterior of the prospective leg into the anterior part of the tail bud (Hinchliffe and Sansom, 1985); (Hornbruch and Wolpert, 1991). The distribution of polarizing potential is refined during development, as

polarizing potential disappears from the flank and remains in the posterior wing and leg bud (Hornbruch and Wolpert, 1991). Hornbruch and Wolpert indicate that polarizing potential disappears from the flank shortly after limb buds have emerged from the body wall, although Yonei *et al.* have suggested that the stage at which polarizing activity is lost from the flank is considerably later (Yonei *et al.*, 1995). Other tissues have also been shown to have polarizing activity when grafted to the chick wing, such as the node, floor plate of the neural tube, notochord, gut and pharyngeal endoderm, genital tubercle, perichondrium, tail bud and tooth germ (Hornbruch and Wolpert, 1986, Wagner *et al.*, 1990, Dolle *et al.*, 1991, Izpisua-Belmonte *et al.*, 1992, Koyama *et al.*, 1996, Roberts *et al.*, 1995, Saunders and Gasseling, 1983) which suggests conservation of the signaling molecules involved in patterning other organ systems in the embryo.

Polarizing activity is not only shared by different organ systems, but has also been shown to be highly conserved among evolutionarily distant vertebrates. A polarizing region was identified in mammals by grafting posterior limb mesenchyme cells from embryonic mice (Tickle *et al.*, 1976), hamsters (MacCabe and Parker, 1976), pigs, ferrets and humans (Fallon and Crosby, 1977) to the anterior margin of a chick wing bud. Reptilian limb buds also contain a polarizing region. Posterior limb mesenchyme from the snapping turtle, painted turtle (Fallon and Crosby, 1977), map turtle, and alligator (Honig, 1984) can induce digit duplications when grafted to the anterior margin of a chick wing. As in birds, polarizing activity within the mammalian and reptilian limb bud appears to be restricted to the posterior, as grafts of anterior cells to the anterior margin of the chick limb have no effect on the pattern of the chick limb.

Figure 1. The Zone of Polarizing Activity (ZPA) patterns the anteroposterior axis of the limb.

A. Diagram of the chick wing bud (left) and mature wing skeleton (right). The zone of polarizing activity (ZPA), shown in red, is involved in patterning the limb across the anterior to posterior axis. In the mature wing (right), the most anterior digit is digit 2 and the most posterior digit is digit 4. **B.** Transplantation of an additional ZPA to the anterior margin of the wing bud (left) left results in mirror-image duplication along the anteroposterior axis, shown of the right. Asterisks next to numbers denote duplicated digits.



2.1 Polarizing activity in urodele amphibians

The principles that govern limb development are shared by all amniotes, and most also apply to amphibians. Much of the early experimental work on vertebrate limb development was done in the 1910's-1920's on urodele amphibians. Harrison identified in the axolotl embryo an area of lateral plate mesoderm cells ventral to the pronephros that was capable of forming a complete limb when transplanted in whole or in part to ectopic positions, and he referred to this as the limb disc (reviewed in Harrison, 1969). In a series of transplantation experiments designed to investigate when limb axes were determined, Harrison uncovered what was later interpreted by Slack to be polarizing activity (Slack, 1976, Slack, 1977a, Slack, 1977b). In these experiments, the limb disc (or presumptive limb) was excised from an embryonic axolotl and transplanted in different orientations either to the flank (heterotopic grafts) or back to the limb (orthotopic grafts) (Harrison, 1969, Slack, 1977a, Stocum and Fallon, 1984). Development of the grafted limb with normal polarity was taken as an indication that the axis had been determined prior to transplantation, whereas development of limbs with reversed polarity indicated that the axis had not yet been determined (reviewed in Stocum and Fallon, 1984). Orthotopic grafts of limb discs with the a-p axis inverted resulted in formation of limbs with their original polarity (accompanied by duplicated limbs on the anterior and posterior sides). When these same experiments were performed with the graft placed heterotopically in the flank, curious differences were observed. Limb discs placed in the flank with their a-p polarity unchanged resulted in formation of limbs with mirror image duplications in the a-p axis. When the a-p polarity of the graft was reversed, however, very few limbs developed duplicated patterns. Subsequent work by Slack (1976, 1977a, b) offered an explanation for these results by demonstrating the importance of peribrachial flank cells. Slack showed that

flank cells posterior to the limb disc have polarizing activity similar to that identified in the chick embryo (see above). Transplantation of flank tissue to the anterior margin of the limb disc induced mirror-image duplication of the digits (Slack, 1976). Interspecific grafts demonstrated that the duplicated digits were not derived from the graft, but had been induced in the host tissue. In urodeles, as described above for the chick, the distribution of cells with polarizing activity extends into the flank, well beyond the posterior limit of tissue competent to form a limb (Slack, 1976, 1977a). Thus, Harrison's transplantation of a forelimb disc into the flank positioned the anterior edge of the limb disc adjacent to flank cells with polarizing activity. If the posterior peribrachial flank cells were included in the graft, which they were in Harrison's experiments, then the limb disc developed with polarizing cells at the anterior and posterior margins. This also explained how anterior fragments of limb disc could "regulate" and give rise to a limb when transplanted to the flank -- the polarizing signal would have been supplied by the adjacent flank cells. Similarly, transplantation of the anterior half of the limb disc to the head would give rise to a limb only when posterior flank tissue was grafted alongside it (Slack 1977a). The ventral half of the limb disc is also unable to develop unless accompanied by the dorsal half (Slack, 1980). Ventral disc tissue transplanted to the flank showed no growth at all, suggesting that the dorsal part of the disc (which includes the pronephros) contained either a permissive or stimulatory factor required for limb development, which may also be involved in dorsoventral patterning (Slack, 1980).

Slack suggested that the limb rudiment consists of a homogeneous population of cells that responds to graded signals, as described for the chick limb (Tickle *et al.*, 1975) rather than a group of polarized cells, as Harrison had argued (Slack, 1977b; Harrison 1969). The observation that

anterior cells grafted to the head do not give rise to a limb suggests that the polarizing signal is not only involved in patterning the limb, but also must be involved in limb outgrowth. These experiments focused on the establishment of pattern and polarity within the limb. They indicate that the distribution of polarizing signal determines the pattern of skeletal elements within the limb.

2.2 Molecular basis of polarizing activity

2.2.1 Retinoic acid

Considerable progress towards identifying the molecular networks involved in limb patterning has been made within the past 15 years. Retinoic acid was the first defined molecule implicated in limb patterning. Tickle *et al.* showed that application of all-*trans* retinoic acid to the chick wing could mimic the effect of a polarizing region graft, which suggested that retinoic acid may mediate the activity of the polarizing region (Tickle *et al.*, 1982). Moreover, like the polarizing region graft, retinoic acid acts in a concentration-dependent manner when applied to the limb, with higher doses specifying more posterior digits (Tickle, Lee, and Eichele, 1985). An interesting distinction between grafts of polarizing region and retinoic acid beads to the anterior limb is that a polarizing region graft does not induce another polarizing region (Smith, 1979) whereas retinoic acid can induce a new polarizing region and RAR β expression in adjacent cells (Noji *et al.*, 1991). Retinoic acid can also convert anterior limb bud mesenchyme cells to polarizing cells *in vitro* (Hayamizu and Bryant, 1992). During normal development, retinoic acid may act upstream of the polarizing signal by inducing a polarizing region that, in turn, signals to cells in the limb. In the chick limb bud, all-*trans* - and didehydroretinoic acid levels are highest posteriorly (Scott *et al.*, 1994, Stratford, Horton, and Maden, 1996, Thaller

and Eichele, 1987). Retinoic acid receptors and binding proteins are also expressed in the limb, indicating that the cellular machinery that would be required for endogenous retinoid activity is present in the limb. Maden *et al.* showed that cellular retinoic acid binding protein is present in a gradient opposite to that of retinoic acid (i.e., highest anteriorly), and Dollé *et al.* found that retinoic acid receptor (RAR) β is expressed proximally and RAR α and γ are expressed throughout the limb buds of 10 day mouse embryos (Dolle *et al.*, 1989, Maden *et al.*, 1988). Loss of function mutations in the retinoic acid receptors and binding proteins individually result in development of surprisingly normal limbs, although compound mutants develop limb defects (Fawcett *et al.*, 1995; Lohnes *et al.*, 1993; Lohnes *et al.*, 1994). These results suggest that endogenous retinoids are involved in limb development, and that functional redundancy in the retinoid receptor machinery allows for single and even compound loss of function mutations without severe pattern alterations (Lohnes *et al.*, 1994).

2.2.2 *Sonic hedgehog*

Recently, transcripts of a vertebrate homolog of the *Drosophila hedgehog* gene, *Sonic hedgehog* (*Shh*), have been found to map to the polarizing region, and grafts of *Shh*-expressing cells, or application of SHH protein to the anterior limb bud induce digit duplications (López-Martínez *et al.*, 1995, Riddle *et al.*, 1993, Yang and Drossopoulou *et al.*, 1997). Polarizing activity is found in other regions of the embryo, such as Hensen's node (Hornbruch and Wolpert, 1986) and the floor plate of the neural tube (Wagner *et al.*, 1990), and these tissues also express *Sonic hedgehog* (Riddle *et al.*, 1993). Flank cells with polarizing potential do not express *Shh*, but can induce digit duplications and activate *Shh* when grafted to the anterior margin of a host wing bud (Hornbruch and Wolpert, 1991, Yonei *et al.*, 1995). Loss of function mutations in *Shh* result in severe limb truncations

at the level of the femur/humerus (Chiang *et al.*, 1996). This is consistent with the role of *Shh* in maintaining limb outgrowth as well as patterning (see below).

Two forms of SHH protein are secreted from the cell as a consequence of autoproteolytic processing (Bumcrot, Takada, and McMahon, 1995). The N-terminal peptide has been shown to possess all of the signaling activity in biological assays (Marti *et al.*, 1995a). More recent work has shown that a component of *Shh* (and *hh* in *Drosophila*) autoprocessing is attachment of cholesterol to the N-terminal peptide (Porter, Young, and Beachy, 1996). Attachment of the lipophilic cholesterol allows the peptide to associate tightly with the surface of the cell. Tethering the active peptide to the cell surface allows a highly local concentration of SHH to be maintained on the surface of the SHH-producing cells (Hammerschmidt, Brook, and McMahon, 1997). *Shh* is involved in long-range and short-range patterning during development (Johnson and Tabin, 1995). If SHH acts as a long-range signal in limb patterning, then it should be distributed in a gradient across the limb bud and signalling should be dose dependent. Surprisingly, the distribution of SHH-N peptide in the limb maps precisely to the domain of mRNA, and protein could not be detected at a distance from the polarizing region (López-Martínez *et al.*, 1995, Marti *et al.*, 1995b). However, Yang and Drossopoulou *et al.* (1997) have found that high concentrations of SHH applied anteriorly in the wing bud induce posterior digits whereas lower concentrations of SHH induce anterior digits. This dose-dependent response of limb cells to SHH signaling suggests that cells could respond to a gradient of SHH. Failure to detect a gradient of SHH protein in the limb could be a problem with the sensitivity of the antibodies being inadequate to detect low levels of protein. Another possibility is that SHH acts indirectly by short-range induction of a secondary signal that acts over a long-range (see below).

Recent work on the SHH transduction pathway, and on the molecular response of limb cells to treatment with candidate signaling molecules, means that the polarizing pathway in the limb is starting to become clear. Retinoic acid induces *Shh* expression (Riddle *et al.*, 1993), and it has been shown that retinoid synthesis is required for normal expression of *Shh* (Lu *et al.*, 1997, Stratford, Kostakopoulou, and Maden, 1997). It now appears that activation of *Shh* by retinoic acid is mediated by the *Hoxb8* gene (discussed below). *Ptc*, a transmembrane protein that is the SHH receptor (Marigo *et al.*, 1996a), is expressed in the posterior mesenchyme of the limb bud in a domain that extends beyond the *Shh* domain (Marigo *et al.*, 1996b). PTC represses its own transcription. When SHH binds PTC, it represses PTC activity, which in turn allows *Ptc* to be transcribed. Marigo *et al.* have therefore proposed that *Ptc* expression indicates that cells have been exposed to SHH (Marigo *et al.*, 1996b). Expression of *cubitus interruptus*, a zinc finger gene in *Drosophila* homologous to the vertebrate *Gli* gene, is necessary for expression of *ptc*. In vertebrates, *Shh* induces *Gli* expression in the limb, and transcriptionally activated form of *Gli* can induce *Ptc* expression (Marigo *et al.*, 1996b). The SHH signaling pathway is negatively regulated by protein kinase A (PKA), and blocking PKA activity by overexpression of a dominant negative form of PKA simulates the effect of ectopic *Shh* expression by activation of *Shh* targets *Ptc* and *Gli* (Epstein *et al.*, 1996).

SHH activates expression of the signaling molecule *Bmp2* in limb bud mesenchyme, and BMP2 could mediate the effects of SHH (Laufer *et al.*, 1994, Yang and Drossopoulou *et al.*, 1997). This appears to be a widely used pathway in vertebrates (Bitgood and McMahon, 1995). Also, in *Drosophila*, *decapentaplegic*, the homologue of *Bmp2*, is activated as a result of *hedgehog* signaling in the wing imaginal disc (Basler and Struhl,

1994). *Bmp2* transcripts map to the polarizing region (Francis et al., 1994). Grafts of *Bmp2*-expressing cells to the anterior wing bud can induce an additional digit 2 (Duprez et al., 1996), but anterior application of BMP2 protein does not lead to digit duplications (Francis et al., 1994). The inability of BMP2 to induce complete digit duplications suggests that it does not act to relay the *Shh* signal. *Bmp2*, *Bmp4* and *Bmp7* are expressed in the mesenchyme and the apical ridge and could therefore participate in signaling between the mesenchyme and the ridge (Francis-West et al., 1995). In *Drosophila*, however, *dpp* signaling is not required for *hh* to exert its effect during eye development, but this independence may be limited to short-range interactions (Burke and Basler, 1996).

2.2.3 *Hox genes in limbs*

Hox genes are transcription factors containing a homeobox, a 180 base pair highly conserved domain that encodes a helix-turn-helix protein (Krumlauf, 1992). *Hox* genes are involved in the specification of positional identity during metazoan embryogenesis. Gain or loss of function mutations involving *Hox* genes can produce dramatic transformations in which one body part or segment is substituted for another (homeotic mutations). These mutations were first identified in *Drosophila*, where genetic analyses led to the proposal that they operate as selector genes, determining where particular structures develop (Lewis, 1978). In *Drosophila*, all *Antennapedia* and *Bithorax*-class *Hox* genes (defined by shared identity in the homeodomain) are located on chromosome 3 in a complex collectively referred to as the Homeotic complex (Krumlauf, 1992). Vertebrate homologues of the *Hox* genes were first identified in the frog (De Robertis, 1994), and are characterized by: (a) sequence similarity to the *Drosophila Hox* complex, (b) organization in gene clusters and (c) correspondence between expression pattern along the embryonic axis ^{and} arrangement on the

chromosome (Kappen, 1996). In all animals so far examined, genes located at the 3' end of the *Hox* cluster are expressed at the anterior end of the animal and genes located at the 5' end are expressed posteriorly. Duboule and colleagues proposed the rule of spatial colinearity to describe this correspondence between *Hox* gene position in the cluster and expression pattern in the embryo (reviewed in Duboule and Morata, 1994). Position within the cluster also correlates with temporal sequence of expression , so that 3' genes are expressed before their 5' neighbors (termed "temporal colinearity"). This results in an embryonic expression pattern in which 3' *Hox* genes are activated anteriorly, prior to expression of more 5' genes in more posterior body regions.

Hox gene expression in tetrapod limbs has been the focus of considerable attention. Most work has centered on *AbdB*-related members of the *Hoxa* and *Hoxd* clusters, but it is now clear that members of all four clusters are activated during bud outgrowth (Nelson et al., 1996). Genes situated 5' in the *Hoxa* and *Hoxd* clusters form a series of overlapping domains centered on distal and posterior-distal regions, respectively, of the early limb bud (Izpísúa-Belmonte and Duboule, 1992). The same *Hoxa* and *Hoxd* genes are expressed in the fore and hindlimb buds (Nelson et al., 1996) and can be activated by retinoic acid, SHH, and BMP2 in the presence of FGF (Duprez et al., 1996, Izpisúa-Belmonte et al., 1991, Riddle et al., 1993)

Overexpression of *Hoxd11* produces local pattern alterations, and an anterior digit in the chick leg appears to be posteriorized (Morgan et al., 1992). The idea that the sole function of *Hox* gene expression domains is to encode position (Tabin, 1992) appears be an oversimplification, and after a recent reinterpretation of the above result, the authors conclude that the effect of overexpression is an altered growth program (Morgan and Tabin,

1994). Duboule has argued that the pattern of cell proliferation and growth is controlled by much earlier expression of Hox genes, and thus, may be the mechanism by which homeosis is achieved (Duboule, 1995). Mesenchyme cells in different regions of the limb bud express different combinations of *Hox* genes. Patterns of *Hox* gene expression are dynamic and do not remain fixed. Early expression patterns are associated with patterning of the stylopod and zeugopod, and this expression period can be subdivided into corresponding proximal and more distal phases (Nelson et al., 1996). A third, distalmost expression phase maps onto the domain of digit development where gene expression extends anteroposteriorly across the bud apex (Izpisúa-Belmonte and Duboule, 1992, Vargesson et al., 1997). Functional inactivation of *Hoxa13* results in loss of digit 1 and malformation of the carpal and tarsals (Fromental-Ramain et al., 1996). When *Hoxd13* is functionally inactivated, digit development is delayed and there are only small changes in digit morphology (Dolle et al., 1993). It is possible that, although not functionally equivalent, *Hoxa13* could partially compensate for the lack of *Hoxd13*. Consistent with this idea, digits are almost completely absent in *Hoxd13/Hoxa13* double mutants (Fromental-Ramain et al., 1996). Similarly, in double homozygous mutants for *Hoxa11* and *Hoxd11* (which are expressed more proximally and anteriorly than the *Hoxa13* and *Hoxd13* genes), the forearm is almost completely absent (Davis et al., 1995).

Unlike these *Hoxa* and *Hoxd* genes, the *Hoxc* gene contribution to the wing is not restricted so closely to the 5' end of the cluster, and the expression domains lie within the anterior proximal region of each bud. Fore- and hindlimb buds express different *Hoxc* genes, and these respect the colinear expression sequence along the body axis. *Hoxc6* is also retinoid responsive, and is downregulated by retinoic acid application (Oliver et al., 1990). *Hoxc6* is associated with development of the shoulder girdle.

Of the *Hoxb* cluster, *Hoxb5*, *Hoxb8*, and *Hoxb9* are expressed during limb development (Nelson *et al.*, 1996). Two of the *Hoxb* genes *Hoxb5* and *Hoxb8*, have been linked to the relationship of limbs to patterning along the body axis. A loss of function mutation in the mouse *Hoxb5* gene causes an apparent shift in the position of the forelimb relative to the axial skeleton (Rancourt, Tsuzuki, and Capecchi, 1995). *Hoxb5* is normally expressed in the region of the shoulder (Wall *et al.*, 1992). It is unclear whether the forelimb bud in mutant mice emerges from cells at a more anterior position, or whether the shifted limb is due to a malformation in the shoulder that results in a "shrugged" anterior orientation of the girdle. The girdle appears to originate at the normal axial level, but is longer and projects anteriorly rather than laterally. The shifted limb is innervated by the normal brachial plexus and the axon trajectories are normal within the limb, although the nerves enter the limb at a more posterior position (Rancourt *et al.*, 1995). These results suggest that the forelimb may not originate from a more anterior position, but may be secondarily shifted instead.

Hoxb8 has been implicated in positioning the polarizing region. *Hoxb8* is normally expressed in lateral plate mesoderm of the anterior hindlimb and flank, with an anterior boundary in the posterior region of the forelimb (Charite *et al.*, 1994, Lu *et al.*, 1997, Stratford, Kostakopoulou, and Maden, 1997). In a transgenic mouse designed to push *Hoxb8* gene expression to a more anterior level, the *Hoxb8* gene was driven by the *RAR β 2* promoter (Charite *et al.*, 1994). The resulting expression of *Hoxb8* throughout the forelimb resulted in formation of an ectopic polarizing region, and as a consequence, a mirror image duplication in the forelimbs (Charite *et al.*, 1994). This result suggested that the anterior boundary of expression may position the polarizing region in the forelimb. Consistent with this idea,

the hindlimbs of the mutants are normal. A more posterior (5') *Hox* gene is presumably involved in positioning the polarizing region in the hindlimb. Stratford *et al.* have recently shown that *Hoxb8* expression in the chick is tightly correlated with the distribution of polarizing potential in the lateral plate mesoderm of the chick embryo (Stratford, Kostakopoulou, and Maden, 1997). There now appears to be a direct link between retinoic acid and *Hoxb8* in induction of the polarizing region, as retinoid treatment can induce *Hoxb8* expression in the limb within 30 minutes and in the absence of protein synthesis (Lu *et al.*, 1997; Stratford *et al.*, 1997). Early expression of *Hox* genes along the embryonic axis may also ^{be} regulated by retinoids (Conlon, 1995), which can interact directly with retinoic acid response elements within enhancers that direct restricted expression (Morrison *et al.*, 1996). *Hox* gene expression along the body axis plays a direct role in limb development by determining where, within the limb, the polarizing region is situated. The possibility that *Hox* genes are involved in specifying limb position is also attractive, and work reported in chapter 4 of this thesis suggests that this is indeed the case.

3. Proximodistal outgrowth and patterning

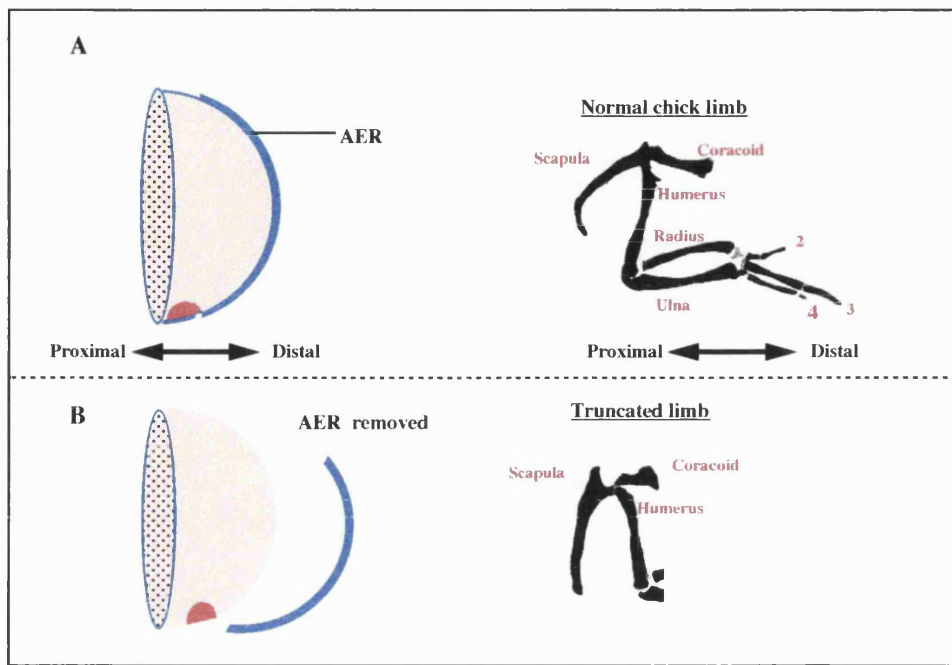
3.1 The apical ectodermal ridge

Outgrowth of the limb bud along the proximodistal (shoulder to digits) axis is controlled by the apical ectodermal ridge. The apical ectodermal ridge (AER) is a pseudo-stratified columnar epithelium that rims the developing limb bud. Surgical removal of the ridge (Saunders, 1948) results in truncation of the limb in a stage-dependent manner; earlier ridge removals result in more severe truncations (Fig. 2) (Summerbell, 1974). Grafting an additional ridge onto the dorsal surface of the limb bud causes a new axis of outgrowth (Zwilling, 1956a). Mutants which have perturbed apical ridge formation exhibit the predicted morphological effects in the limb, such as the

Eudiplopoidia mutant, which develops an ectopic apical ridge on the surface of the limb and consequentially, ectopic limb structures develop. *Limbless* and *wingless* embryos fail to form a normal apical ridge and as the names imply, they lack both wings and legs, and wings alone, respectively (Fallon *et al.*, 1983, Zwilling, 1956b).

Figure 2. The Apical Ectodermal Ridge (AER) maintains proximodistal outgrowth of the limb.

A. The chick wing bud is rimmed by the apical ectodermal ridge (left, in blue) which maintains proximodistal outgrowth of the limb. The mature wing skeleton is organized along a proximal to distal (proximodistal) axis, with the scapula and coracoid being the most proximal structures and the digits being the most distal. **B.** Removal of the apical ectodermal ridge from the limb bud (left) results in loss of distal structures in the mature limb (right).



3.2 Molecular basis of ridge signaling

3.2.1 Fibroblast growth factors

There is increasing evidence that signaling by the AER is mediated by fibroblast growth factors (FGFs). The FGF family of signaling molecules consists of at least 10 members. The size of the protein is variable among the different members, ranging from 155 to 267 amino acids, but all are characterized by the presence of a conserved region of approximately 125 amino acids (Thomas, 1993). Although only \approx members contain recognizable secretory signal sequences (Abraham *et al.*, 1986, Thomas, 1993), alternate mechanisms have been proposed to account for release of FGF1 and FGF2 from the cell. In several systems, studies have shown that FGF2 is not released from the cell unless cell death or damage occurs (reviewed in Thomas, 1993). McNeil has proposed that transient, non-lethal wounding of the plasma membrane may be a mechanism of bFGF release (McNeil, 1993), and Mignatti and Rifkin have suggested that exocytosis may be a means by which bFGF could escape from the cell (Mignatti and Rifkin, 1991).

Fgf8 is expressed throughout the ridge from very early in limb development, while transcripts of *Fgf4* are detected later and are posteriorly restricted in the ridge. FGF2 protein can be detected at high levels in the ridge and ectoderm and at lower levels in limb mesoderm. Experimental work has shown that the apical ectodermal ridge signal can be replaced by application of FGF8 (Crossley *et al.*, 1996, Vogel, Rodriguez, and Izpisúa-Belmonte, 1996), FGF4 (Niswander *et al.*, 1993) or FGF2 (Fallon *et al.*, 1994). The posterior ridge, or FGF4, also maintains signaling activity in the polarizing region (Vogel and Tickle, 1993). A positive feedback loop, coordinating limb outgrowth and patterning, involves reciprocal maintenance between *Shh* in the ZPA, and *Fgf4* in the AER (Laufer *et al.*, 1994,

Niswander *et al.*, 1994). The polarizing region signal, in conjunction with FGF4, may establish the progress zone at the tip of the bud and allow continued patterning of limb structures (Niswander *et al.*, 1993).

FGF binds to a group of 4 receptor tyrosine kinases (FGF receptor [FGFR] 1-4) with varying affinity (Green, Walsh, and Doherty, 1996, Ornitz *et al.*, 1996). Different isoforms of FGFR1-4 can be generated by alternative splicing, which can alter the ligand binding properties of the receptor(Green, Walsh, and Doherty, 1996). Several FGF receptors are expressed in the emerging limb buds, although expression patterns of the different isoforms are, for the most part, not yet known (see below). In the mouse embryo, FGFR1 is expressed in mesenchymal cells and FGFR2 is expressed in the overlying ectoderm, including the AER (Orr-Utreger *et al.*, 1991, Peters *et al.*, 1992). Both receptors can bind FGF1- FGF6, but not FGF7 (Johnson *et al.*, 1990, Mansukhani *et al.*, 1990, Miki *et al.*, 1992, Orr-Utreger *et al.*, 1993, Werner *et al.*, 1992). FGF7 is the ligand for KGF Receptor (KGFR), a splicing variant of FGFR-2 encoded by the *bek* gene (Miki *et al.*, 1992), which is expressed only in the ectoderm (Orr-Utreger *et al.*, 1993). Although FGF8 is expressed in the ridge, it seems to show the strongest affinity for FGFR4 (a relative of the chicken FREK gene) (Marcelle *et al.*, 1994) which is expressed in muscle cells of the limb. The affinity of FGFs for their receptors is increased by heparin and heparan sulphate proteoglycans (Green, Walsh, and Doherty, 1996, Yayon *et al.*, 1991). *Syndecan1*, a member of the Syndecan family of heparan sulphate proteoglycan family, is expressed in limb bud mesenchyme in a similar pattern to FGFR1 (Bernfield, Hinkes, and Gallo, 1993). The *Syndecan1* promoter contains binding sites for homeoproteins, suggesting that expression of both Syndecans and FGFs (see below) may be regulated by *Hox* gene expression during development (Bernfield, Hinkes, and Gallo, 1993).

3.3 The progress zone

The proximo-distal pattern of the limb elements is determined in the mesenchyme at the tip of the limb bud, known as the progress zone. Cells in the progress zone at the distal tip of the bud are kept in a rapidly proliferating undifferentiated state by the overlying ridge (Summerbell, Lewis, and Wolpert, 1973). Summerbell *et al.* proposed that the p-d identity of limb bud mesenchyme cells is determined by the length of time they spend dividing in the progress zone, either by a mitotic clock or other mechanisms involving exposure to a local factor (such that exit from the progress zone equates with a positional stamp indicating when this cell left the influence of the zone). The cell then interprets this information, or value, as a positional address along the p-d axis. As the cell number increases in the progress zone, cells furthest from the ridge exit the zone and are left behind (proximally) in the limb. According to the model, the first cells to exit this region are specified to give rise to the most proximal structures.

3.4 Candidate molecules expressed in the progress zone

Msx1 and *Msx2*, two related homeobox genes, are expressed in the progress zone, and *Msx1* can be maintained by FGF (Vogel, Roberts, and Niswander, 1995). *Msx2* is expressed in the apical ridge and anteriorly in the progress zone (Coelho *et al.*, 1991, Davidson *et al.*, 1991). *Cek8*, a receptor tyrosine kinase, is also expressed in the progress zone, and, like *Msx1*, expression of *Cek8* is dependent upon FGF signals from the apical ridge (Patel *et al.*, 1996). *Msx* and *Cek8* genes may be involved in integrating and interpreting apical ridge signals. *Wnt5a*, a short-range signaling molecule closely related to the *Drosophila Dwnt5* gene (Eisenberg, Ingham, and Brown, 1992), is also expressed in the limb with highest levels in the progress zone and the apical ridge (Dealy *et al.*, 1993,

Parr *et al.*, 1993). This is particularly interesting because *Dwnt5* is thought to be a downstream target of *Distal-less (Dll)* (Eisenberg, Ingham, and Brown, 1992), and several vertebrate homologues of *Dll (Dlx)* are expressed in the apical ridge overlying the progress zone (Bulfone *et al.*, 1993, Dolle, Price, and Duboule, 1992, Ferrari *et al.*, 1995). *Wnt12* is also expressed in the apical ridge (Christiansen *et al.*, 1995). Based on homology to *Drosophila* signaling networks, an interesting possibility is that in the apical ridge DLX induces expression of *Wnt5a* (and possibly other *Wnts*) which could, in turn, induce *Bmp* expression. (If the ability of *dll* to induce *dpp* in *Drosophila* has been conserved in vertebrates, then DLX may directly induce *Bmp* expression.) *Wnt* genes cooperate with FGF to induce mesoderm in *Xenopus* (Christian, Olson, and Moon, 1992). Moreover, mouse mammary tumor virus (MMTV) has been found to activate transcription of *Wnt1*, *Wnt3*, *Fgf3* and *Fgf4* in mouse mammary tumors, and an attractive possibility is that these factors cooperate in carcinogenesis and development (reviewed in Nusse and Varmus, 1992). It will be interesting, therefore, to determine whether *Wnt* genes are involved in induction of *Fgf* in the apical ridge, and whether *Wnt* gene expression in the underlying progress zone (i.e., *Wnt5a*) is dependent on FGF signaling.

4. Dosoventral polarity

Dorsoventral polarity (d-v) of the limb bud is initially established in the lateral plate mesoderm, and this information is subsequently transferred to the ectoderm, where it feeds back on the mesoderm (Geduspan and MacCabe, 1989, MacCabe, Errick, and Saunders, 1974, Saunders and Reuss, 1974). The latter interaction results in the establishment of polarized gene expression within the limb bud mesenchyme. A signal secreted by the dorsal ectoderm, WNT7a, contributes to limb patterning along the dorsoventral axis (Parr and McMahon, 1995) by inducing expression of *Lmx1*, a

transcription factor in the dorsal mesenchyme (Riddle *et al.*, 1995, Vogel *et al.*, 1995). *Shh* expression is also maintained by *Wnt7a* (Yang and Niswander, 1995). Expression of *engrailed1(en1)*, a homeobox gene, in the ventral ectoderm antagonizes *Wnt7a* expression, and thereby inhibits formation of dorsal structures on the ventral surface (Logan *et al.*, 1997, Loomis *et al.*, 1996). Involvement of *Wnt7a* and *en1* in dorsoventral patterning is supported by the phenotypes of the *Wnt7a* and *en1* knockout mice, which develop with a double ventral and a double dorsal pattern, respectively, in the limbs (Parr and McMahon, 1995; Loomis *et al.*, 1996).

LMX1 is a relative of the

Drosophila LIM domain gene *apterous*, and, like *Wnt7a* in the ectoderm, expression of this gene is activated very early in lateral plate mesoderm, even before a limb bud is formed (Riddle *et al.*, 1995, Vogel *et al.*, 1995). It is striking that *apterous* is also expressed in the dorsal compartment of the *Drosophila* wing disc (Blair, 1995). Infection of chick wing bud ectoderm with a retrovirus containing *Wnt7a* results in ectopic activation of *LMX1* in ventral mesoderm, and when presumptive limb is infected with a retrovirus containing *LMX1*, parts of the ventral limb are dorsalized (Riddle *et al.*, 1995, Vogel *et al.*, 1995).

The link between dorsoventral patterning and apical ridge formation has been emphasized in several recent studies on the chick *limbless* mutant. In three independent studies, the *limbless* mutation was shown to affect dorsoventral polarity of the limb bud. The entire limb is dorsalized and expresses *Wnt7a* and *Lmx1* throughout. In the absence of a d-v boundary, the apical ridge fails to form (Grieshammer *et al.*, 1996, Noramly *et al.*, 1996, Ros *et al.*, 1996). *Radical Fringe (R-fng)* is normally expressed in the dorsal ectoderm of the emerging bud (Laufer *et al.*, 1997, Rodriguez-Esteban *et al.*,

1997). The AER forms in the ectoderm at the boundary of *R-fng* expressing and non-expressing cells. *En1* also represses *R-fng* ventrally, thereby creating the border of *R-fng* expression which positions the AER at the apex of the limb bud. However, in the absence of *en1*, an apical ridge is induced which expands into the ventral ectoderm (Loomis et al., 1996). This is surprising, because if *en1* acts to repress *R-fng*, then *R-fng* expression should be found throughout the limb ectoderm. Thus, in the absence of apical expression boundaries, one would predict complete absence of an AER in *en1* mutants. Although this is not the case in *en1* mutants, this condition is seen in *limbless* mutants; *R-fng* is expressed throughout the limb ectoderm and the ridge fails to form (Laufer et al., 1997). The pattern of *R-fng* expression in *en1* knockout mouse is not yet known, but the fact that the ridge is not completely deleted suggests that the role of *R-fng* in AER formation is likely to be more complicated than that initially proposed by Laufer et al. (1997) and Rodriguez-Esteban et al. (1997).

Two recent studies of dorsoventral polarity have shed new light on the developmental origin of the limb. Based on a series of chick-quail grafting experiments, Michaud et al. reported that the ectoderm overlying the medial (presumptive dorsal) somatic mesoderm gives rise to the apical ridge, the ectoderm overlying the somites and kidney gives rise to dorsal limb bud ectoderm, and the ectoderm of the lateral somatopleure makes-up the ventral half of the limb bud ectoderm (Michaud, Lapointe, and Le Douarin, 1997). They argue that cells from each half oppose each other, but do not mix, at the apical ridge. Altabef et al. addressed the same problem using Dil labeling, and obtained different results (Altabef, Clarke, and Tickle, 1997). Altabef et al. found that the ectoderm over the medial somatopleure gave rise to dorsal limb bud ectoderm and apical ridge cells. They also found that ectoderm over the lateral somatopleure forms the ventral limb ectoderm and

apical ridge cells. However, in contrast to the sharp boundary seen by Michaud *et al.*, Altabef *et al.* observed dorsal and ventral cells intermingling in the apical ridge, although ventral cells did not cross the ridge into the dorsal ectoderm nor did dorsal cells cross into ventral ectoderm. Both papers indicate that the limb ectoderm consists of two lineage-restricted compartments (dorsal and ventral), although the results conflict over the question of whether or not cells mix in the apical ridge boundary. Michaud *et al.* also demonstrate that the somites are a source of a dorsalizing factor and the lateral somatopleure is the source of a ventralizing factor, and although their model does not indicate a molecular basis for this induction, it does indicate that local environmental cues establish the initial dorsoventral polarity in the limb. Identification of these signals will be important for understanding how dorsoventral position of limb buds is established with respect to the main body axis.

5. Evolutionary conservation of signaling networks

Limb outgrowth is linked to interconnected genetic networks which pattern all three primary axes. The same genetic networks are deployed during development of many different organ systems within the embryo. In vertebrates, for example, there are common components in the molecular networks of limb, gut, lung, face, central nervous system, hair and feather, tooth, mammary gland and eye (Bitgood and McMahon, 1995, Dudley, Lyons, and Robertson, 1995, Hebert *et al.*, 1994, Liem *et al.*, 1995, Luo *et al.*, 1995, Nohno *et al.*, 1995, Peters *et al.*, 1994, Roberts *et al.*, 1995, Thesleff, Vaahtokari, and Partanen, 1995, Wall and Hogan, 1995). Moreover, these networks appear to be evolutionarily conserved because they are used by crustacea, insects and vertebrates during embryonic development (reviewed in Shubin, Tabin, and Carroll, 1997).

Several parallels have been identified between gene expression patterns in tetrapods and teleosts (the major subgroup of ray-finned fishes), and functional comparisons of gene regulation are now possible. Sonic hedgehog is expressed at the posterior margin of zebrafish fin bud mesoderm (Sordino, van der Hoeven, and Duboule, 1995) and, as in tetrapods, treatment with retinoic acid induces ectopic *Shh* expression in the anterior part of the fin bud (Akimenko and Ekker, 1995). Several zebrafish FGF receptors have been identified, and at least one is expressed in the mesoderm underlying the fin bud apical ridge (Thisse, Thisse, and Weston, 1995). *Engrailed1* is expressed in the ventral half of the pectoral fin bud ectoderm (Hatta et al., 1991). As in tetrapod limb buds, *Msx* genes are expressed in the mesenchyme and *Msx* and *Dlx* genes are expressed in the apical ridge of teleost fins buds (Akimenko et al., 1995, Akimenko et al., 1994). Significantly, in fins the ridge extends distally as an ectodermal fold, enclosing the developing dermal fin rays. Sordino and Duboule speculate that these rays may physically interrupt ectodermal signalling to the mesoderm, thereby truncating fin endoskeletal outgrowth (Sordino and Duboule, 1996). If this is correct, then a key question in the evolutionary transition from fins to limbs concerns the nature of the mechanism which evolved to prevent early fin-ray development, before such primitive bud-truncation occurs. Further analyses of zebrafish mutants and experimentally manipulated fin buds are likely to reveal additional differences and similarities between fin and limb development. *Hox* gene expression patterns in fin development are already beginning to uncover aspects of both.

Hox gene expression in zebrafish paired fins provides an informative comparison with tetrapod limbs. 5' *Hoxa* and *Hoxd* genes are expressed in pectoral and pelvic fins. *Hoxb* gene expression patterns in fin pairs are

currently undescribed, but *Hoxc6* is expressed in a wedge-shaped domain at the anterior-proximal region of pectoral fin buds, similar to the pattern seen in tetrapod limbs (Molven *et al.*, 1990). *Hox* gene expression domains in zebrafish fin-pairs are abbreviated distally, however, and appear to be mono- or biphasic (Sordino, van der Hoeven, and Duboule, 1995) instead of triphasic as in limb buds (Nelson *et al.* 1996). These simpler expression patterns correlate impressively with shorter and simpler appendicular skeletons of zebrafish fins, relative to their tetrapod homologues.

6. Patterning the primary body axis

6.1 *Hox* genes

Members of the *Hoxa*, *Hoxb*, *Hoxc*, and *Hoxd* clusters interact to encode positional identity in vertebrate embryos. It now appears that this involves a complex program of cell behavior involving cell proliferation and adhesion, factors that are pivotal to the developmentally later event of growth (Dolle *et al.*, 1993, Duboule, 1995, Yokouchi *et al.*, 1995). Evolution of the *Hox* genes themselves may have played an important role in the elaboration of the vertebrate body plan. The evolutionary diversity of chordate *Hox* gene clusters is becoming increasingly clear (Fig. 3). Amphioxus, a cephalochordate, has only a single cluster, but this has members of at least 10 out of the 13 parologue gene groups identified in the four clusters of jawed vertebrates (Holland and Garcia-Fernandez, 1996, Sharman and Holland, 1996). This suggests that during early vertebrate evolution a *Hox* gene cluster resembling that of amphioxus underwent four-fold duplication,

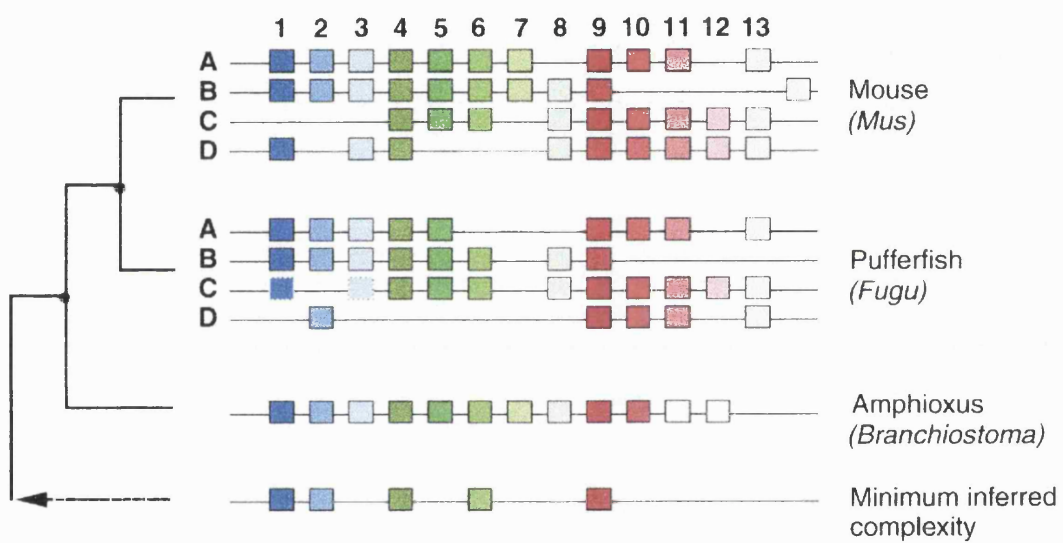
at a locus or loci preceding the divergence of lamprey and jawed vertebrate lineages (Pendleton *et al.*, 1993, Sharman and Holland, 1996). Moreover, the amphioxus *Hox* gene complement must itself have arisen from lateral duplications of the genes in successively simpler, more primitive *Hox* clusters (Kappen, 1996). Thus, even within a single *Hox* cluster, gene

duplications have occurred, and these events have allowed changes to accumulate in orthologous genes without altering existing developmental processes. Indeed, these changes may have facilitated acquisition of new developmental roles. Clues about the pattern of these events derive from *Hox* gene sequence analyses which identify three interrelated sets: *anterior*- (1-3), *medial*- (4-8), and *posterior*-groups (9-13) (Fig. 3) (Kappen, 1996).

Since these fundamental duplication events, instead of further expansion of the *Hox* gene network, jawed vertebrate cluster evolution seems to have been characterised by gene deletions. This much is apparent from direct comparison of amphioxus with mouse clusters (Fig. 3) (Holland and Garcia-Fernandez, 1996). Cluster structures in other, non-mammalian, vertebrates are less well documented, and information about the zebrafish (*Danio rerio*), a teleost, is only just becoming available (Prince *et al.*, 1997, van der Hoeven *et al.*, 1996). However, the recent report of *Hox* cluster organisation in the pufferfish *Fugu rubripes*, an advanced teleost, shows major differences relative to mammalian clusters , indicating quite separate patterns of gene loss in tetrapod and teleost lineages (Aparicio *et al.*, 1997). Furthermore, absence of *Hoxd12* in *Fugu* (Aparicio *et al.*, 1997) but presence in *Danio* (van der Hoeven *et al.*, 1996), already points to variation within the teleost fishes (Fig. 3).

Figure 3. *Hox* gene cluster diversity and evolution

Tree shows evolutionary relationships of representative chordates in which complete *Hox* cluster organization is known. Numbers indicate paralogous *Hox* gene groups and letters indicate *Hox* gene clusters. Mouse *Hox* genes from Sharman and Holland (Sharman and Holland, 1996), *Hoxb13* from Zeltser *et al.* (Zeltser, Desplan, and Heintz, 1996), pufferfish *Hox* genes from Aparicio *et al.* (Aparicio *et al.*, 1997) and Amphioxus *Hox* organization from Garcia-Fernandez and Holland (Garcia-Fernandez and Holland, 1994). Minimum inferred complexity of arthropod-chordate ancestral *Hox* gene cluster, and interrelationships of anterior (blue) medial (green) and posterior (red) *Hox* gene groups from Kappen ((Kappen, 1996)). Inter-gene distances are not indicated with the exception of *Hoxb13*, which is out of register with the other group 13 genes (Zeltser, Desplan, and Heintz, 1996). Open boxes in Amphioxus cluster indicate incompletely characterized genes (Sharman and Holland, 1996), and dotted boxes in pufferfish cluster indicate possible pseudogene remnants of *Hoxc1* and *Hoxc3* (Aparicio *et al.*, 1997).



6.2. *Hox genes and axial patterning.*

During vertebrate development, the head-tail body axis is established during gastrulation, when cells are assigned anteroposterior positional identities (Beddington and Smith, 1993). The paraxial mesoderm, which forms the vertebrae, musculature and dermis, is a useful model for studying axial patterning because segmented somites have particular identities, and changes in these can be detected in the vertebral pattern. Kessel and Gruss showed that retinoid treatment could alter *Hox* gene expression boundaries along the A-P axis of paraxial mesoderm (Kessel and Gruss, 1991). These alterations result in apparent homeotic transformations of vertebral identity. Further evidence for the role of *Hox* genes in specifying vertebral identity comes from experiments in which *Hox* genes are knocked-out or overexpressed (Krumlauf, 1994).

Evolutionary changes in regional identity within a series of vertebral segments, such as conversion of the first lumbar vertebra to a thoracic, is known as transposition (Goodrich, 1930). Initial comparative studies of axial *Hox* expression have already begun to relate 'transposed' (Goodrich, 1930) vertebral anatomical landmarks and regions to shifts in conserved expression boundaries (Burke *et al.*, 1995, Gaunt, 1994). In tetrapods the anteroposteriorly staggered expression domains of *Hox* genes from the same parologue group are probably evolutionarily derived. These spatial differences, or dispersal, probably appeared with the evolution of axial regional boundaries such as the lumbar-thoracic division and sacrum (Gaunt, 1994; Burke *et al.*, 1995). This interpretation is based upon the premise that members of each parologue group primitively shared coincident expression boundaries. A clear prediction of this hypothesis is that simpler colinear expression patterns should be found in experimental subjects with less highly regionalized equivalent domains of axial

organisation (e.g. the vertebral column of the zebrafish, *Danio rerio*). Preliminary results from such a study appear to support this hypothesis. Prince and Ho report that, in comparison with tetrapods, zebrafish *Hox* genes of paralogue groups 6 to 8 share significantly closer anterior expression boundaries in the paraxial mesoderm (Prince *et al.*, 1997). Because these paralogues probably derive from a single ancestral gene, they suggest that the ancestral expression pattern has been retained and the boundaries became dispersed in tetrapods with increased specialization of the axial skeleton

6.3 Retinoids, limbs and the body plan

The earliest link between retinoids and limb formation may be coupled to more global specification of positional identity along the body axis. This is demonstrated by the dramatic experiments of Rutledge *et al.*, in which systemic administration of retinoic acid to morula-stage mouse embryos resulted in duplications of the lower body, including the limbs (Rutledge *et al.*, 1994). Ectopic limbs were almost always induced posterior to the normal hindlimbs. Niederreither *et al.* repeated these experiments in a systematic study of the phenomenon, and classified the morphological effects into 4 groups; supernumerary limb buds (paired buds ventral and caudal to the normal hindlimbs), supernumerary axis (lower body axis with tail, limbs, and occasional genitalia) , unilateral twin (a single ectopic bud joined to the original bud along the a-p axis), and misshapen (normal buds with abnormal protrusions) (Niederreither *et al.*, 1996). While the mechanisms by which this operates is unclear, it seems unlikely that retinoic acid acts on *Hox* genes in these experiments, because *Hox* gene expression is not known to be activated at morula stages. The authors suggest that retinoic acid may act to regulate secondary signaling molecules which act during or after gastrulation.

Retinoic acid has also been shown to transform regenerating tails into limbs (Maden, 1993, Mohanty-Hejmadi, Dutta, and Mahapatra, 1992, Muller, Streicher, and Muller, 1996). This dramatic effect of retinoic acid may be explained in light of recent work on the proximalizing effect of retinoic acid on the regenerating limb of the newt (Gardiner *et al.*, 1995). The effect of retinoic acid on limb regeneration suggested some important differences between development and regeneration, the most obvious being that retinoids posteriorize the developing limb and proximalize the regenerating limb. Hox genes located at the 5' end of the complex are associated with posterior and distal positional values in the limb (Izpísúa-Belmonte and Duboule, 1992). Accordingly, transformation of positional identity from anterior to posterior involves activation of these 5' genes. If proximalization of the blastema by retinoic acid is mediated by Hox genes, then the predicted effect of retinoic acid would be to downregulate 5' genes, leaving blastemal cells with a pattern of Hox gene expression characteristic of more a proximal position. Gardiner *et al.* (1995) found that *Hoxa13*, which is re-expressed during limb regeneration, is indeed downregulated by retinoic acid treatment. If Hox genes are involved in the positional memory required for normal tail regeneration, then retinoic acid may act to reset the pattern of Hox gene expression from "tail" to "leg", which will almost certainly involve downregulation of group 13 Hox paralogues. If this is correct, then the tail to leg transformation may reflect loss of 5' Hox gene expression, which typically anteriorizes cells along the body axis. This interpretation is consistent with the idea that a particular combination of Hox genes could determine where limbs develop along the main body axis.

7. How are limbs induced?

The search for the origin of factors involved in limb induction has led

to the suggestion that medial tissues play a role in signaling to the lateral plate mesoderm. In the grafting experiments involving the limb disc of urodeles, the dorsal region of the peribrachial flank was found to be required for development of the limb (Slack, 1980, Stocum and Fallon, 1984). The dorsal region of the disc contains the pronephros, and several researchers have since argued on the basis of experimental evidence that the kidney plays an important role in limb development. Geduspan and Solursh found that ablation of the mesonephros in pre-limb bud stage chick embryos resulted in reduction or absence of the limb bud on the operated side (Geduspan and Solursh, 1992b). Chick-quail grafting experiments demonstrated that the medial part of the lateral plate mesoderm gives rise to the limb (Geduspan and Solursh, 1992a), and the proximity of this tissue to the mesonephros suggests that an inductive signal, whether it originated from or was transferred by the mesonephros, would not have to diffuse over a long range to affect prospective limb cells. Stephens and McNulty found that insertion of a foil barrier between the mesonephros and lateral plate mesoderm of the prospective wing between stages 12 and 15 inhibited wing development (Stephens and McNulty, 1981). Other work showed that paraxial mesoderm was necessary for limb initiation (Kieny, 1971), but this effect was early and transient, as removal of the somites at later stages had no effect on limb patterning, although the limbs lacked muscle (Chevallier, Kieny, and Mauger, 1978). Raynaud also suggested that paraxial mesoderm played a stimulatory role in reptilian limb induction, and reported that removal of the brachial somites from lizard embryos prevented limb development (Raynaud, 1977).

Limb determination is related to the prospective limb tissue moving past the node early in development. Rudnick showed that tissue transplanted from a level anterior to the node into the coelom of a host

embryo could differentiate into a limb, whereas tissue taken from posterior to the node did not (Rudnick, 1945). Chaube constructed a fate map of the early lateral plate mesoderm using chalk, and from this the relative movements of the prospective limbs and the node were determined (Chaube, 1959). Chaube found that the prospective wing cells pass the node between stages 8 and 9, which is precisely the same point at which these cells become competent to form a limb when transplanted to the coelom (Chaube, 1959). In a series of barrier experiments, Stephens *et al.* investigated the possibility that mediolateral progression of an inductive signal was involved in limb induction (Stephens *et al.*, 1991). Barriers placed immediately lateral to Hensen's node at stages 6 to 8, between the segmental plate and intermediate mesoderm between stages 10 and 11, and between the intermediate and lateral plate mesoderm between stages 13 and 15 resulted in absence or malformation of the wing. When barriers were placed between the neural tube and somites, or between the somites and intermediate mesoderm at stages 13 to 15, the limbs were normal in all cases (Stephens *et al.*, 1991). The authors argue that their results, when taken together with the experiments mentioned above, indicate that an inductive factor passes from Hensen's node to the segmental plate prior to stage 11, and at stage 12 it moves from the segmental plate to the intermediate mesoderm. The factor would then pass to the adjacent the lateral plate mesoderm, where limb development would be induced. These experiments raised the possibility that a limb-inducing signal originates from the axial midline or is produced as a consequence of signals that originate medial to the lateral plate. The means by which limb induction is localized to two positions along the primary body axis could be either by localizing the inductive signals or by localizing the response to a more widespread signal, and this may involve repression of limbs in the flank.

7.1 Ectopic limb development

Formation of an appropriate number of limbs at appropriate positions does not always occur. Bateson addressed the question of extra limb formation, and reviewed several cases of vertebrates with additional limbs (Bateson, 1894). Interestingly, in his description of a frog with an extra hind limb, he noted that the extra leg may have had pattern duplications within it. In light of current knowledge of the distribution of polarizing potential in lateral plate mesoderm, this phenotype suggests that cells with polarizing activity were not confined to one side of the extra leg. Balinsky showed experimentally that competence to form a limb was not restricted to the regions that normally form the limb. He found that transplantation of otic placode, nose rudiment or hypophysis to the flank of an embryonic newt could induce formation of an ectopic limb bud that would develop into a complete limb (Balinsky, 1925, Balinsky, 1933, Balinsky, 1965). Balinsky noted that the identity of the ectopic limb (forelimb or hindlimb) was related to position along the body axis, and the polarity of these limbs was not always the same as that of the normal limbs. Some of these extra limbs may also have had pattern duplications in the a-p axis (Slack, 1977a). These experiments highlight the problems of how limb position is determined within the broad region of competent lateral plate mesoderm, and raise questions about the nature of the limb inducing signal.

7.2 Initiation of limb budding

The lateral plate mesoderm proliferates at a uniform rate along the anteroposterior axis prior to limb budding (Searls and Janners, 1971). The earliest differential can be seen when a localized thickening appears at the site of the prospective forelimb bud. Searls and Janners demonstrated experimentally that limb buds emerge at discrete positions along the lateral plate mesoderm as a result of localized maintenance of cell proliferation.

Their analysis showed that the mitotic index of limb and flank regions is the same up to stage 16, but the index decreases rapidly in the flank between stages 16 and 17, when the limb buds become visible. As Balinsky and Harrison initially showed in amphibians (see above), the chick flank is also competent to participate in limb development. Transplantation of prospective limb mesoderm to the flank results in development of an ectopic limb, and flank cells have been found within both the limb bud and differentiated cartilage (Dhouailly and Kieny, 1972). Limb mesenchyme transplanted under flank ectoderm induces the flank ectoderm to form an apical ridge (described below), which supports outgrowth of the ectopic bud into a complete limb (Carrington and Fallon, 1984, Saunders and Reuss, 1974). Flank cells transplanted under the apical ridge of a limb bud, however, can not support the ridge and the ridge flattens over the flank cells. Thus, the region of lateral plate that actually forms limbs is only part of the region that is competent to form limbs, which suggests that signals localized to specific axial levels determine the positions at which limbs emerge. Moreover, these experiments suggest that the signal acts not only to maintain cell proliferation, but also changes the character of the cells from flank to limb, thereby allowing them to participate in the inductive interactions required for limb morphogenesis.

Very little is known about the molecular basis of limb bud initiation. Application of disulphiram (inhibitor of retinoid synthesis) to pre-limb bud stage chick embryos inhibits limb bud formation, suggesting that initiation of limb development is dependent on retinoic acid synthesis (Stratford, Horton, and Maden, 1996). Retinoic acid does not have limb inducing activity, however, as local application of retinoic acid to the flank of pre-limb bud stage chick embryos does not result in additional limb formation, although patterning of the normal legs can be affected (Wilde, Wedden, and Tickle,

1987). At the beginning of the work described in this thesis, FGFs were known to be involved in maintenance of limb outgrowth, and the possibility had arisen from overexpression studies by Heath and colleagues that FGF may also be involved in the initial budding of the limbs (see chapter 3). The work described in this thesis focuses on the role of FGF in initiation of vertebrate limb development. The work described in chapter 3 asks whether direct and local application of FGF to the flank of chick embryos can induce limb budding, and addresses the problem of establishing signaling regions in the bud. Chapter 4 describes experiments which investigate the role of Hox genes in controlling the position at which limbs are specified in lateral plate mesoderm of chick embryos. In pythons, loss of specialization along the body axis is accompanied by loss of forelimbs and severe truncation of hindlimbs. In chapter 5, I investigate the developmental basis of limblessness and axial regionalization in pythons, with particular emphasis on the mechanisms controlling limb position, limb bud initiation and patterning, and regional identity in the axial skeleton.

CHAPTER TWO: Materials and Methods

1. Application of FGF beads to chick embryos

Fertilized chicken eggs were incubated at 38°C and the embryos were staged by counting somites according to Hamburger and Hamilton (Hamburger and Hamilton, 1951). Experiments were performed on embryos between stages 10 and 22. To improve visibility, a small amount of India or drawing ink (Pelikan) diluted 1:4 in tissue culture medium was injected under the blastoderm, or a small chip of 1% neutral red in 1% agar was placed on the vitelline membrane. The vitelline membrane was torn away from the right side of the embryo, and a small transverse slit was made with electrolytically-sharpened tungsten needles in the ectoderm covering the lateral plate mesoderm at a particular somite level. Heparin acrylic beads (H5263, Sigma) 125 - 250 µm in diameter were soaked in a 2µl drop of Minimum Essential Medium (MEM, Gibco-BRL) containing one of the following proteins for at least 1 hour at room temperature prior to implantation: FGF-1 (1mg/ml; 132-FA-025 R&D Systems), FGF-2 (1mg/ml; 133-FB-025, R&D Systems), FGF-7 (1mg/ml; 251-KG-010, R&D Systems), or FGF-4 (700µg/ml; kindly provided by Prof. John Heath, Birmingham). A bead was inserted into the slit and manipulated into the appropriate anteroposterior position under the ectoderm. A few drops of tissue culture medium (MEM supplemented with 10% fetal calf serum, 1:100 antibiotic/antimycotic and 2mM L-Glutamine, all from Gibco-BRL) were added to the egg before it was resealed and returned to the incubator. Embryos were incubated for a total of 9-10 days.

2. Application of SHH beads to chick embryos

SHH beads were prepared using a recombinant form of the mouse SHH protein corresponding to the complete amino peptide (extending to

amino acid 198, kindly provided by Prof. Andy McMahon, Harvard; described in Yang and Drossopoulou *et al.*, 1997). Affigel CM beads approximately 150 µm in diameter were rinsed for 2-3 minutes in Tris chloride/sodium chloride buffer and then soaked in a 2 µl drop of SHH (16 mg/ml) for at least 1 hour at room temperature. Beads soaked in this concentration of SHH can induce full digit duplications when applied anteriorly in chick wing buds (Yang and Drossopoulou *et al.*, 1997). Embryos were prepared as described above for FGF beads.

3. Application of retinoic acid beads to chick embryos

Retinoic acid preparation and experiments were carried out in the dark. All-trans-retinoic acid (Sigma) was diluted in dimethylsulphoxide (DMSO) to the desired concentrations and stored at -20°C until needed. AG1-X2 beads in formate form (Biorad) between 200 -250 µm in diameter were soaked in retinoic acid/DMSO for 20 minutes at room temperature. Beads were then rinsed in tissue culture medium (as described in method 1) and implanted into the desired position in the embryo.

4. Whole-mount skeletal preparations: Alcian green staining

Embryos were removed from the egg, washed in 1X phosphate-buffered saline (PBS) and the membranes and internal organs were removed prior to overnight fixation in 5% trichloroacetic acid (TCA). They were then transferred to 0.1% Alcian green in acid alcohol for 6-16 hours. Alcian green was removed and the embryos were differentiated in acid alcohol overnight, dehydrated in 100% alcohol and cleared in methyl salicylate for analysis of skeletal patterns.

5. Whole-mount skeletal preparations: Alcian blue and Alizarin red staining

Embryos were washed in 1X PBS and fixed in 80% ethanol overnight. Skin, viscera and adipose tissue was cleared away and embryos were transferred to 96% ethanol for 24 hours. Embryos were then placed in acetone for at least 2 days, rinsed in 96% ethanol and stained for 2-6 hours, according to size, at 37°C. 10 ml of staining solution was prepared with 1 ml of 0.3% Alcian blue stock , 1 ml Alizarin red stock, 1 ml acetic acid and 17 ml 70% ethanol (Alcian blue stock: 0.3% Alcian blue in 70% ethanol, filtered; Alizarin red stock: 0.1% Alizarin red in 96% ethanol, filtered). Embryos were rinsed in 96% ethanol for 1-2 hours, rinsed in tap water for a further 1-2 hours, and cleared in 1% Potassium Hydroxide (KOH) until the skeleton was visible. Clearing was continued in a graded sequence of 1% KOH/Glycerine as follows: 20% Glycerine, 50% Glycerine, 80% Glycerine for 2-5 days at each step. Embryos were then transferred to 100% Glycerine for photography and storage.

6. Scanning Electron Microscopy

SEM was used to examine early morphology of treated embryos. Embryos were incubated up to 56 hours following FGF application, then removed from the egg into PBS for washing and removal of membranes. They were fixed and stored in modified Tyrode's solution (1% gluteraldehyde) at 4°C. After post-fixation in 1% osmium in 0.1M phosphate buffer for 1 hour, the specimens were dehydrated in graded ethanol washes and placed in amyl acetate. They were then dried by critical point-drying, mounted on metal studs, and sputter coated with gold particles. The embryos were observed using a Hitachi S-530 scanning electron microscope.

7. Whole-mount *in situ* hybridization

For whole-mount *in situ* hybridization, embryos were removed from the egg and washed and dissected in 1x PBT (PBS with 0.1% triton). Embryos were fixed overnight in 4% paraformaldehyde at 4°C and dehydrated in a series of graded methanol washes. Embryos were stored in 100% methanol at -20°C. Processing and hybridization was carried out following the published protocol of Nieto *et al.* (Nieto, Patel, and Wilkinson, 1996), using digoxigenin-labelled riboprobes for the chick *Hoxb9* (kindly provided by Dr. Robb Krumlauf, NIMR, *Shh* (kindly provided by Dr. Juan Carlos Izpisúa-Belmonte, Salk Institute), *Hoxd9* and *Hoxd13* (kindly provided by Prof. Denis Duboule, Geneva), *Hoxc9* and *Ptc* (kindly provided by Dr. Cliff Tabin, Harvard), and *Fgf8* (kindly provided by Prof. Gail Martin, UCSF) genes.

8. Tissue transplantations

Grafts of chick and python flank tissue to host wing buds were performed as follows. Donor embryos were removed from the egg, staged and dissected in 1x PBS on a cold block. Pieces of flank tissue approximately 200-300 µm were excised from the appropriate position using electrolytically-sharpened tungsten needles. For chick embryos, somites were counted and used as a landmark for determining axial level in the lateral plate mesoderm, and for snakes, the coiling pattern of the embryo was used for this purpose. Host limb buds were prepared by removing enough of the vitelline membrane and amnion to expose the wing bud. The apical ridge was lifted away from the anterior or posterior limb bud mesenchyme using a tungsten needle to make a loop, and the graft was manipulated into the loop. The egg was resealed with clear adhesive tape and returned to the incubator.

Grafts of limb bud mesenchyme from python to chick were performed as follows. Python embryos were rinsed in 1X PBS, and the hindlimb bud was dissected off. The bud was divided into anterior, middle and posterior thirds, and the middle third was discarded. The anterior and posterior third were then divided into proximal and distal halves, and the distal halves were transferred separately to a 2% solution of Trypsin (1:250, Gibco-BRL) to remove the ectoderm. The mesenchymal tissue was then rinsed in tissue culture medium and grafted to chick wing buds as described above.

9. Iontophoretic application of Dil and DiAsp

Small deposits of the lipophilic membrane dye Dil (Molecular Probes D-282) were applied *in ovo* to the lateral plate mesoderm of the flank, prospective limb bud, or limb bud by iontophoresis. Microelectrodes with a tip diameter of approximately 3 μ m were filled at their tips with a small quantity of Dil (3 mg/ml dimethyl formamide) and then backfilled with 1M lithium chloride. These were then inserted into an electrode holder connected to the positive pole of a 9 volt battery. The electrode was carefully micromanipulated through the ectoderm and into the somatic layer of the lateral plate mesoderm at the appropriate position. The dye was driven out of the electrode by completing the circuit with a second silver wire placed into the egg albumin and attached to the battery's negative terminal. Completing the circuit for about 8-10 seconds was sufficient to label a small patch of cells. Dye application was done under a dissecting microscope and the success and position of labelled cells then checked on an epifluorescent microscope fitted with an extra long working distance x20 objective. For double label experiments the membrane dye DiA (Molecular Probes D-3883) was applied in exactly the same way. The embryos were then allowed to develop for the stated time points and examined using Nikon fluorescence microscopy. For subsequent analysis of *Hoxb9* expression in

labelled embryos, the embryos were fixed and mounted in 4% paraformaldehyde, photographed, and then dehydrated in graded methanol washes prior to processing for *in situ* hybridization.

10. Dig-FGF2

Dig-FGF2 at a concentration of 0.25 mg/ml was a kind gift from Professor John Heath, Birmingham. Activity of Dig-FGF2 at 0.25 mg/ml was tested by soaking heparin beads in 2 µl of protein under the same conditions described for unlabeled FGF, and then applying the beads to the flank of chick embryos. Presence of Dig FGF *in situ* was detected as follows. Embryos were fixed in 4% paraformaldehyde at 4°C overnight. Embryos were then washed in PBT twice for 5 minutes each, and then twice for 30 minutes each. Embryos were then blocked for 2-3 hours in PBT with 15% goat serum and 2% Bovine Serum Albumin (BSA). Anti-digoxigenin antibody (Boehringer Mannheim) was added at a concentration of 1:1000 and embryos were incubated at 4°C overnight. Embryos were washed 4 times for 1 hour each in PBT with 0.1% BSA, and then transferred into NTMT alkaline phosphatase buffer, containing 100mM Tris-HCl, pH 9.5 + 50mM MgCl + 100mM NaCl + 0.1% Triton, for 30 minutes. Color reaction was achieved by transferring the embryos into a glass dish containing BM purple AP substrate (Boehringer Mannheim) and rocking the embryos in the dark at room temperature. Reaction was monitored and stopped by washing the embryos in PBS. Embryos were fixed and stored in 4% paraformaldehyde.

11. Microinjection of Dig-FGF2

Dig-FGF was lightly colored so that injection of the protein could be confirmed visually. Coloration was achieved by dipping a needle first into a 2% solution of fast green and then into the FGF solution. Colored Dig-FGF was loaded into a micropipette with a tip diameter of approximately 3µm, and

the micropipette was carefully micromanipulated through the ectoderm and into the somatic layer of the lateral plate mesoderm at the appropriate position. Dig-FGF was driven out of the pipette and into the tissue by pressure-injection using a picospritzer (General Valve). Microinjection was done under a dissecting microscope and the success was confirmed visually, as described above. Embryos were fixed in 4% paraformaldehyde at stated time points, and processed for immunostaining as described for Dig-FGF beads.

12. Antibody staining

Monoclonal antibodies against LMX1 (Riddle *et al.*, 1995), MSX (Liem *et al.*, 1995) and HOXC8 (Shashikant *et al.*, 1995) (all 3 kindly provided by Dr. Monica Ensini, Columbia), and polyclonal antibodies against FGF2 (Dono and Zeller, 1994) (kindly provided by Dr. Rolf Zeller, EMBL), DLX (Panganiban *et al.*, 1995) (kindly provided by Dr. Grace Panganiban and Prof. Sean Carroll, Wisconsin), EN (Davis *et al.*, 1991) (kindly provided by Prof. Alex Joyner, NYU), SHH (Bumcrot, Takada, and McMahon, 1995, Marti *et al.*, 1995b) (kindly provided by Prof. Andy McMahon, Harvard), HOXC6 (Oliver *et al.*, 1988a) (kindly provided by Prof. Eddy De Robertis, UCLA) and HOXB5 (Wall *et al.*, 1992) (kindly provided by Dr. Nancy Wall, Wisconsin) were used to compare expression in chick and python embryos. Staining protocols varied according to the antibody and are listed below. All secondary antibodies were horseradish peroxidase-coupled (Jackson Immunochemicals) and for whole-mount staining, all steps were done on a rocking platform unless otherwise stated.

12a. Whole-mount antibody staining

Whole-mount staining with HOXC8 and SHH antibodies was carried-out on embryos fixed in ice cold 4% paraformaldehyde for 4-12 hours. Embryos were washed thoroughly in PBS and blocked and bleached in PBS

with 10% goat serum (heat inactivated), 1% BSA and either 1% H₂O₂ for 15 minutes at room temperature (SHH) or 0.5% H₂O₂ overnight at 4°C. Embryos were then washed in PBT and incubated with the primary antibody (1:5 for HOXC8 and 1:500 for SHH) in PBT with 1% goat serum and 1% BSA overnight at 4°C plus 6 hours at room temperature. Embryos were washed in PBS with 1% goat serum and incubated with goat anti-mouse (1:500, HOXC8) or goat anti-rabbit (1:250, SHH) secondary antibodies in PBT with 1% goat serum overnight at 4°C plus 6 hours at room temperature. Embryos were then washed in PBS, pre-incubated for 1 hour in 0.5 mg/ml 3,3'-diaminobenzidine tetra hydrochloride (DAB, Sigma) at room temperature before color detection with activated DAB solution (containing 0.003% H₂O₂). The reaction was stopped with several rinses in PBS.

Whole-mount staining with antibodies against EN and HOXB5 was carried-out on embryos fixed in Dent's fixative (methanol:DMSO [4:1]) overnight at 4°C, then bleached in Dent's with 5% H₂O₂ for 5 hrs at room temperature. Embryos were stored in methanol at -20°C. Embryos were then rehydrated through a graded methanol series into PBS, transferred into PBS with 2% instant skim milk powder + 0.5% triton (PBSMT) and washed twice for 1 hour each. Primary antibody was added to PBSMT at a concentration of 1:500 (EN) or 1:200 (HOXB5) and embryos were incubated at 4°C overnight. Embryos were then washed in PBSMT five times and incubated with a goat anti-rabbit secondary antibody at a concentration of 1:200 (EN) or 1:500 (HOXB5) in PBSMT overnight at 4°C. Embryos were washed in PBSMT, rinsed in PBT with 2% BSA, and pre-incubated in 0.6 mg/ml DAB in PBT for 30 minutes. Color reaction was started by adding 0.03% H₂O₂ to fresh DAB solution, and was stopped with several washes in PBT.

Whole mount staining with the HOXC6 antibody was carried out on embryos fixed in Dent's fix for 1-2 hours at 4°C, then bleached in Dent's with 5% H₂O₂ for 24 hours at room temperature. Embryos were washed twice in tris buffered saline pH 7.4 (TBS: 0.01M tris + 0.1M MgCl) with 0.1% tween (TBST) before incubating with primary antibody (1:75) in TBST with 20% goat serum overnight at 4°C. Embryos were washed three time in TBS (1 hour each), and then incubated overnight at 4°C with the secondary antibody, goat anti-rabbit (1:500), in TBST with 20% goat serum. Embryos were washed three times (1 hour each) in TBS, pre-incubated in 0.5 mg/ml DAB in TBS for 30 minutes, and the reaction was carried-out by adding 0.02% H₂O₂ to the DAB solution. The reaction was stopped by washing in TBS.

Whole mount antibody staining with the DLX antibody was as follows. Embryos were fixed overnight at 4°C in a 1:3 mixture of 37% formaldehyde : fix buffer (fix buffer consisted of 1.33X PBS with 67mM EGTA). After washing 3 times in methanol, embryos were treated with 3% H₂O₂ in methanol for 5 minutes, and washed another 3 times in methanol. Embryos were stored at -20°C in methanol. Embryos were rehydrated through a graded methanol series into PBS, blocked in PBT with 2% BSA for 2 hours at 4°C, and incubated overnight at 4°C with primary antibody (1:36) in PBT with 2% BSA. After washing 10 times (12 minutes each) in PBT, embryos were incubated with secondary antibody, goat anti-rabbit (1:400), in PBT for 4 hours at 4°C. Embryos were washed as before and pre-incubated in 0.5 mg/ml DAB before the color reaction was started by adding 0.03% H₂O₂ to fresh DAB solution. The reaction was stopped with several rinses in PBT.

12b. Antibody staining frozen sections

Frozen sections were stained with antibodies against MSX, LMX1, FGF2, and EN using the Vectastain Elite ABC Kit (Vector Labs). Embryos

were fixed in 4% paraformaldehyde overnight at 4°C, washed in PBS, and equilibrated in 30% sucrose. Embryos were then embedded in OCT and placed in a -70°C freezer. Frozen blocks containing the embryos were mounted on studs and 10 µm sections were cut using a cryostat. Sections were collected on Superfrost slides (Fisher) and allowed to air dry. Sections were washed with PBS, bleached with 0.05% H₂O₂ in PBS, washed again and blocked in 5% horse (MSX and LMX1) or goat (FGF2 and EN) serum in PBT. Primary antibodies were added (MSX @ 1:4; LMX1 @ 1:30; FGF @, 1:400; EN @ 1:500) to PBT with 1% horse or goat serum (as above) and slides were left to incubate overnight in a humid, airtight box at 4°C. Slides were then washed with PBS and a biotinylated secondary antibody (horse anti-mouse for MSX and LMX1 and goat anti-rabbit for FGF2 and EN) was added according to the manufacturer's instructions. Slides were washed, incubated for 30 minutes in Vectastain ABC reagent, and washed again before pre-incubating them in DAB (0.5 mg/ml) for 5 minutes. Color reaction was carried-out by adding fresh DAB solution containing 0.006% H₂O₂ and the reaction was stopped with PBS. Slides were then washed in distilled H₂O, dried overnight, dehydrated through a graded ethanol series, immersed in histoclear twice (5 minutes each) and covered with Permount and a coverslip.

13. Nile Blue Sulphate staining

The pattern of cell death in python and chick limbs was visualized by staining with Nile Blue Sulphate. Limbs were dissected from embryos taken directly from the incubator, quickly rinsed in PBS that had been pre-warmed to the incubation temperature, and transferred to a pre-warmed solution of 1% Nile Blue Sulphate in a 35mm petri dish. The petri dish was immediately returned to the incubator for 2- 5 minutes, after which the limbs were rinsed in PBS and photographed.

CHAPTER THREE: FGF and Limb Initiation

1. Background

Although the molecular networks that operate in the limb bud have received much attention (see Chapter 1), very little is known about the molecular basis of limb bud initiation. A recent clue has emerged from work on chimeric mice combining wild type blastocysts or morulae with pluripotent embryonic stem (ES) cells which constitutively express FGF4. Overexpression of FGF4 leads to dramatic malformations in chimeric embryos, including reduction or deletion of the diencephalon and eyes, and development of multiple small limb bud structures from the flank (Abud *et al.*, 1996). The latter result suggested the possibility that FGFs may be involved in the initiation of limb budding. This chapter reports the results of experiments carried out in chick embryos to examine whether fibroblast growth factors are involved in initiation of limb development. The major finding is that FGF induces development of additional limbs. This discovery gave rise to a number of related questions that are presented in this chapter. Early development of additional limb buds was investigated to determine how a limb bud is established from flank cells and how signaling regions arise in the limb. Grafting experiments were performed to investigate the competence of flank cells to express *Shh*. In light of the ability of FGF to activate *Shh* in flank cells, the effects of direct application of SHH to the flank were assayed. Finally, FGF and SHH were applied simultaneously to determine whether this affected the anteroposterior polarity of additional limbs.

2. Results

2.1 FGF beads induce additional limbs in chick embryos

Beads soaked in FGF (-1, -2 or -4) and implanted in presumptive flank lead to the development of additional limbs (Figure 4A-F). A major set of experiments was carried-out with FGF2, in which FGF2 beads were placed at different levels along the primary body axis in the lateral plate mesoderm of chick embryos between stages 13 and 17. Stage 13 is well before there is any sign of limb development, and at stage 17 a slight thickening in the lateral plate mesoderm marks the place where buds will form. When beads are placed in lateral plate mesoderm opposite somites 20 to 26 (presumptive flank lies between somites 21 and 25), additional limbs developed in 35 out of 42 embryos (Table 1). Both complete wings (Fig. 4a) and complete legs (Fig. 4c) could develop from the flank (summarized in Table 1 and Fig. 4). The rib cage often appeared to be pushed together distally on the treated side, but vertebral identity was unchanged (Fig. 4c). When beads soaked in FGF2 were placed anterior to somite 15 in the neck region ($n = 4$), or in the tail bud ($n = 3$), no additional limbs were produced.

Application of FGF2 to the flank prior to stage 13 did not result in additional limb formation. Embryos treated between stages 10 to 12 ($n = 6$ cases) did not develop additional limbs, but the wing and leg were sometimes shifted along the body axis and appeared to be drawn together. Loss or fusion of limb elements, cleft neural arches, and rib fusions were also observed in these embryos. Ability of the flank to produce complete additional limbs lasts at least through stage 17, when wing and leg buds are present, but additional limbs could not be induced between stages 19 and 22 ($n=7$).

FGF1 and FGF4 beads applied to the flank of stage 13-16 embryos

also induced additional limbs, but the limbs were less complete than those induced by FGF2, in that they rarely developed digits. Beads soaked in FGF7 (also known as Keratinocyte Growth Factor or KGF) and applied to the flank of stage 14-16 embryos did not lead to the development of additional limbs ($n = 10$). Nine of 10 embryos receiving FGF7 beads developed normally; however, a single embryo developed with a duplicated pattern in the leg (duplicated fibula and digit pattern $x^a II\ I\ I\ II\ III\ IV$; x^a = unidentifiable digit).

Beads soaked in PBS and implanted at flank levels had no detectable effects on embryo development ($n = 4$).

2.2 Identity and morphological pattern of additional limbs

The nature of the limb that developed was related to the position at which the FGF bead was placed along the body axis (Table 1). When FGF beads were placed in the anterior part of the flank (opposite somites 21 and 22), 8 of the 9 limbs that developed were additional wings. FGF beads implanted to the mid-flank (opposite somite 23; $n = 9$) resulted in the development of either wings (5 cases) or legs (3 cases). The morphology of 2 remaining limbs was not unequivocally characteristic of either wings or leg and was therefore classified as "limb", and one embryo developed two ectopic limbs; an ectopic leg and an ectopic limb. FGF beads placed slightly more posteriorly (opposite somite 24) also resulted in the formation of either wings (3 cases) or legs (3 cases). However, FGF beads placed still more posteriorly in the flank (opposite somite 25) induced only legs (5 cases).

A few implants were made at levels where the wing and leg would normally form. Two of these resulted in additional limbs which articulated near the normal leg and appeared to contain proximal leg elements and

wing digits (Fig. 4b and e). Unexpectedly, one of the FGF beads placed at wing level induced an extra leg.

Only one of the additional limbs with digits had a normal antero-posterior polarity and four limbs developed with unidentifiable digits. In all other cases, the a-p axis was clearly reversed (18 of 23 cases; Fig. 4a-c, e and f). Fig. 4a shows a good example; the additional wing has a sequence of digits **432**, reading from anterior to posterior, which is reversed compared to the sequence of normal wing digits **234**. In Fig. 4c, the additional leg has a reversed sequence of toes **IV III II I**, compared to the normal leg pattern **I II III IV**.

Many of the limbs which developed wing digits following implantation of FGF beads in anterior or mid-flank (somites 20-23) also had an extra digit **3** inserted into the pattern (6 of 11 cases). This gave, for example, patterns such as **4332** reading anteriorly to posteriorly (Fig. 4b and f). Limbs with reversed polarity which resulted from FGF beads in the posterior flank never had extra digits (Fig. 4a and c). Additional limbs could be fused with the normal wing. Fig. 4f shows an example of such a fusion which produced a mirror-image digit pattern of **2344332**, with posterior digits in the middle. In some cases, forearm bones at the interface of the two limbs were fused into one wide element and posterior digits did not form (Fig. 4e).

In addition to causing ectopic limbs to develop, application of FGFs could cause the wing to shift posteriorly along the body axis (Fig. 4d). Occasionally wing and leg appeared to be drawn together, even when additional limbs did not form, and this could be accompanied by fusion of pelvic and shoulder girdles. FGF beads could also cause development of a single lateral outgrowth, extending from the anterior of the wing to the

posterior limit of the leg, rather than discrete limb buds. This led to development of a single outgrowth containing leg and wing skeletal elements. The skeletal pattern of these specimens was unlike that seen in bud fusions, in that proximal elements began as a single large bone which branched to give a humerus and a very wide femur. Similarly, the ulna and tibia began as one large bone which bifurcated at mid-shaft, but the radius and fibula appeared normal. There were no wing digits, but the foot was complete.

Histological analysis revealed the presence of muscles tendons and nerves in additional limbs, and the tendon pattern in the feet indicated that the dorsoventral axis is not reversed. Innervation of extra limbs was also examined in whole mount with the 3A10 antibody against neurofilament proteins. Although ectopic limbs contain nerves, the pattern of innervation is not complete. Interestingly, spinal axons which enter ectopic limbs do not originate from the same axial level as the limb, but instead they migrate along the trunk and into the limb from one or both of the normal plexi. Trunk nerves at the level of the extra limb undergo more branching on the side of the limb than those on the contralateral side, but they rarely enter the limb.

Table 1. Effects of beads soaked in FGF2 and implanted into the lateral plate mesoderm of chick embryos.

| Bead position (somite level) | ADDITIONAL LIMB DEVELOPMENT | | | | | | | | ADDITIONAL LIMB MORPHOLOGY | |
|---------------------------------|-----------------------------|--------------------------------------|------------------------------|-----------------------------------|--|---|--|-----------------------------------|-------------------------------------|--|
| | Total n | Normal (no ectopic limbs) n | Normal limb(s) shifted | Girdle structures only n | Additional wing structures n (n) ^a | Additional leg structures n (n) ^a | Additional limb structures n (n) ^a | Reversed digit pattern n | Duplicated digit pattern n | |
| 2 0 | 3 | 0 | 2 | 0 | 1 (0) | 1 (1) | 1 (1) | 1 | 1 | |
| 2 1 | 7 | 0 | 5 | 1 | 4 (3) | 1 (1) | 0 | 2 (1 ^b) | 1 | |
| 2 2 | 4 | 0 | 3 | 0 | 4 (4) | 0 | 0 | 4 | 3 | |
| 2 3 | 9 | 0 | 5 | 0 | 5 ^c (3) | 3 (2) | 2 ^c (0) | 3 | 1 | |
| 2 4 | 10 | 1 | 4 | 2 | 3 (1) | 3 (2) | 1 | 3 | 0 | |
| 2 5 | 7 | 0 | 0 | 2 | 0 | 5 (4) | 0 | 4 | 0 | |
| 2 6 | 2 | 1 | 1 | 0 | 1 (1) | 0 | 0 | 1 | 0 | |
| Flank Totals^d | 37 | 1 | 17 | 5 | 16 (11) | 12 (9) | 3 (0) | 16 (1b) | 5 | |
| Totals | 42 | 2 | 20 | 5 | 18 (12) | 13 (10) | 4 (1) | 18 (1b) | 6 | |

^a (n) = number of additional limbs with digits.

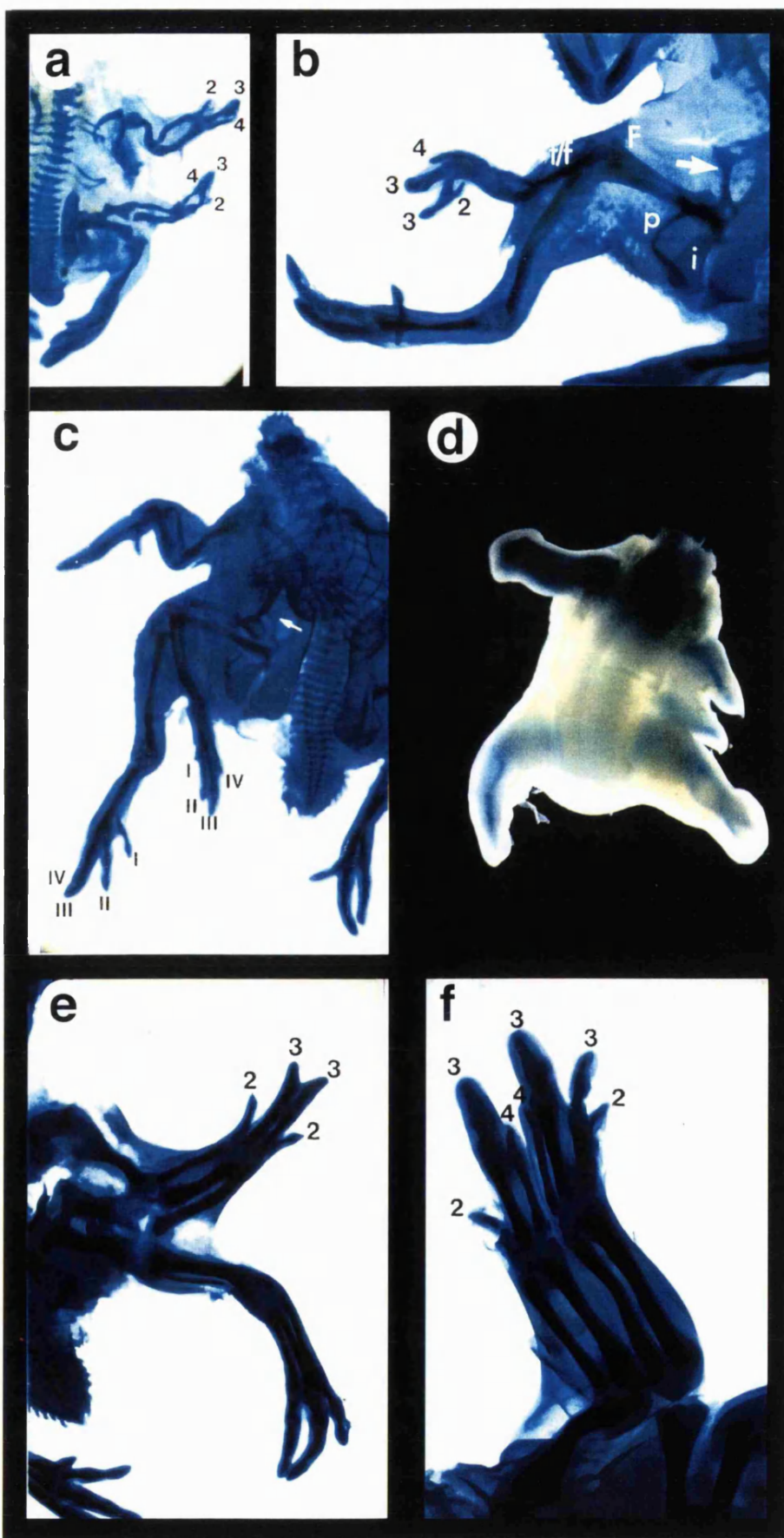
^b Polarity could not be determined

^c Embryo developed 2 extra limbs and is included in 2 categories.

^d Flank includes somites 21-25

Figure 4. Additional limbs produced by application of FGF2 beads to the flank

Whole-mount chick embryos stained with Alcian green to reveal skeletal patterns. **b, c, e** and **f** at 10 days of development. **a** at 9 days, and **d** at 6 days. Anterior at top of page, except in **f**. **a.** Additional wing that developed between normal wing and leg after implantation of a bead opposite somite 24 at stage 17. Note the reversed polarity of the digits, with a pattern of **432** compared to the normal wing pattern of **234**. Dorsal view. **b.** Additional limb that developed after implantation of an FGF2 bead opposite somite 20, at stage 14. The limb consists of proximal leg structures (femur [F], tibia and fibula [t/f]) with wing digits. Note reversed digit pattern, **4332**, with duplicated digit 3. Additional femur is anterior and articulates between the pubis (p) and an additional ischium (arrow). Normal ischium (i). Ventral view **c.** Additional leg that developed following bead implantation to the mid-flank, opposite somite 23 at stage 15, with digit pattern in reversed polarity (**IV III II I**). Digit **IV** is not complete. Note additional ischium (arrow), as in **b**. Ventral view. **d.** Embryo stained but not cleared 4 days after bead implantation opposite somite 21. The wing on the treated (right) side is truncated and appears to be shifted posteriorly along the body axis. The additional limb is also truncated. Dorsal view. **e.** Fusion of additional limb and normal wing following bead implantation opposite somite 26 at stage 13. The forearm of the fused limb consists of radius, ulna, radius and the digit pattern is **2332**. Note absence of digit 4 and single ulna. Dorsal view. **f.** Fusion of additional wing and normal wing following bead implantation opposite somite 23 at stage 14. The normal wing, with digit pattern of **234**, is connected by soft tissue to the additional wing, which has a reversed sequence of digits in a pattern of **4332**. Proximally there is a double set of skeletal elements. Anterior is to the left; dorsal view.



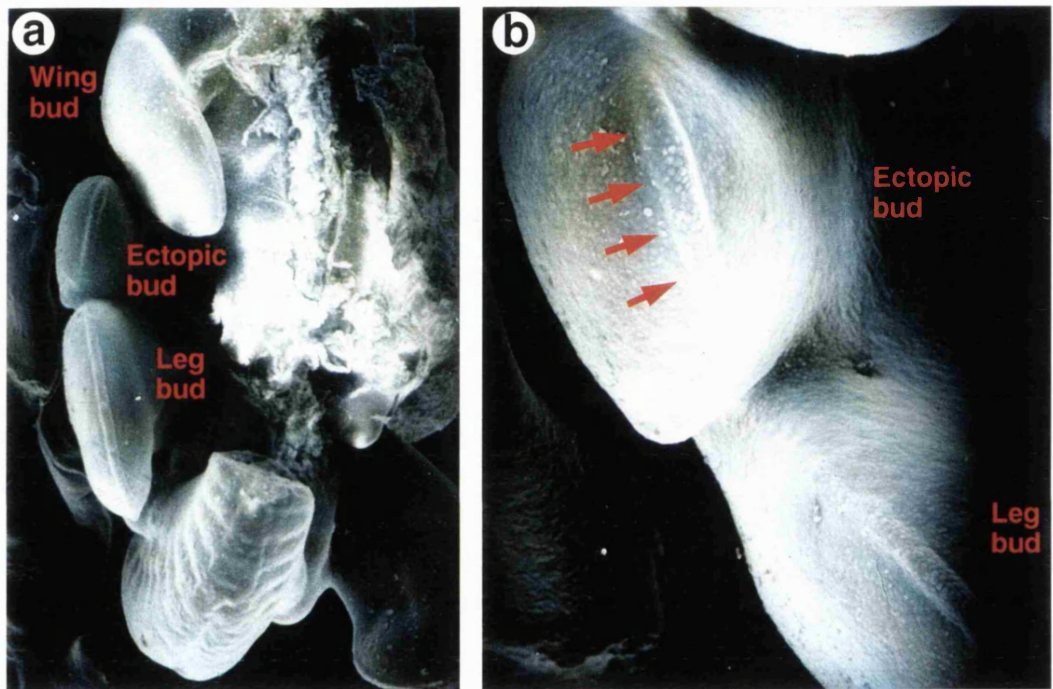
2.3 Early development of additional buds

By 24 hours after insertion of an FGF2 bead in the flank, a small swelling was seen adjacent to the bead. By 48 hours, an additional limb bud was present between wing and leg buds (Fig. 5a and b). Initial formation of additional limb buds was slightly delayed in comparison to normal limb buds, and this is why additional buds often appeared smaller than the normal buds (Fig. 5a). The bud was capped with a well-developed apical ectodermal ridge (Fig. 5a and b). At this time, the bead could be found proximal to the bud.

The shape of additional limb buds was variable. Comparison of limb bud shape 48-72 hours after FGF treatment with the skeletal pattern of the additional limb at 10 days revealed that normal-shaped buds developed into complete limbs, while very narrow buds gave rise to truncated limbs. In some embryos, as the extra bud continued to grow, the original wing bud remained small and often took on an abnormal, pointed shape. These buds lagged behind the extra bud and the leg bud, and resulted in truncated wings often consisting of only a humerus or a humerus and radius. Occasionally, the additional limb bud was fused with the wing bud, and the types of patterns seen in Fig. 4e and f were obtained.

Figure 5. Scanning electron micrograph of embryo with ectopic limb bud 48 hours after bead implantation

Ventral view. **a.** Low power view showing position of ectopic bud between wing bud and leg bud. Thickened apical ridge on ectopic bud marked by arrows. Note tail posteriorly. **b.** High power view of ectopic bud (upper bud) showing apical ectodermal ridge (arrows). Compare with ridge of leg bud at bottom right.



2.4 FGF acts within two hours

A series of experiments was performed in which FGF2 beads were implanted in the flank and the embryo was reincubated for a fixed time, at which point the FGF bead was removed from the tissue through a small slit made with a tungsten needle. The embryo was then reincubated to embryonic day 10. Removal of the FGF bead as early as 2 hours after implantation, at stage 14/15, did not interfere with bud outgrowth, and the bud went on to develop into an additional limb. One interpretation of this is that a brief exposure to FGF sets in train a cascade of gene expression which results in limb formation. Alternatively, FGF could be sequestered in the extracellular matrix and act after the bead has been removed.

To further investigate the distance and time over which FGF acts, digoxigenin-tagged FGF2 was used to allow detection of the protein *in vivo* by immunochemistry with an antibody against digoxigenin. Beads soaked in 0.25 mg/ml Dig-FGF2 induced development of additional limb buds ($n=3$). Embryos fixed for Dig antibody staining between 1:30 and 43 hours after implantation of Dig-FGF2 beads to the flank showed intense staining on the surface of the bead ($n=7/7$). Six of 7 embryos showed Dig staining on surrounding cells up to 5-6 μm from the bead (Figs. 6a and b). The remaining embryo (fixed at 27 hours) showed diffuse rather than localized staining. Diffuse staining also resulted when beads were implanted deeper in the lateral plate so that they came to lie in the coelom ($n=2$, Fig. 6c). This may be due to the bead not being embedded in tissue, but being wedged into a space, which would facilitate free diffusion wherever the bead is not in contact with tissue.

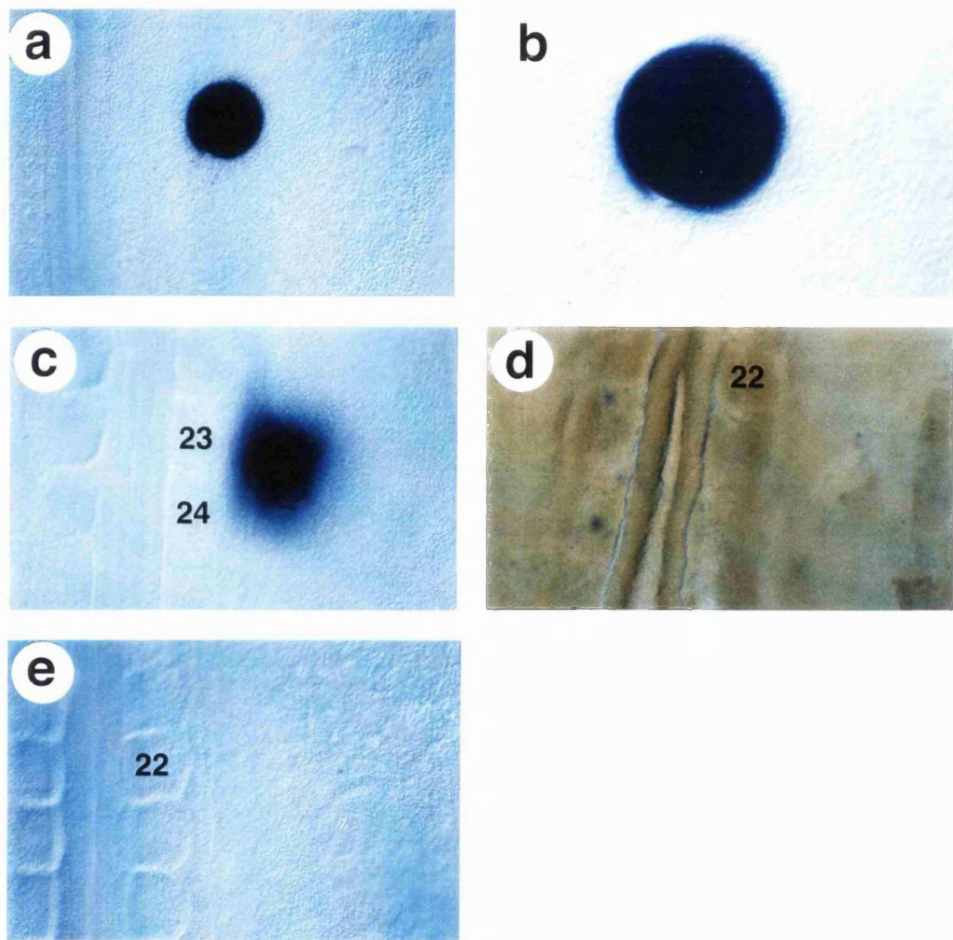
To determine whether FGF could still be detected after removal of the bead from the flank, Dig-FGF beads were implanted in the flank

somatopleure and embryos were reincubated for either 1.6 or 2 hrs, at which point the bead was removed and the embryo was fixed immediately for antibody staining. In 3 of 3 cases, no staining could be detected in the tissue after removal of the Dig-FGF bead (Fig. 6d). These specimens were processed with embryos in which the bead was left in place, and positive staining in the latter served as an internal control. The absence of detectable FGF in the flank after removal of the bead suggests that FGF acts on the flank cells within the 2 hour exposure period.

These results suggest that brief exposure to a local FGF signal is sufficient to induce limbs. To test whether a local source of FGF is necessary, Dig-FGF2 colored with fast green was microinjected into the somatopleure of the flank. Stage 15 embryos were injected with Dig-FGF2/fast green opposite somite 23 (n=2) or 24 (n=3), reincubated, and fixed at 2.5, 3.5 or 72 hours for antibody staining. At 72 hours embryos had not developed ectopic limbs (n=2), and Dig-FGF2 could not be detected by antibody staining. Embryos fixed and stained at 2.5 and 3.5 hours were also negative for Dig-FGF (n=3, Fig. 6e). To determine whether fast green interferes with activity or detectability of Dig-FGF2, fast green-treated Dig-FGF2 was loaded onto heparin beads and applied to the flank. Additional limb buds developed and Dig-FGF2 could be detected immunochemically in all cases (n=3). Thus, microinjection of FGF is not sufficient to induce ectopic limbs and no FGF can be detected in the targeted tissue, suggesting that when FGF is injected (rather than presented localized on a bead surface) it appears to dissipate in the tissue.

Figure 6. Distribution of Digoxigenin-tagged FGF2 after application to the chick flank

Dorsal views. **a.** Dig staining 2 hours after a bead soaked in Dig-FGF2 was applied to the flank of a stage 13 chick embryo. Note absence of stain in tissue surrounding the bead. **b.** High power view of the bead shown in panel **a** indicates that FGF is limited to the surface of the bead and cells immediately around the bead. **c.** Dig staining 1.6 hrs after Dig-FGF bead was implanted into the coelomic cavity of the flank at the level of somites 23 and 24. Note that FGF can be detected much further from this bead compared to that shown in **a** and **b**. **d.** Embryo in which a Dig-FGF bead was implanted opposite somite 22, and removed after 2 hours via a small slit made opposite somite 23. This specimen was immediately fixed and probed with the anti-Dig antibody. Staining is absent. **e.** Embryo 3.5 hours after Dig-FGF2 was microinjected opposite somite 22. Staining is absent.

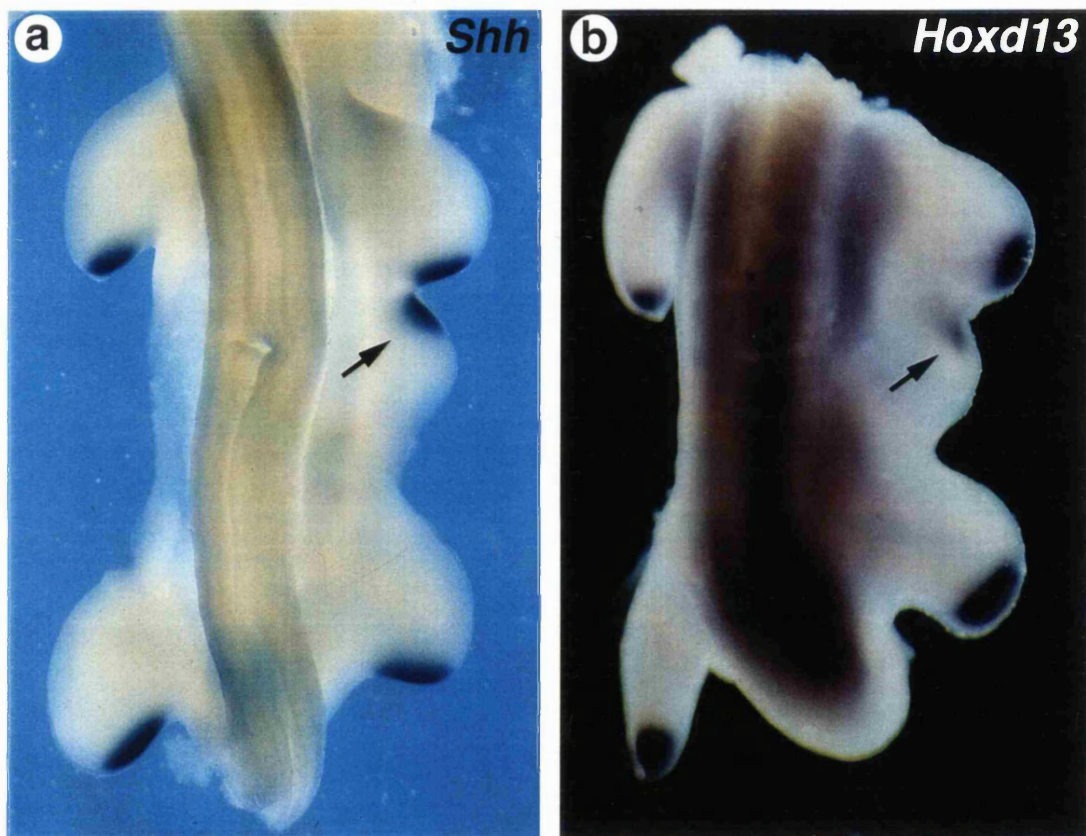


2.5 Molecular polarity of early buds

Polarity of early limb buds was investigated by looking at expression of 2 genes, *Sonic hedgehog* and *Hoxd-13*, which are normally expressed posteriorly. Whole mount *in situ* hybridization was carried out between 4 and 48 hours after FGF2 bead implantation. The first run of *in situ*s for *Shh* was carried out by Juan Carlos Izpisúa-Belmonte on embryos manipulated by me, and all subsequent runs were carried out by me. The earliest time at which *Shh* transcripts could be detected in the flank is 24 hours after FGF bead implantation (1 of 2 cases). All embryos examined from 25.5 to 48 hours after FGF bead implantation were positive for *Shh* in the additional bud ($n = 10$; Fig. 7a). *Shh* transcripts could not be detected in the flank of any of the embryos examined between 4 and 23.5 hours after bead implantation ($n = 6$), nor in the second embryo examined at 24 hours. *Shh* expression in the notochord was used as a control, and each specimen was positive for *Shh* in the notochord. Similarly, low levels of *Hoxd-13* expression could be detected in the flank at 24 hours after application of FGF (1 of 2 cases). At 48 hours after FGF2 application, additional limb buds had been established and an ectopic domain of *Hoxd-13* expression was clearly seen in addition to the ectopic *Shh* expression domain ($n = 3$; Fig. 7). Transcripts of both genes were restricted to the anterior margin of the additional limb buds, which is opposite to normal buds in which these genes are expressed posteriorly. Thus, additional limb buds are established with the molecular polarity reversed in the anteroposterior axis.

Figure 7: *Sonic hedgehog* and *Hoxd13* are expressed in additional limb buds

Distribution of *Hoxd-13* (**a**) and *Sonic hedgehog* (**b**) transcripts in whole-mount preparations of embryos with additional limb buds 48 hours after FGF2 bead implantation. Regions to which the probes have hybridized are stained purple. Expression of *Hoxd-13* and *Sonic hedgehog* is restricted to the posterior margin of the normal wing and leg buds, but is found anteriorly (arrows) in the additional limb buds.



2.6 Competence of flank cells to express *Shh*

Activation of *Shh* in flank cells indicates that although these cells do not normally express *Shh*, they have the potential to do so when presented with FGF. Activation of *Shh* only at the anterior margin of ectopic limbs, although the entire bud is rimmed by an apical ridge, suggests that competence to express *Shh* is not uniformly distributed throughout the flank. Consistent with this idea is the observation that when cells taken from different positions along the anteroposterior axis of the prospective flank are grafted to the anterior margin of a wing bud, anterior cells have higher polarizing activity than do posterior cells (Hornbruch and Wolpert, 1991). To determine whether these results reflect differential competence to express *Shh*, flank somatic mesenchyme from different axial levels ranging from somites 21-25 was taken from stage 17 embryos and transplanted under the anterior apical ridge of stage 20 wing buds. Embryo receiving grafts were assayed for *Shh* expression by *in situ* hybridization between 12 and 27 hours after transplantation. *Shh* could not be detected in grafted tissue from any position prior to 21.5 hours, although in all cases a normal pattern of *Shh* expression was detected in the host ($n=3$). *Shh* expression is activated in flank tissue in a graded fashion, with anterior flank cells being capable of expressing higher levels of *Shh* than posterior cells, between 21.5 to 27 hours. Thus, when flank tissue opposite somite 21 was grafted under the apical ridge of a host limb, strong *Shh* expression ^{was} detected in the graft (2 of 4 cases, the remaining 2 grafts were completely negative; Fig. 8a). Flank tissue opposite somite 22 also expressed high levels of *Shh* (2 of 2 cases, Fig. 8b). In contrast, when tissue opposite somite 23 was grafted to a host wing, considerably lower levels of *Shh* were observed in the graft ($n=1$, Fig. 8c). At similar time points, *Shh* expression was barely detectable in grafts of flank tissue originating opposite somite 24, and then only in cells immediately under the apical ridge ($n=1$, Fig. 8d). Tissue grafted from

opposite somite 25 also failed to activate *Shh* (n=2, Fig. 8e).

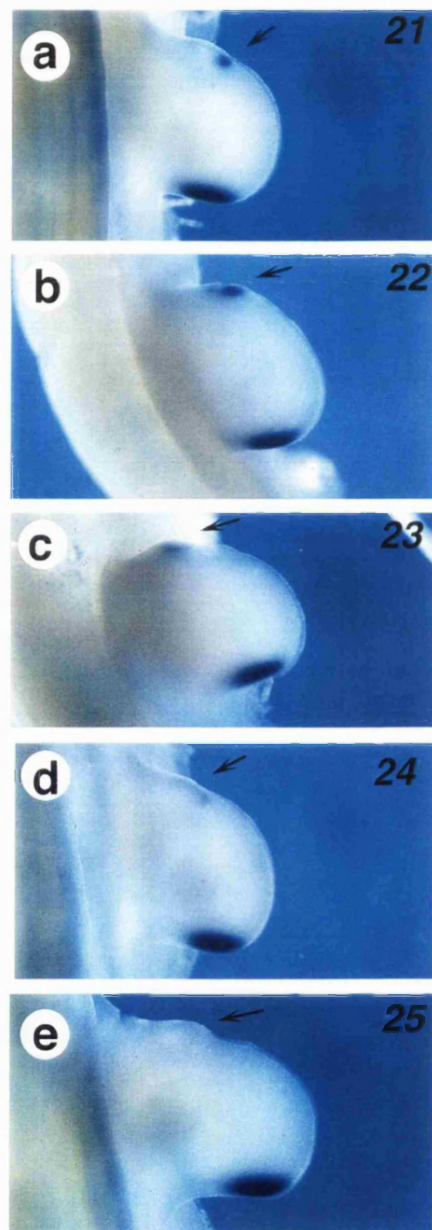
To compare directly these results with polarizing potential as demonstrated by Hornbruch and Wolpert (1991), two embryos which received grafts of flank opposite somite 22 and 25 were allowed to develop to E10. Analysis of the skeletal pattern of these embryos showed that flank cells from opposite somite 22 induced a digit pattern **433234**, reading from anterior to posterior, and cells originating opposite somite 25 induced **2234** pattern of digits. These results indicate that the potential to express *Shh* is distributed in an anterior to posterior gradient in the flank, consistent with the graded distribution of polarizing potential.

Figure 8. Activation of *Shh* in flank cells transplanted under the apical ridge

Lateral plate mesoderm (LPM) transplanted from different positions in the flank to the anterior margin of a chick wing, under the apical ridge, were assayed for expression of *Shh*. Axial level was determined using the somites (parax = paraxial mesoderm) as landmarks. Anterior is at the top of the page. Arrows indicate position of graft in limb. Strong *Shh* expression is detected in flank cells grafted from LPM opposite somites 21 (**a**) and 22 (**b**). **c.** *Shh* expression is also detected in flank cells grafted from LPM opposite somite 23, but expression appears weaker than that seen in **a** and **b**. **d.** Very weak *Shh* expression is detected in flank cells grafted from LPM opposite somite 24. **e.** Flank cells grafted from LPM opposite somite 25 do not express *Shh*.

Parax LPM

| | |
|----|--|
| 21 | |
| 22 | |
| 23 | |
| 24 | |
| 25 | |



2.7 Application of SHH to the flank

Establishment of a polarizing region is a key step in limb development. Application of SHH to the anterior of established limb buds induces anterior expansion of the *Fgf4* and *Fgf8* expression domains in the overlying ectoderm, and reproduces the positive feedback loop between the polarizing and the apical ridge (Laufer *et al.*, 1994, Niswander *et al.*, 1994, Ohuchi *et al.*, 1997) The above results (also see introduction) show that application of FGF to the flank activates *Shh* in the flank. In order to determine whether activation of *Shh* in the flank is sufficient to induce ectopic limb formation, SHH protein was applied directly to the flank of chick embryos between stages 14 and 17. Application of SHH beads to the flank of chick embryos did not result in formation of additional limbs (n=18; Table 2). SHH beads were applied at different positions in the flank between somites 22 and 25, as well as opposite somite 26 in the prospective leg. Forty-eight hours after application of SHH to the flank, a small thickening of flank cells could be seen lateral to the bead, which is consistent with the proposed mitogenic effect of SHH on mesenchymal cells (Fan and Tessier-Lavigne, 1994) (Fig. 10c). Although application of SHH did not induce additional limb development, irrespective of the position at which it was applied, several aspects of normal limb development were affected. Malformations of shoulder and pelvic girdles were observed, including shortened scapula (Fig. 9a), anteriorly or medio-laterally expanded ilium, thickened ischium, and fused pubis, ischium, and ilium (n=6; Fig. 9b). In one case in which the entire innominate was fused, the leg was completely absent (Fig. 9B). Rib malformations also resulted. Ribs with distal bifurcations were observed in 7 of 18 embryos, and ectopic ribs were observed in 3 embryos (Table 2; Fig. 9c, d).

When SHH was applied the posterior flank, opposite somite 24 or 25,

or to the anterior of the prospective leg bud, opposite somite 26, the leg could develop with duplicated digits ($n=2$; Table 2; Fig. 10a and b). Application of SHH to the anterior margin of the chick wing results in anterior extension of the apical ridge and *Fgf8* expression (Ohuchi et al., 1997). In order to determine whether application of SHH to the flank could extend the apical ridge of the leg bud, *Fgf8* expression was examined by *in situ* hybridization 48 hours after application of SHH to the posterior flank. Application of SHH opposite somite 25 resulted in anterior extension of *Fgf8* expression in the leg bud and a separate domain of weak expression in the flank (Fig. 10c, d). *Ptc* expression was also localized to the flank cells around the bead, but surprisingly, ectopic *Ptc* transcripts could not be detected in the leg (Fig. 10c). Thus, SHH alone can induce expression of *Fgf8* in flank ectoderm and local proliferation of flank cells, but this is not sufficient to induce additional limb development.

2.8 Application of FGF2 and SHH to the flank

Establishment of a polarizing region is necessary for outgrowth and patterning of the limb, and the position of the polarizing region dictates limb polarity. In order to determine whether application of SHH to the posterior flank could affect the a-p polarity of the extra limb, FGF2 was applied to the posterior flank and at the same time mSHH198 beads were implanted adjacent to the FGF beads (Table 2B). When FGF beads alone are placed opposite somites 24 and 25, additional limbs develop in 12 of 17 cases (Table 2). When SHH beads alone are placed opposite somites 23 and 24, no additional limbs develop in 10 of 11 cases, and the remaining embryo develops a leg with duplicated digits. However, when both SHH beads and FGF beads were implanted simultaneously, so that the SHH and FGF beads were opposite 23 and 24 respectively or 24 and 25 respectively, 4 of 5 embryos developed with a pattern duplications in the leg. The digit patterns

were II-I-I-II-III-IV and III-III-II-II-III IV (anterior to posterior), and 2 embryos had duplicated fibulae (Fig. 10*e*). Thus, simultaneous application of FGF and SHH appears to interfere with the limb inducing activity of FGF, and instead results in leg duplications. An additional limb (a leg) developed in only 1 of 5 cases (Table 2B), and surprisingly, the additional leg still had a reversed pattern of digits. When SHH was added to the posterior flank 24 hours after FGF application, only one of 4 embryos had a duplicated leg, and the remaining 3 embryos developed additional legs, all with reversed polarity (Table 2B). These results suggest that, during normal development, expression of SHH defines a boundary which spatially limits the extent of cells that can participate in limb bud formation. Thus, the position of the Shh domain initially defines the posterior edge of the limb bud, and controls the anteroposterior pattern of elements that develop within the bud.

Table 2. Effects of mSHH198 beads applied to lateral plate mesoderm of chick embryos*

A. mSHH198

| Somite position | n | Normal | Duplicated leg | Bifid ribs | Ectopic ribs | Malformed girdle |
|-----------------|-----------|----------|----------------|------------|--------------|------------------|
| 22 | 2 | 1 | 0 | 0 | 0 | 1 |
| 23 | 6 | 1 | 0 | 5 | 1 | 1 |
| 24 | 5 | 1 | 1 | 1 | 1 | 2 |
| 25 | 2 | 0 | 1 | 1 | 1 | 1 |
| 26 (leg) | 3 | 1 | 2 | 0 | 0 | 1 |
| Totals | 18 | 4 | 4 | 7 | 3 | 6 |

*embryos may be included in more than 1 category

B. mSHH198 + FGF2

Effects of mSHH198 and FGF2 beads applied to flank mesoderm

| <u>Protein</u> | <u>somite level</u> | <u>n</u> | <u>Additional limb</u> | <u>Duplicated leg</u> |
|-------------------------|---------------------|----------|------------------------|-----------------------|
| mSHH 198 | 23 | 6 | 0 | 0 |
| | 24 | 5 | 0 | 1 |
| | 25 | 2 | 0 | 1 |
| FGF2 | 23 | 9 | 9 | 0 |
| | 24 | 10 | 7 | 0 |
| | 25 | 7 | 5 | 0 |
| mSHH 198 | 23/24 | | | |
| + | + | 5 | 1 | 4 |
| FGF2 | 24/25 | | | |
| FGF + | 23/24 | 2 | 2 | 0 |
| mSHH 24 hr later | + | | | |
| | 24/25 | 2 | 1/2 | 1/2 |

Figure 9. Skeletal malformations induced by application of SHH protein to the flank

Ten day chick embryos stained with Alcian green and cleared to reveal the skeletal pattern. **a.** Application of SHH to flank opposite somite 23 at stage 14 resulted in development of a shortened scapula on the treated (right) side compared to the untreated (left) side (red arrows). **b.** Application of SHH opposite somite 24 at stage 15 resulted in severe malformation of the innominate and loss of the leg on the treated side. **c.** High power view of the embryo showed in **a**, showing severe malformation of the ribs, including bifurcation, fusion, and truncation. One additional rib has also developed on the treated side, resulting in 9 ribs on the right and 8 ribs on the left. **d.** Disorganization of the ribs resulting from application of SHH opposite somite 23 at stage 16.

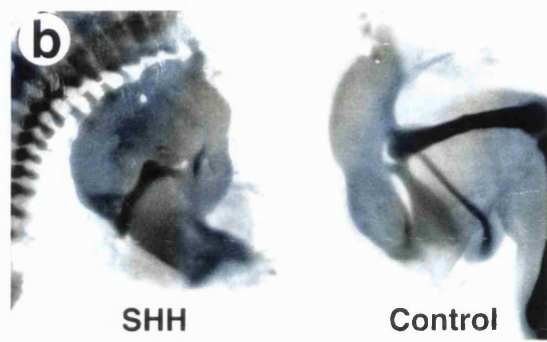
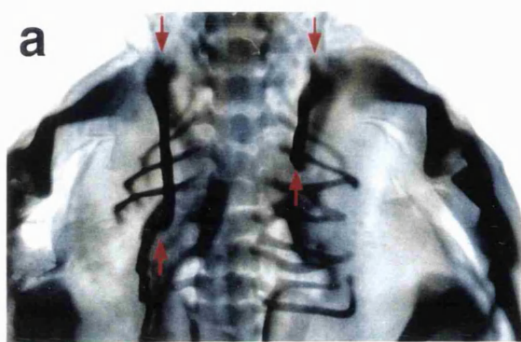
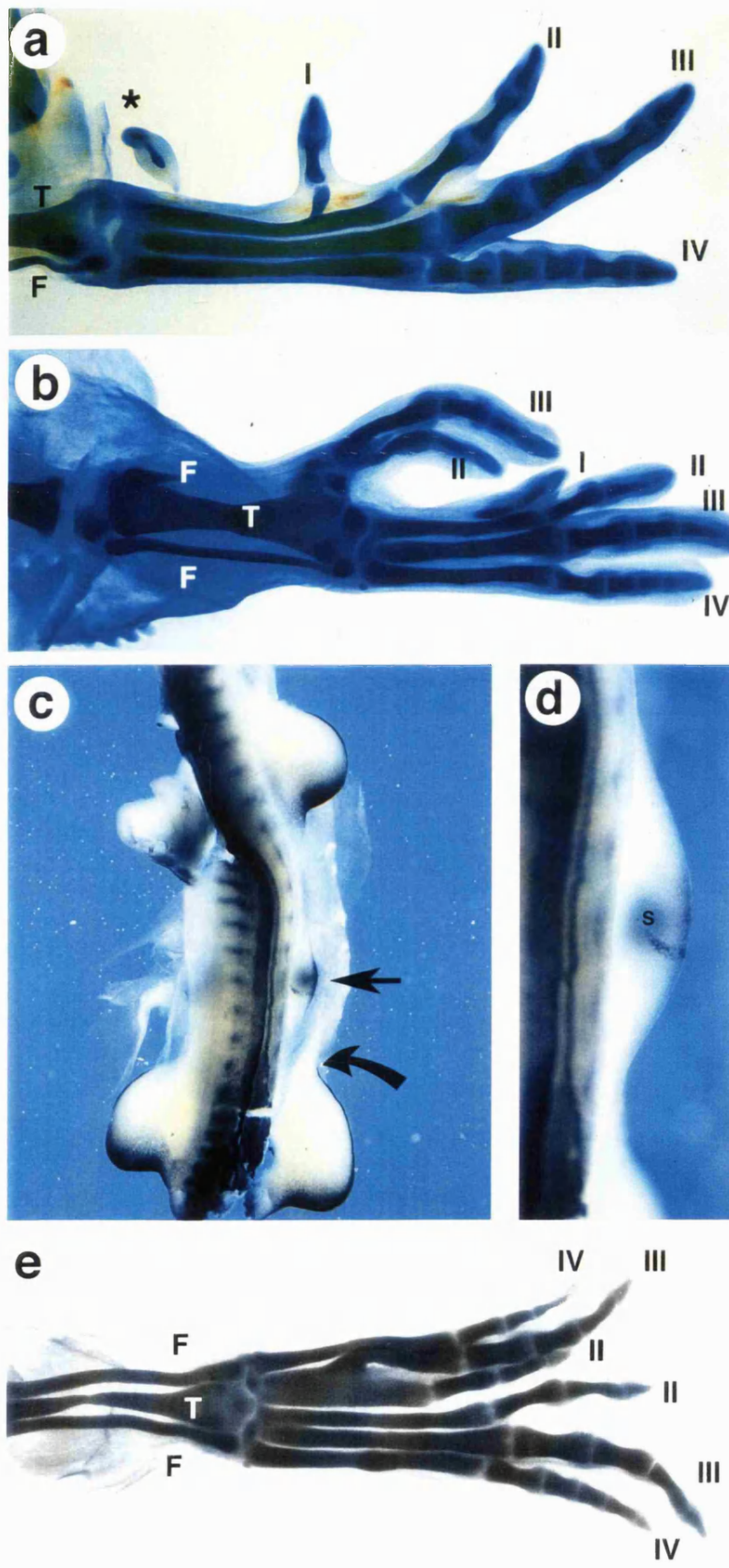


Figure 10. Application of SHH beads to posterior flank alters patterning of the leg

Anterior is at top of page. **a, b** and **e** are 10 day embryos stained with Alcian green. The embryo shown in **c** and **d** was fixed 48 hours after SHH application opposite somite 25. **a.** Application of SHH opposite somite 25 at stage 15 resulted in development of a small extra digit (*) anterior to digit I in the foot. The identity of this digit is unclear, although the number of phalanges suggests that it may be an extra digit I. **b.** Application of SHH opposite somite 24 at stage 15 resulted in duplication of digit III and digit II, and the proximal fibula (F). **c, d.** Image shown in **d** is a high power view of embryo shown in **c**. Forty-eight hours after application of SHH opposite somite 25, a small bud had formed in the flank (straight arrow). *Fgf8* expression was detected in flank ectoderm over the bud, and *Ptc* expression was detected around the SHH bead (S). *Fgf8* expression in the apical ridge of the leg bud extends further anteriorly on the treated side (curved arrow in **c**) than on the untreated (left) side. **d.** Simultaneous application of a FGF bead opposite somite 25 and a SHH bead opposite somite 24 at stage 15 resulted in a severely duplicated pattern in the foot. A complete extra fibula and duplicated digits IV, III and II are seen anterior to the normal structures. Digit I has been eliminated from the pattern.

Roman numerals = digit identity, T = tibia, F = fibula and S = SHH bead.



3. Discussion

Local application of FGF protein to the flank of the chick embryo initiates development of a limb bud which establishes a new axis of proximo-distal outgrowth and can develop autonomously into a complete limb. Limb identity is determined by position of the FGF bead, with anteriorly placed beads inducing mostly wings and posteriorly placed beads inducing mostly legs. Additional limbs have reversed anteroposterior polarity and mesenchyme cells in the anterior flank are competent to express high levels of *Shh*, which determines the anterior position of the polarizing region. A brief exposure to FGF is sufficient to induce limb formation, and FGF acts very locally rather than long-range. Although FGF induces Shh expression in the flank, application of SHH alone does not initiate limb development. SHH does, however, appear to define the anteroposterior limit of the limb bud, and application of SHH adjacent to the anterior edge of the FGF bead inhibits formation of a discrete limb bud, and results in an anteroposteriorly compressed outgrowth that becomes entrained into the leg. These results suggest that local production of a fibroblast growth factor determines limb position along the body axis, the type of limb that forms depends on position of the initiation signal, and the same signal can induce both wings and legs.

3.1 Initiation of a Limb by Application of FGF

Application of FGF elicits limb formation from the flank in chick embryos. Thus the flank has a limb forming potential that is normally not realized. Constitutive FGF4 expression in chimeric mice also stimulates limb bud outgrowth from the flank (Abud *et al.*, 1996). Fibroblast growth factors can promote proliferation of limb mesenchyme cells (Niswander and Martin, 1993), and FGF could act to maintain cell proliferation in the region where limb buds will form (see Searls and Janners, 1971). However, the fact that SHH can induce cell proliferation and expression of *Fgf8* yet no limb forms

suggests that cell proliferation is not enough, and the character of the flank cells must somehow be changed to limb. Additional limbs developed even when the FGF bead was removed as early as two hours after bead implantation, and 22-23 hours prior to activation of *Shh*. The late response of *Shh* to FGF suggests that intermediate steps are involved and *Shh* is not directly activated by the FGF bead. When Dig-labelled FGF is used in bead removal experiments, labelled protein could not be detected in the embryo after the bead was removed. It is therefore unlikely that in these experiments FGF released from the bead could be sequestered in the extracellular matrix (Klagsbrun and Baird, 1991) and act after the bead has been removed. A more likely hypothesis is that FGF acts within two hours to induce a cascade of gene expression in flank cells, and, at least between 2 hours (when the bead is removed) and 17 hours (when endogenous *Fgf10* is induced [Ohuchi et al., 1997]) this pathway is not dependent on continuous presence of FGF. Moreover, the cascade must be initiated by a very small group of cells, as the effect of the FGF bead is very short-range, on the cells immediately surrounding the bead.

3.2 Reversed Polarity of the Additional Limbs

A striking feature of additional limbs is that they almost always have a reversed antero-posterior polarity. In ectopic buds, *Shh* and *Hoxd-13* expression is found at the anterior margin (the reverse of the normal limb) and this correlates with the reversed pattern of digits. Occasionally, the ectopic bud is fused with the normal wing bud and these develop into limbs which have a mirror-image pattern of digits, with posterior digits in the middle. This pattern is consistent with signaling from a shared polarizing region.

The results in this chapter show that *Sonic hedgehog*, although not

normally expressed in the flank, can be activated in flank cells with potential polarizing activity. Previous grafting experiments have shown that potential for polarizing activity extends from the posterior of the prospective wing bud to cells in the posterior flank in chick embryos, but the intensity of polarizing potential appears to be distributed in a gradient that is highest anteriorly (Hornbruch and Wolpert, 1991). Although this activity normally remains dormant in the flank, the cells can produce a polarizing region signal and induce digit duplications when transplanted to a wing bud. Grafting flank cells under the apical ridge results in activation of *Shh* in the graft within 22 hours. Similarly, transcripts first appear as the extra limb bud begins to emerge around 24 hours after bead implantation. The graded potential of flank cells to activate *Shh* correlates with polarizing activity demonstrated by Hornbruch and Wolpert (1991), and this explains the anterior position of the polarizing region in ectopic buds. Although cells at the posterior limit of the flank have very weak polarizing activity, they do not appear ^{to} switch on *Shh* (or at least there is no detectable *Shh*) when grafted under the ridge. Polarizing activity in these cells may be mediated by signals downstream of *Shh*, such as *Bmp2*, which has been shown experimentally to be able to activate *Fgf4* and *Hoxd13* and induce formation of digit 2 independent of *Shh* (Duprez *et al.*, 1996). Buds that develop when FGF is applied to anterior flank often have additional digit 3's, although only a discrete region expressing *Shh* is induced. The slope of the gradient of potential polarizing activity is shallow in anterior flank (Hornbruch and Wolpert, 1991) and therefore, cells next to *Shh*-expressing cells could have weak polarizing activity which specifies the additional digit(s).

3.3 Establishment of the polarizing region

It seems likely that cells with highest potential polarizing activity are induced by FGF to express *Shh* and form a polarizing region. During normal

development, cells with this potential lie at the posterior edge of the region that normally forms the limb bud, and activation of *Shh* in these cells leads to development of a discrete polarizing region. Charite *et al.* (1994) have shown that anterior extension of the *Hoxb8* domain in transgenic mice, so that it is expressed throughout the early forelimb bud, results in ectopic *Shh* at the anterior margin of the forelimb bud. *Hoxb8* and potential polarizing activity are coextensive in the flank (Lu *et al.*, 1997, Stratford *et al.*, 1997), creating a situation in the flank that is similar to that seen in the forelimb of the transgenic mouse; i.e., expression of *Hoxb8* throughout the bud. In both the forelimb of the transgenic mouse and the ectopic limb of the chick flank, *Shh* is activated in a discrete domain. How does a discrete domain of *Shh* expression form in limb buds which express *Hoxb8* throughout? In slightly older limb buds, both retinoic acid and FGF are required for ectopic activation of *Shh* (Niswander *et al.*, 1994), and retinoic acid appears to induce polarizing activity by induction of *Hoxb8* (Stratford *et al.*, 1997; Lu *et al.*, 1997). An attractive hypothesis is that retinoids induce polarizing potential through *Hoxb8*, and FGF allows this potential to be realized. The domain of *Shh* expression may be defined in response to different threshold levels of FGF8 and HOXB8 protein, such that in the presence of *Hoxb8*, an appropriate concentration of FGF can switch on *Shh*. In essence, the range of FGF diffusion determines the location of the *Shh* domain. Consistent with this idea, Stratford *et al.* (1997) have shown that high levels of FGF inhibit transcription of *Hoxb8*. Thus, *Shh* transcription would be induced in *Hoxb8* expressing cells exposed ^{to} _^ FGF8, as long as the concentration of FGF8 remains below the threshold that inhibits *Hoxb8*. The *Shh* domain would end at the position where FGF has diffused below the minimum concentration required for *Shh* expression. This hypothesis can account for expression in a discrete patch at the edge of the apical ridge, rather than adjacent to or a distance from the ridge, in normal, ectopic and duplicated

limbs.

The ability of SHH to modulate the limb-inducing ability of FGF is curious. The apposition of *Shh* and *Fgf* domains at multiple sites in the embryo (Bueno *et al.*, 1996) such as the posterior limb bud, suggests that *Shh* may limit the extent of FGF. One possibility is that high levels of SHH inhibit *Fgf* expression (which would keep FGF below levels which inhibit *Shh* expression). If the above hypothesis is correct, then duplication of the leg, rather than an ectopic limb, may arise when SHH and FGF are applied together because SHH inhibits activation of *Fgf8* in the flank ectoderm anterior to the SHH bead. As a result, the flank cells posterior to the FGF bead may be entrained into the normal leg, and polarized by the SHH bead. Under these conditions, it may not be necessary to reprogram the flank cells to take on a limb identity, as other work has shown that flank cells can participate in limb development when mixed with normal limb cells (Dhouailly and Kieny, 1972). The occasional appearance of duplicated legs resulting from application of SHH alone to posterior flank may be a consequence of SHH respecifying pre-bud mesenchyme. The lack of *Ptc* expression in anterior leg is probably due to SHH acting on the leg at much earlier stages, or transcript levels being below the level of detection.

It has been proposed that a polarizing region signal and a fibroblast growth factor cooperate to establish a progress zone (Niswander *et al.*, 1993). Once a polarizing region has been established in the presumptive limb, mesenchyme cells under the influence of FGF will form a progress zone. Grafts of *Shh*- or *Bmp2*-expressing cells to the normal limb bud can induce *Hoxd-13* expression in the progress zone (Riddle *et al.*, 1993; Duprez *et al.*, 1996). Thus, activation of the *Shh* pathway could lead to activation of *Hoxd* genes in the presence of FGF.

3.4 Which FGF member initiates limb development in the normal embryo?

This work shows that at least 3 members of the FGF family can induce limb development from the flank. Although FGF1, FGF2 and FGF4 are able to elicit bud formation, none of these are likely to be the signal that normally initiates limb development. *Fgf4* transcripts can only be detected in the limb once a bud is formed, and although expression in the dermamyotome is detectable at the time of limb bud initiation, it is not localized to limb levels (Niswander and Martin, 1992). FGF2 protein has been detected in limb and flank cells (Dono and Zeller, 1994, Savage *et al.*, 1993), yet no additional limbs develop from the flank, suggesting that endogenous FGF2 is not a probable candidate. *Fgf1* also lacks a known signal sequence. However cells can be experimentally induced to release the protein in response to heat shock (Jackson *et al.*, 1992). Since the findings reported in this chapter were published (Cohn *et al.*, 1995), 2 new candidate FGFs have emerged as limb initiation signals from very recent work carried out in several labs. *Fgf8* has been shown to be expressed in the limb ectoderm as buds begin to emerge in the mouse, suggesting a possible role in very early stages of limb budding (Crossley and Martin, 1995, Ohuchi *et al.*, 1994). Application of FGF8 (specifically, the FGF8b isoform) to the flank can induce *Fgf8* expression in the overlying ectoderm and result in ectopic limb development (Crossley *et al.*, 1996, Vogel, Rodriguez, and Izpisúa-Belmonte, 1996). *Fgf8* is expressed in the mesonephros prior to the stage at which limb budding is initiated. Crossley *et al.* proposed the hypothesis that FGF8 secreted from the mesonephric mesenchyme adjacent to the lateral plate is the endogenous signal that initiates limb budding and induces the limb ectoderm to express *Fgf8* (Crossley *et al.*, 1996). It is difficult for *Fgf8* expression in the mesonephros to account for localized limb induction, as

the expression domain is out of register with the region that forms the limb buds (Crossley et al., 1996, Vogel et al., 1996). Furthermore, *Fgf8* is expressed in the mesonephros at flank levels at stages 13-14, a period when flank cells are responsive to an FGF inductive signal. Although expression in the flank is transient (Crossley et al., 1996), it is clear that only a brief exposure (<2 hrs) is required to induce limb development (see section 2.4 in this chapter). Thus both FGF8 and FGF2 would require spatially restricted receptors, for example, if they are acting as endogenous limb inducers. *Fgf8* expression in the limb ectoderm is detectable from stage 16 (Crossley et al., 1996, Vogel et al., 1996), after limb budding has been initiated, which suggests that it may be involved in maintaining limb bud outgrowth but it cannot be responsible for initiation of the bud. Ohuchi et al. (1997) have recently reported that the *Fgf10* gene is expressed in the lateral plate mesoderm of the prospective limbs prior to *Fgf8* expression in the limb ectoderm. FGF10 can induce additional limb development when applied to the flank, but the window of competence occurs between stages 12-13, which is earlier than that of other FGFs. FGF10 induces expression of *Fgf8*, and FGF8 induction of *Fgf8* appears to be mediated by FGF10. Thus, at this point it appears that FGF10 is the best candidate for the endogenous limb inducer, and FGF8 is a downstream target of FGF10. It should be noted, however, that FGF10 is expressed in the flank at a time when the flank can be induced by exogenous FGF10 to form a limb. Thus, if FGF10 is the endogenous inducer, then localized induction of a limb must require additional mechanisms (other than *Fgf10* expression), such as repression of limbs in the flank that can be overcome by higher levels of FGF10.

FGF10 can induce limbs at earlier stages than other FGFs. FGF10 is believed to act through an ectoderm-specific FGF receptor (Ohuchi et al., 1997), and the ectoderm may, in turn, relay a signal to the mesenchyme at

stages when other FGFs that act on the mesenchyme are able induce limbs. Thus, failure of additional limbs to develop when the (ectoderm-specific) KGF receptor is targeted could be due to a requirement for activation of a mesenchymal receptor at later stages of development. It will be interesting to test whether KGF can induce limbs at stages when FGF10 is known to act. The above would imply that induction of extra limbs by FGF1, FGF2, FGF4, and FGF8 after stage 13 may act to mimic a secondary signal that is may be induced by FGF10.

3.5 Control of limb position

The results suggest that local production of a fibroblast growth factor controls limb position. The nature of the signal that switches on FGF production at a particular axial level, and how its production is controlled are unknown. The position at which this signal is produced could be encoded by the pattern of *Hox* gene expression along the body axis. For example, in mice, frogs and zebrafish, upper limbs (fins) develop at a level that corresponds approximately to the anterior limit of expression of *Hoxc6* in the somites. (Oliver *et al.*, 1988; Molven *et al.*, 1990). Loss of function mutations in the *Hoxb5* gene result in development of a shoulder girdle that appears to be situated anterior to the normal position (Rancourt, Tsuzuki, and Capecchi, 1995). The next chapter will exploit the finding that FGF can induce additional limbs to investigate the relationship between *Hox* genes and limb position.

3.6 Molecular basis of limb induction

Application of FGF induces formation of a limb at a level where limbs do not usually form. The entire flank can form limbs, but no additional limbs form when FGF is applied more anteriorly in the neck, or posteriorly in the tail. This supports the view that the field with limb forming potential extends

from the anterior edge of the upper limb to the posterior edge of the lower limb (Balinsky, 1965). The present results cast new light on experiments carried out over 70 years ago. Locatelli and Kiortsis deflected brachial nerves to the flank of newts and showed that limbs could regenerate from this position (Kiortsis, 1953, Locatelli, 1924). Interestingly, it has been suggested that early events in amphibian limb regeneration may be initiated by release of FGF-like molecules from traumatized nerves (Metscher and Gospodarowicz, 1979), and it is now known that FGF can substitute for nerve during regeneration of denervated limbs (Mullen *et al.*, 1996). Balinsky grafted otic vesicle and nose rudiment to the flank of newt embryos and induced formation of additional limbs, often with reversed polarity (Balinsky, 1925, Balinsky, 1933). It is now known that the mouse otic vesicle expresses *Fgf-3* (Wilkinson, Bhatt, and McMahon, 1989) and the nasal placode and epithelium express *Fgf-8* (Crossley and Martin, 1995, Heikinheimo *et al.*, 1994, Ohuchi *et al.*, 1994). Thus, production of a fibroblast growth factor could be the molecular basis of the limb inducing ability of the tissues used by Balinsky.

CHAPTER FOUR: *Hox Genes and Specification Of Limbs*

1. Background

Specification of limb position, number and type is a component of patterning the body axis, and must involve production of limb initiating signals at specific axial levels and interpretation of those signals by lateral plate mesoderm cells to determine limb type (forelimb versus hindlimb). The previous chapter showed how local application of Fibroblast growth factors (FGFs) to the prospective flank of chick embryos induces development of ectopic limbs with reversed anteroposterior polarity (Cohn et al., 1995). The same signal (FGF) can initiate formation of a wing or a leg but the position of FGF application along the lateral plate mesoderm determines whether forelimb or hindlimb forms. FGF applied to anterior flank induces ectopic wings and FGF applied to posterior flank induces ectopic legs. This suggests that the wing field is contiguous with the leg field in lateral plate mesoderm. The hypothesis that ectopic wings and legs are derived from separate cell populations was tested by tracing cell lineage during ectopic limb formation.

There is substantial evidence that patterns of Hox gene expression govern development of paraxial mesoderm into different types of vertebrae (Carroll, 1995). By analogy, Hox genes are good candidates for encoding positional identity in the lateral plate mesoderm. One particular combination of Hox gene expression could determine where a wing develops and another combination could determine where a leg develops. If this is the case, then formation of additional limbs at an inappropriate axial level should involve changes in Hox gene expression in the flank, and different patterns of Hox expression should be seen according to whether an additional wing or an additional leg is induced. This chapter examines the

role of Hox genes in patterning lateral plate mesoderm, by mapping expression of the *Hox* group 9 paralogues in lateral plate mesoderm during normal chick development, and comparing this with *Hox* expression patterns in embryos treated with FGF to induce ectopic limbs. Transplantation experiments were also carried-out in order to define the mechanisms that control *Hoxb9* expression during subsequent limb development.

2. Results

2.1 Cell lineage in ectopic wings and legs

In experiments described in the previous chapter, ectopic wings formed when FGF beads were placed in anterior flank and ectopic legs formed when FGF was applied to posterior flank. These results suggested the presence of two adjacent cell populations in the flank, one with the potential to form a wing and another with the potential to form a leg. To directly determine whether cells that form ectopic wings constitute a separate population to cells that form ectopic legs, a bead soaked in FGF2 was implanted in the flank either opposite somite (s) 21 (anterior flank), which induces mostly ectopic wings, or opposite s25 (posterior flank), which induces ectopic legs (data from Table 1; wing bud develops opposite s15-20, flank opposite s21-25, and leg bud opposite s26-32). A small number of flank cells were then labelled with the fluorescent dyes Dil or DiA at different distances along the anteroposterior axis from the FGF bead, and positions of labelled cells were examined 48-72 hours later. FGF beads placed in anterior flank induced an ectopic bud posterior to the bead, and flank cells opposite s22 to 25, the entire span of the prospective flank, were incorporated into the bud (n=7; Fig. 11a). Cells just anterior to the FGF bead did not contribute (n=2). FGF beads placed in posterior flank induced an ectopic limb anterior to the bead, and cells opposite s22 to 24 were seen in ectopic buds (n=9), but neither cells opposite s21 (n=3) nor cells

immediately posterior to the bead ($n=1$) were incorporated (Fig. 11b,c). These results show, rather surprisingly, that when FGF beads are placed at opposite ends of the flank, almost the same population of cells contributes to the ectopic bud, which will form either wing or leg according to the position of the FGF bead. Thus, FGF can induce bidirectional changes in cell fate, and flank cells can be anteriorized to give rise to an ectopic wing or posteriorized to form an ectopic leg.

Figure 11. FGF induces bidirectional transformations in flank cell fate to induce ectopic wings and legs.

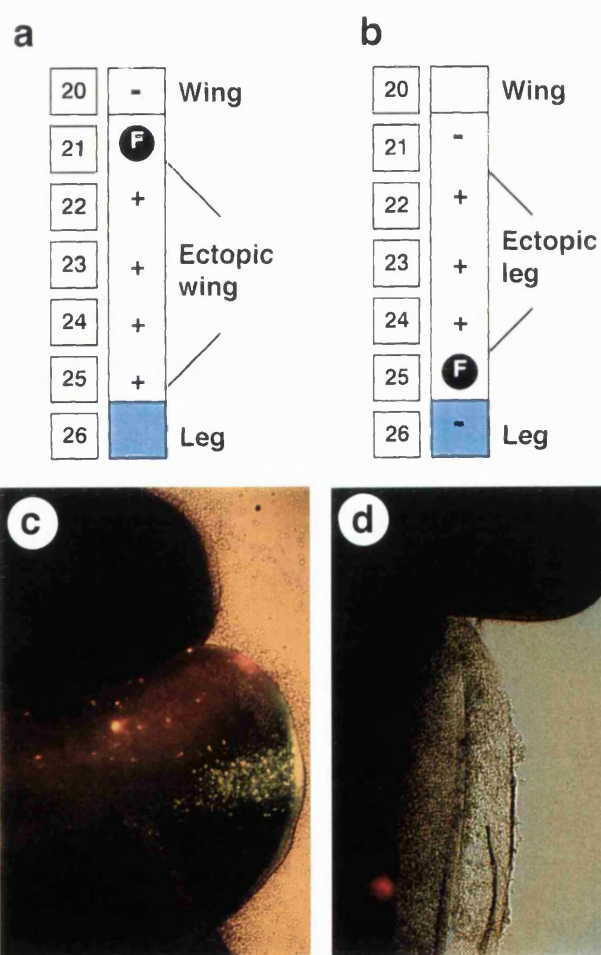
(a, b) Schematic representation of lateral plate mesoderm with FGF bead (F) placed in anterior flank opposite s21 (a), a position which generally results in ectopic wings formation, or in posterior flank opposite s25 (b), a position which generally results in ectopic legs. FGF beads were implanted in the lateral plate mesoderm of the flank of stage 14-15 chick embryos and a small patch of cells at one or two positions were labelled with Dil and/or DiA at the time of bead implantation. Embryos were viewed under fluorescence microscopy 48 to 72 hours later. (+) indicates that cells labelled at this position contributed to the ectopic limb bud and (-) indicates that labelled cells did not contribute. Anterior at top.

(a) When beads were implanted opposite s21, cells labelled opposite s22 (n=1), 23 (n=1), 24, (n=3), and 25 (n=1/2) were located in the ectopic bud. Cells labelled anterior to the bead, opposite s20 in the normal wing, were not detected in ectopic limbs (n=2).

(b) When beads were placed opposite s25, cells labelled opposite s24 (n=1), 23 (n=4), and 22 (n=3/4) contributed to ectopic limbs. Cells in the anterior flank opposite s21 (n=3) and cells posterior to the bead, opposite s26 (n=1), were not detected in ectopic limbs.

(c) Triple exposure photomicrograph of ectopic limb bud to reveal positions of fluorescent cells 72 hours after implantation of a FGF bead opposite s25. At the time of bead implantation, flank cells were labelled with Dil (red) opposite s22 and DiA (green) opposite s23. Cells from both positions have contributed to the ectopic limb bud. Note the extent of cell spread in both anteroposterior and proximodistal axes compared to normal embryo shown in (d).

(d) Double exposure photomicrograph of a normal chick embryo in which flank cells opposite s22 had been labelled with Dil 48 hours earlier. Labelled cells remain in the flank as a small patch. There is no contribution to the limb buds and the cells have remained tightly clustered.



2.2 Dynamics of *Hoxb9* expression in lateral plate mesoderm

Hox genes are involved in patterning lateral plate mesoderm along the body axis (Charite *et al.* 1994; Rancourt *et al.* 1995), however, in contrast to paraxial mesoderm, patterns of Hox gene expression in lateral plate mesoderm are not well characterized. Preliminary observations of *Hoxb9* expression in limb bud stage mice and chicks suggested that the anterior expression boundary in lateral plate mesoderm could be related to limb position (Fig. 12a). *Hoxb9* expression pattern was therefore mapped from stage 4, the definitive primitive streak stage through stage 24, when limb development is well underway. This work was carried out in collaboration with Ketan Patel (NIMR and UCL).

Hoxb9 expression could not be detected prior to stage 5, when it is initiated lateral to the posterior primitive streak (Fig. 12b). Expression then spreads anteriorly and by stage 8 the anterior boundary of *Hoxb9* in the mesoderm lies within the region identified by Chaube (1959) as the prospective wing (Fig. 12c,d), but is more posterior than the anterior boundary in the neuroectoderm (Fig. 12c). The mesodermal expression boundary continues to co-localize with the prospective wing bud, and by stage 13, the segmentation of the paraxial mesoderm at wing level allows the use of somites as landmarks. From this stage, the anterior boundary of expression in lateral plate and paraxial mesoderm is at the level of the somite 18/19 junction (Fig. 12e). Transverse sections of embryos at stage 13 show that *Hoxb9* is expressed in both layers of the lateral plate mesoderm; the somatic layer that will form the limbs and body wall and the splanchnic layer that will form the smooth muscle of the gut. At the onset of wing budding at stage 16, the anterior boundary of *Hoxb9* in the wing still lies opposite somite 18/19, and expression extends posteriorly throughout the

flank and leg bud. The anterior boundary of *Hoxb9* expression in the paraxial mesoderm also lies at the somite 18/19, but expression in the dorsal root ganglia and neural tube extends much more anteriorly to the level of somite 9 (Fig. 12e). At stage 18, however, the anterior expression boundary in the somites has regressed posteriorly to somite 21, out of register with the lateral plate mesodermal boundary opposite somite 18/19. At around stage 20, the anterior boundary in the lateral plate mesoderm shifts posteriorly out of the wing to mark the junction between the flank and posterior wing, opposite somites 20/21, and the wing bud no longer expresses the gene (Fig. 12f). The domain of high levels of *Hoxb9* expression extends throughout the flank, with a posterior boundary of high expression marking the site of leg bud outgrowth, opposite somite 26 (Fig. 12a). At stage 20, the leg bud expresses lower levels of *Hoxb9*, and this pattern then resolves to high levels of *Hoxb9* in anterior and distal leg bud by stage 21 (Fig. 12g). Expression in the rest of the leg bud becomes progressively weaker until it is undetectable in posterior and central mesenchyme at stage 24 (Fig. 12h).

2.3 Comparative analysis of *Hoxb9*, *Hoxc9* and *Hoxd9* in lateral plate mesoderm

Paralogous *Hox* genes are known to interact to influence patterning in the limbs (Davis *et al.*, 1995) and axial skeleton (Condie and Capecchi, 1994, Horan *et al.*, 1995). To compare the *Hoxb9* pattern with that of other *Hox* group 9 paralogs in lateral plate mesoderm, expression of *Hoxc9* and *Hoxd9* was also analyzed. Particular emphasis was placed on the relationship between *Hox9* gene expression and the different regions of lateral plate mesoderm along the main body axis; prospective wing, prospective leg and the intervening flank. Prior to initiation of limb budding, at stage 14, anterior expression boundaries of *Hoxb9*, *c9* and *d-9* in lateral plate mesoderm are staggered within prospective wing region, and

expression is strong throughout prospective flank and leg regions (Fig. 13a-d). When limb budding is initiated at stage 16, a secondary phase of *Hox9* gene expression along the main body axis occurs, boundaries of expression begin to realign and levels of expression change locally. The anterior boundary of *Hoxd9* expression shifts anteriorly from the flank-wing junction to the anterior limit of the wing bud (Fig. 13e). Thus, in the secondary phase, the wing bud expresses *Hoxd9* throughout, and *Hoxb9* and *Hoxc9* posteriorly (Fig. 13f). *Hoxd9* expression in the flank is subsequently reduced and ultimately switches off (Fig. 13i), so that by stage 18 the flank expresses *Hoxb9* and *Hoxc9*, but not *Hoxd9* (Fig. 11j). Decreased levels of *Hoxb9* expression in the leg bud, which produce the posterior boundary that separates strong flank expression and weaker leg expression at stage 17 (Fig. 13g), result in a leg bud expression pattern of weak *Hoxb9* with strong *Hoxc9* and *Hoxd9* (Fig. 13j). The anterior boundary of *Hoxc9* expression follows a similar pattern to that described for *Hoxb9*, in that it remains at the same position as in the primary phase until the buds are well-developed (Fig. 13g,h,j). Thus, these 3 *Hox* genes are expressed in regionally specific patterns related to limb specification and budding.

2.4 *Hox9* gene expression and induction of ectopic limbs

In order to determine whether respecification of flank to form limbs involves changes in *Hox* gene expression, FGF was applied to either anterior flank to induce additional wings or to posterior flank to induce additional legs and expression of *Hoxb9*, *Hoxc9* and *Hoxd9* was monitored. Specific changes were observed in the pattern of *Hox* gene expression in lateral plate mesoderm, according to the position at which FGF is applied. Changes in expression were almost always confined to boundaries; local patches of downregulation around the FGF bead were not detected.

FGF beads in anterior flank, which lead to ectopic wings, induced a posterior shift of the anterior boundaries of *Hoxb9* and *Hoxc9* expression (Fig. 14a,b,c; Table 3a). The posterior boundary of *Hoxb9* expression could be seen, but was not affected (Fig. 14b). In contrast to the posterior shift of *Hoxb9* and *c9* anterior boundaries, the anterior boundary of *Hoxd9* was unaffected, but *Hoxd9* expression was maintained in the flank where, during normal development, it would have been switched off (Fig. 14d). Thus, the combination of *Hox* genes expressed in the flank after anterior FGF application is transformed from the normal flank pattern to a pattern normally found at wing level (Fig. 14e).

FGF beads in posterior flank, which lead to ectopic legs (Table 1), induced an anterior shift of the posterior boundary of the *Hoxb9* domain (Fig. 14g; Table 3a), stronger *Hoxc9* expression in the flank (Fig. 14h) and *Hoxd9* expression was again maintained in the flank (Fig. 14i); anterior boundaries of *Hoxb9* and *Hoxc9* were unaffected. These changes transformed the normal flank pattern of *Hox* gene expression to a pattern normally found at leg level (Fig. 14j).

FGF applied to mid-flank, opposite s22-24, which results in either wing or leg development, induced shifts of both boundaries of *Hoxb9*, sometimes in the same embryo (Table 3a,b). FGF beads placed at any position within the flank occasionally induced single lateral outgrowths extending from anterior wing to the posterior limit of the flank (n=8), which were associated with posterior shifts in the *Hoxb9* anterior boundary (Table 3b).

Changes in the primary pattern of *Hox* gene expression were detected as early as 12 hours after FGF application, when the anterior boundary of

Hoxb9 had shifted posteriorly in the lateral plate mesoderm over a distance of one somite (Table 3a). Activation of expression of genes that encode signaling molecules which control outgrowth and patterning occurs later in ectopic buds. Ectopic *Fgf-8* transcripts are first detectable in flank ectoderm 14-16 hours after FGF application (Crossley et al., 1996) , and ectopic *Shh* is first expressed in flank mesenchyme at 24 hours (Cohn et al. 1995) . Two to 3 days after application of FGF, ectopic limb buds show specific changes in the complex patterns of *Hox* gene expression characteristic of normal wings (e.g., downregulation of *Hoxb9*; Fig. 14a) or legs (e.g., asymmetric downregulation of *Hoxb9*; Fig. 14f; Table 3b), indicating that a cascade of gene expression characteristic of either wing or leg has been set in train in flank cells (see below).

Figure 12 *Hoxb9* expression during normal chick development.

Hoxb9 transcripts were detected by whole-mount *in situ* hybridization. All embryos are oriented with anterior at top and are dorsal views.

- a** Stage 20 chick embryo. *Hoxb9* expression can be detected in the somites as far anterior as somite 21. High levels of expression exist in the lateral plate mesoderm of the flank between the posterior wing bud opposite somite 20 and the anterior leg bud opposite somite 26. The dotted line marks the boundary between different levels of transcripts in the flank and leg bud. *Hoxb9* is also expressed in the neural tube and dorsal root ganglia.
- b** Transcripts are first detectable at stage 5. Arrowhead marks anterior limit of expression lateral to posterior primitive streak.
- c, d.** Stage 8 embryos. Anterior boundary in mesoderm (M, arrow) in **c** appears to mark the region identified as prospective wing in **d** (after Fig. 3 of Chaube, 1959). **c** *Hoxb9* expression extends further anteriorly in the neuroectoderm (N, arrowhead) than in the mesoderm.
- e** Stage 15 embryo. *Hoxb9* is expressed in lateral plate and somitic mesoderm posterior to somite 18, and in the neural tube posterior to somite 9.
- f** Stage 18 (left), 20+ (middle), and 24 (right) embryos. At stage 18, the anterior boundary (arrows) of *Hoxb9* expression in the lateral plate mesoderm is in the posterior wing bud opposite somites 18/19. At stage 20+, the anterior boundary shifts posteriorly out of the wing and comes to mark the junction between the posterior wing bud and the flank. The position of the anterior boundary (note arrow on stage 24 embryo) remains at the flank-wing junction through late limb stages.
- g** Stage 21 leg bud. Levels of *Hoxb9* expression in the leg are no longer uniform as expression in the central and posterior mesenchyme weakens.
- h** By stage 24, *Hoxb9* is no longer expressed in the central-posterior leg bud, but high levels of expression can be seen anteriorly and distally.

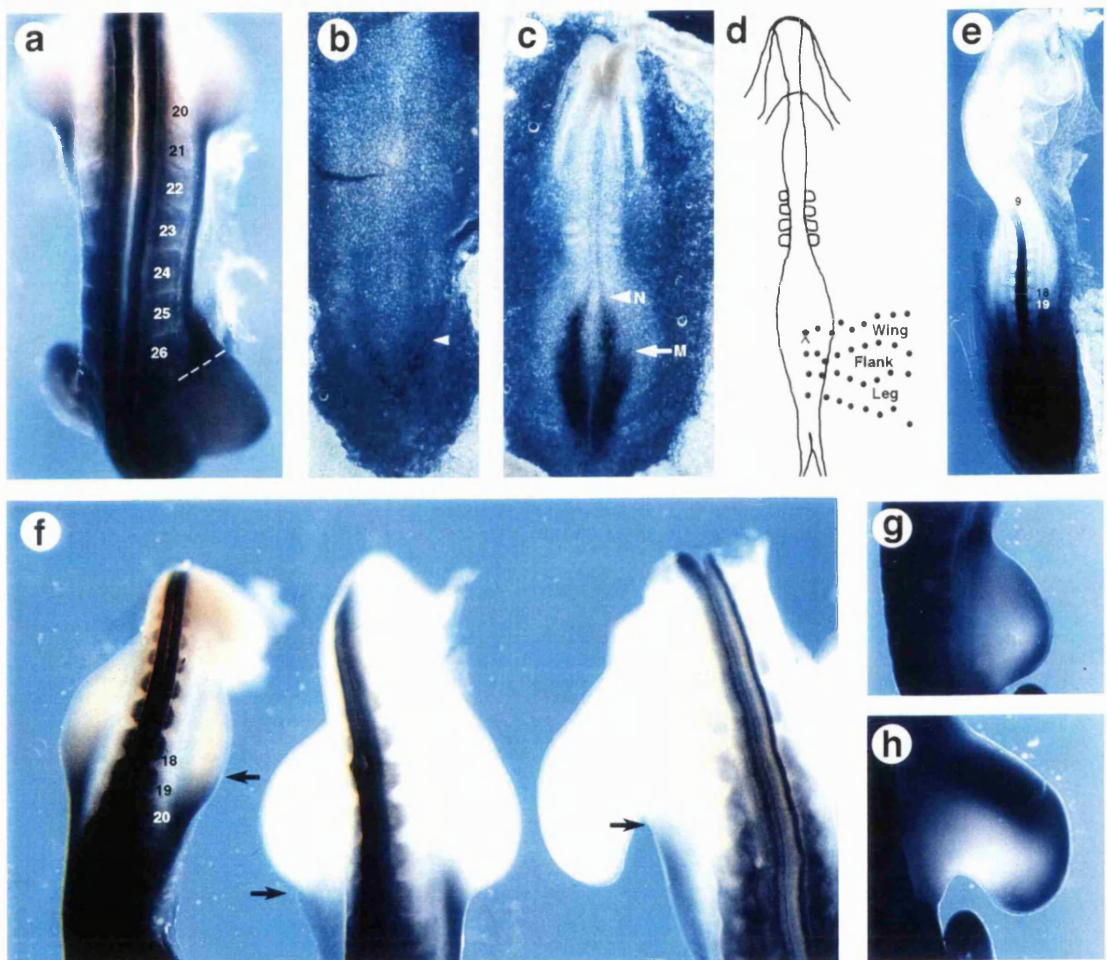


Figure 13. Expression of *Hox* group 9 paralogues in lateral plate mesoderm of normal chick embryos

Hoxb9 (**a, g**), *Hoxc9* (**b ,h**) and *Hoxd9* (**c,e , i**) transcripts detected by whole-mount *in situ* hybridization. Embryos are oriented with anterior at top and are dorsal views, except **e**, which is a ventrolateral view. Black lines mark boundaries of expression domains in lateral plate mesoderm of normal embryos; arrows mark boundaries on FGF-treated side and arrowheads are on the contralateral (untreated side) of embryos.

a-c. Pre-limb bud stage chick embryos (stage 14-15). **a.** Anterior boundary of *Hoxb9* expression in lateral plate mesoderm lies opposite the junction between s18 and 19. **b.** Anterior boundary of *Hoxc9* in lateral plate mesoderm lies opposite s19. **c.** Anterior boundary of *Hoxd9* in lateral plate mesoderm lies opposite s20-21. These patterns are summarized in panel **d**, in which the staggering of the boundaries in the prospective wing region is shown. **e.** Stage 16 embryo in which limb budding has been initiated and the anterior boundary of *Hoxd9* has shifted anteriorly from s20-21 to s15 at the anterior margin of the emerging wing bud. **f.** Schematic illustration summarizing *Hoxb9*, *c9* and *d9* expression at stage 16. **g.** Stage 18 and (**h**) stage 19 chick embryos. The anterior boundaries of *Hoxb9* (**g**) and *Hoxc9* (**h**) are still at the same axial level as shown in **a** and **b**. In **g**, a clear posterior boundary of *Hoxb9* expression has appeared opposite s26 between the strong flank expression and the weaker leg expression, but no such change is seen in *Hoxc9* (**h**), which is uniformly expressed in flank and leg. **i.** Stage 17-18 embryo. *Hoxd9* is now clearly downregulated in the flank between the wing and leg buds (arrows). **j.** Summary of *Hoxb9*, *Hoxc9* and *Hoxd9* expression at stage 19. Dark and light purple represent intensity of *Hoxb9* expression.

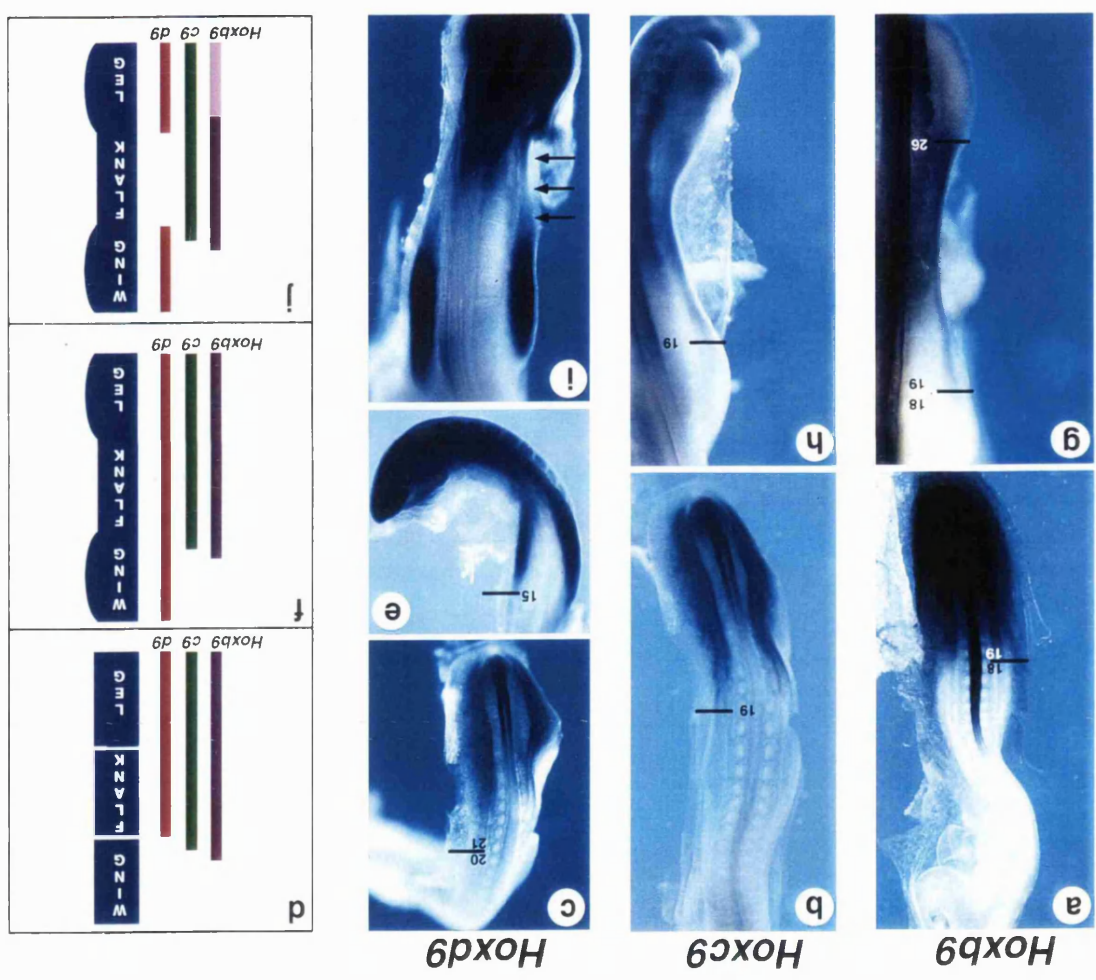
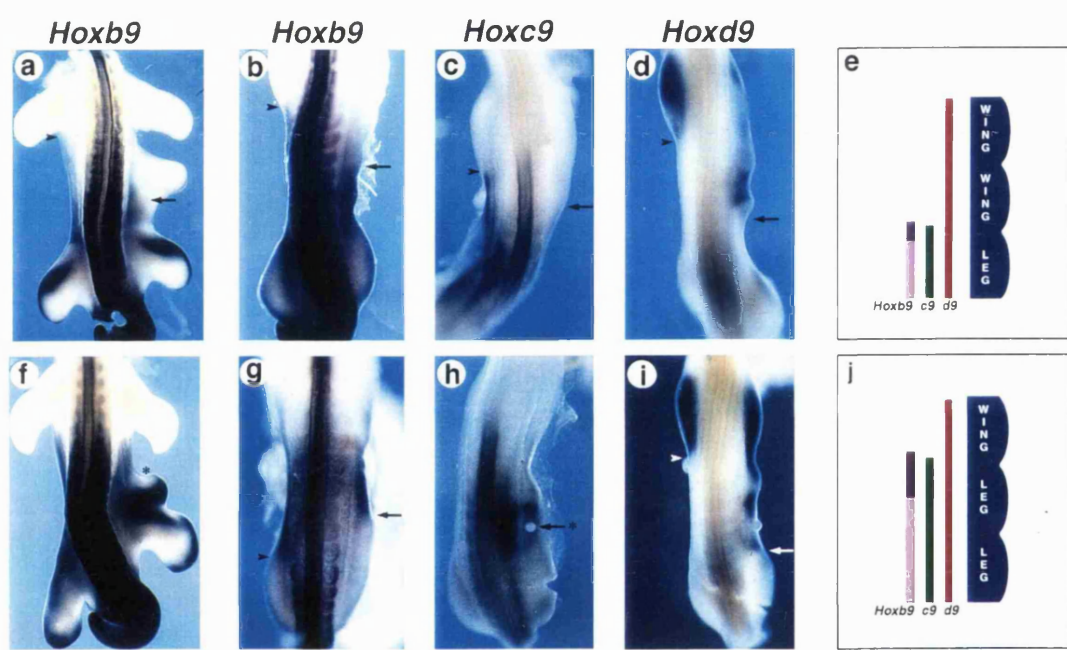


Figure 14 Expression of *Hox* group 9 paralogues in chick embryos treated with FGF to induce ectopic limbs.

a 57 hours after application of the FGF bead opposite s23, the posteriorly displaced anterior (ant.) boundary of *Hoxb9* expression lies at the junction between the ectopic limb bud and the remaining flank (arrow), creating a wing-like pattern in the flank. The boundary of expression on the contralateral side marks the junction between the normal wing bud and ant. flank (arrowhead). **b.** Chick embryo 26 hours after implantation of a FGF bead in the lateral plate mesoderm opposite s23. The ant. boundary of *Hoxb9* expression in the lateral plate mesoderm is shifted posteriorly (arrow) compared to the boundary on the contralateral side (arrowhead), which is unaffected. The posterior (post.) expression boundary in the lateral plate mesoderm and expression in the somites are unaffected. **c, d.** Chick embryos 18 hours after application of FGF opposite s21. **c.** The ant. boundary of *Hoxc9* has shifted posteriorly over a distance of 3 somites (arrow). Compare with contralateral side, where ant. expression boundary lies at the post. edge of the emerging wing bud (arrowhead). **d.** The ant. boundary of *Hoxd9* remains at the ant. limit of the wing bud, but the domain is posteriorly extended into the flank (arrow), whereas on the left side (arrowhead) *Hoxd9* has been switched off. Note that on the treated (right) side, although the ant. boundary is at the appropriate axial level, the expression in the wing is patchy. By this stage, expression in the leg buds has started to weaken. **e.** Schematic diagram summarizing the patterns of *Hoxb9*, *c9* and *d9* expression in the flank when it is anteriorized by FGF to take on a wing identity. **f.** 72 hours after application of a FGF bead opposite s24, the post. boundary of *Hoxb9* expression is no longer visible, as expression in the ectopic bud has taken on a leg-like pattern. *Hoxb9* has been downregulated at the ant. margin of the ectopic bud (*), reproducing the pattern of the normal leg but with a reversed antero-posterior pattern. **g** 17 hours after application of a FGF bead opposite s22, the posterior boundary of *Hoxb9* expression in the lateral plate mesoderm on the treated side has shifted anteriorly (arrow). Expression in the somites and the boundary on the contralateral side (arrowhead) are unaffected. **h.** 19 hours after application of FGF opposite s25, the boundaries of *Hoxc9* expression are unaffected. *Hoxc9* expression is increased in the flank around the bead (*) and arrow). **i** 18 hours after application of FGF opposite s25, *Hoxd9* expression has been extended throughout the entire flank (arrow). **j.** Schematic diagram summarizing the patterns of *Hoxb9*, *c9* and *d9* expression in the flank when the flank is posteriorized by FGF to take on a leg identity.



2.5 Application of FGF to paraxial mesoderm

Hoxb9, *c-9* and *d-9* have different expression boundaries in neural tube, paraxial mesoderm and lateral plate mesoderm. Boundaries of expression in paraxial mesoderm, like lateral plate mesoderm, are dynamic, whereas in neural tube, anterior expression boundaries of *Hoxb9* and *d-9* appear to be fixed early and are generally maintained. FGF application to the flank alters *Hoxb9*, *c9* and *d9* boundaries only in lateral plate mesoderm; expression boundaries in somites and neural tube were unchanged (Fig. 14a-d and f-i). This is consistent with the observation that vertebral identity is not altered in embryos which develop ectopic limbs (Chapter 3). These results demonstrate that Hox gene expression in lateral plate and paraxial mesoderm can be regulated independently. As reported in Chapter 3, Dig-FGF2 does not appear to diffuse far from the bead, therefore the failure of paraxial mesoderm to respond to FGF treatment of the lateral plate could be due to distance from the FGF source. Alternatively, Hox gene expression in paraxial mesoderm may not respond to FGF. To explore these possibilities, FGF2-soaked beads were placed directly in the paraxial mesoderm of stage 13-16 chick embryos, and embryos were examined 24-48 hours later. Application of FGF to the paraxial mesoderm resulted in formation of ectopic limb buds from the flank, and although the anterior boundary of *Hoxb9* in lateral plate mesoderm was shifted posteriorly in all cases, *Hoxb9* expression in paraxial mesoderm was not affected ($n=4$, Fig. 15). These results indicate that *Hoxb9* expression in paraxial mesoderm is not sensitive to FGF at stages when expression in lateral plate can be altered.

Figure 15. *Hoxb9* expression in chick embryo 48 hours after application of FGF to paraxial mesoderm

FGF bead was implanted in somite (s)23. *Hoxb9* expression in the somites appears normal, but the anterior boundary of expression in the lateral plate mesoderm (LPM) has shifted posteriorly from somite 21 to somite 23 (arrow).

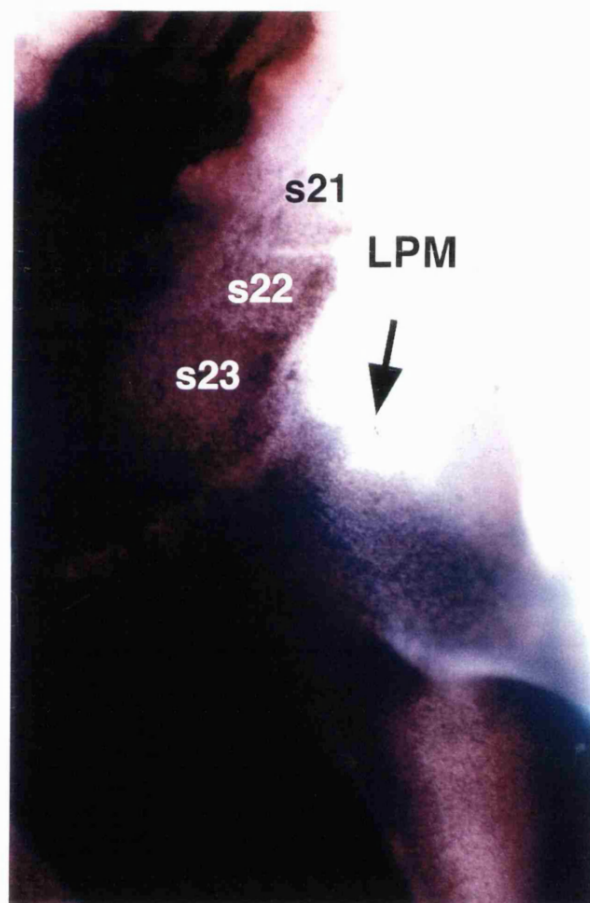


Table 3 Effects of FGF on *Hox* gene expression in lateral plate mesoderm of the chick**A. Pattern of *Hoxb9* expression between 12 and 24 hours after application of FGF to the flank**

| Axial level of FGF bead | Number of embryos assayed | Anterior boundary shifted | Posterior boundary shifted | Both boundaries shifted | Boundaries Unchanged |
|-------------------------|---------------------------|---------------------------|----------------------------|-------------------------|----------------------|
| Somite 21 | 6 | 3 | 0 | 0 | 3** |
| Somite 22 | 3 | 0 | 1 | 0 | 2 |
| Somite 23 | 6 | 3 | 1 | 0 | 2* |
| Somite 24 | 1 | 0 | 0 | 1 | 0 |
| Somite 25 | 3 | 0 | 3 | 0 | 0 |

B. Pattern of *Hoxb9* expression between 25-75 hours after application of FGF to the flank

| Axial level of FGF bead | Number of embryos assayed | "Anteriorized" Wing-like expression pattern | "Posteriorized" Leg-like expression pattern | Expression pattern altered [§] | Pattern Unchanged |
|-------------------------|---------------------------|---|---|---|-------------------|
| Somite 21 | 9 | 7 (1 [†]) | 1 | 0 | 0 |
| Somite 22 | 9 | 3 | 6 | 0 | 0 |
| Somite 23 | 8 | 2 (2 [†]) | 1 | 2 | 1 |
| Somite 24 | 9 | 0 (2 [†]) | 5 | 1 | 1 |
| Somite 25 | 11 | 2 (3 [†]) | 6 | 0 | 0 |

* Upregulation within expression domain (* = 1 case).

† Fin-like outgrowth extending from anterior limit of wing to anterior limit of leg.

§ Expression domain altered but without clear resemblance to wing or leg pattern.

2.6 Effects of retinoic acid on *Hoxb9* expression at wing level

The anterior expression boundary of *Hoxb9* lies approximately at the same axial level as the anterior limit of polarizing potential in lateral plate mesoderm during limb initiation (This chapter and Hornbruch and Wolpert, 1991). Retinoic acid can activate the polarizing region pathway and expression of *Hoxb8* in anterior limb bud mesenchyme (Lu *et al.*, 1997; Stratford *et al.*, 1997). To test whether retinoic acid can activate *Hoxb9* expression, beads soaked in 0.1 mg/ml retinoic acid were applied to the anterior margin of stage 19 and 20 wing buds. There was no detectable induction of *Hoxb9* at 9 hours (n=2) or at 22 hours (n=2) after retinoic acid application, although the normal posterior domain of *Hoxb9* was present. A control embryo which was treated the same way and left to develop to 10 days had a **43234** pattern of digit duplication. A higher dose of retinoic acid applied at an earlier stage of development also did not induce *Hoxb9* expression. Beads soaked in a 1mg/ml solution of retinoic acid were applied to the anterior margin of stage 17-18 wing buds, when *Hoxb9* expression is present in the posterior wing, and the embryos were assayed between 5 and 24 hours. No ectopic *Hoxb9* could be detected in embryos examined at 5 hours (n=2), 16 hours (n=2), or 24 hours (n=1), and control embryos had **4334** and **43234** digit duplication patterns. These results suggest that *Hoxb9* expression in the wing is neither induced by retinoic acid nor required for induction of polarizing activity.

2.7 *Hoxb9* boundaries and cell lineage in the wing bud

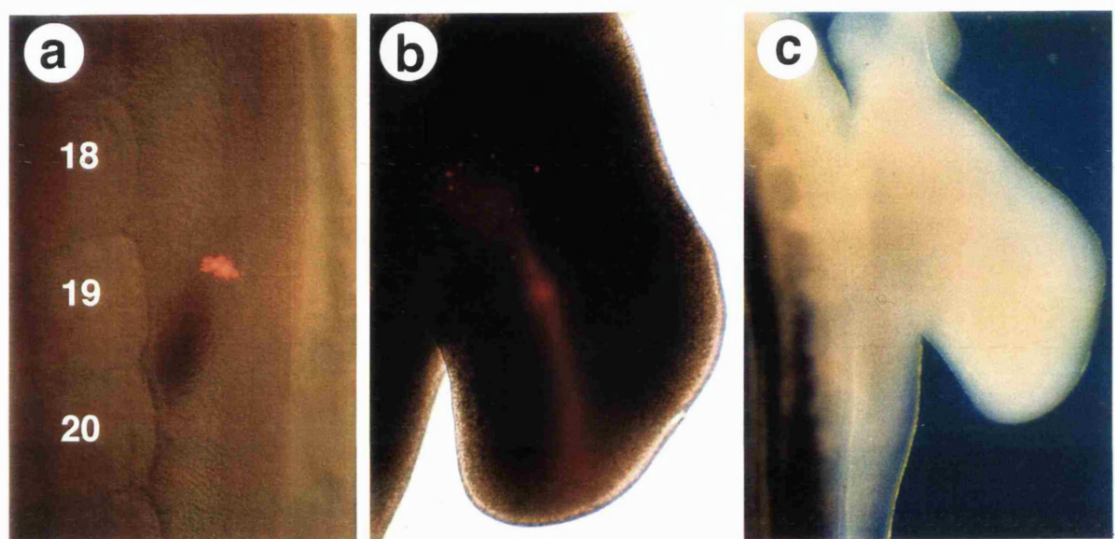
A striking change in *Hoxb9* expression occurs in the posterior of the wing bud between stages 20 and 21. Up to stage 20, *Hoxb9* is expressed posteriorly in the wing bud, with an anterior boundary opposite somite 18/19. One stage later, however, *Hoxb9* is no longer expressed in the wing, but is still expressed in the flank, with an anterior boundary at the flank-wing

junction. The posterior shift of the *Hoxb9* anterior boundary from the wing bud to the flank could be due either to cell movement or to cells in the wing bud switching off expression of the gene. To test these two possibilities, cells in the posterior wing opposite somites 18-20, where *Hoxb9* is expressed (see Fig. 12), were labelled with the fluorescent lipophilic membrane dye Dil between stages 16 and 19 (Fig. 16a), and the embryos were allowed to develop beyond the time at which the boundary shift occurs. The position of fluorescent cells was recorded and then whole mount *in situ* hybridization was performed on the same specimens to determine whether labelled cells expressed *Hoxb9*. In all cases, fluorescent cells remained in the wing, the original spot of labelled cells had expanded into a streak along the proximodistal (p-d) axis of the wing (Fig. 16b), and none of these cells expressed *Hoxb9* (Fig. 16c, n=9). This indicates that the posterior shift in the anterior *Hoxb9* expression boundary during normal wing development is due to cells in the wing switching off *Hoxb9* expression.

Figure 16. Analysis of cell lineage and *Hoxb9* expression in the posterior wing bud.

Dorsal views, anterior at top.

- a Cells in the *Hoxb9* domain of the posterior wing bud, opposite somite 19, of a stage 16 chick embryo were labelled with Dil. Double exposure photomicrograph using fluorescence and lightfield was taken at time of injection.
- b Forty-eight hours after injection, fluorescent cells have remained in the wing bud, which is now at stage 24, and are distributed in a stripe along the p-d axis.
- c Embryo shown in b after whole-mount *in situ* hybridization for the *Hoxb9* gene. Cells in the wing no longer express *Hoxb9*.



2.8 Loss of *Hoxb9* expression in posterior limb buds

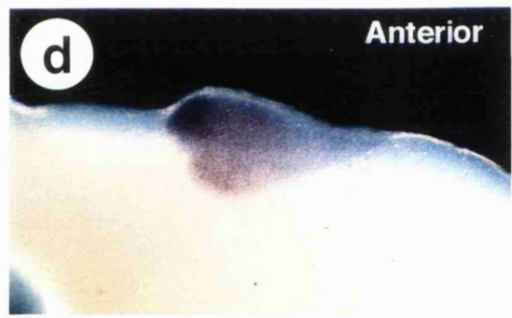
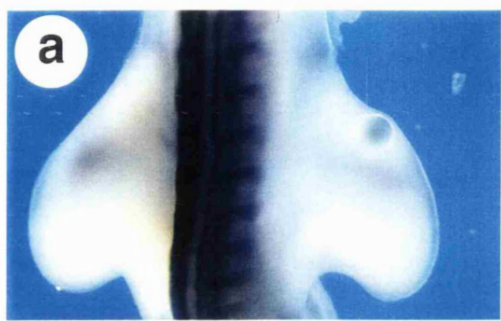
In section 2.2, I showed that *Hoxb9* is initially expressed in the posterior wing bud and throughout the leg bud, and expression later disappears from the posterior region of both limbs. Why does *Hoxb9* switch off in posterior wing and leg, but remain on in the flank and anterior leg? The posterior part of the buds, in which *Hoxb9* expression is downregulated during outgrowth, is a source of several secreted factors (SHH, BMP2, FGF4), and reduction of *Hoxb9* expression occurs after these signaling molecules begin to be expressed. These factors are not expressed in the flank, where *Hoxb9* expression is maintained. Retinoic acid and SHH are known to regulate Hox gene expression (Izpisúa-Belmonte *et al.*, 1991, Riddle *et al.*, 1993), and both signals are present in the posterior wing and leg. Therefore, the possibility that these signals may switch off *Hoxb9* was investigated by directly exposing limb bud cells to retinoic acid and SHH. When retinoic acid (0.1 mg/ml) was applied to the anterior margin of the leg bud at stage 20, expression of *Hoxb9* was either switched off or severely reduced in all cases (n=3, Fig. 17a). Application of mSHH198 (16 mg/ml) to the anterior leg also reduced *Hoxb9* expression (n=2, Fig. 17b). Application of SHH to *Hoxb9*-expressing regions of the flank at stage 14 (n=3) and to the neural tube at stage 20 (n=1) had no effect on *Hoxb9* expression 24 hours after application. These results indicate that both SHH and retinoic acid can reduce *Hoxb9* expression in the limb, but that the sensitivity of *Hoxb9* expression to these factors appears to be restricted to limb buds.

To determine whether exposure of *Hoxb9*-expressing flank cells to endogenous cues in the posterior limb bud could affect *Hoxb9* expression, flank tissue opposite somites 21-24, in which *Hoxb9* is continuously expressed (Fig. 12), was transplanted from stage 14 (n=2) or stage 18 (n=4) donors to the posterior wing bud of stage 19-20 hosts. The embryos were

allowed to develop for 24 to 48 hours after grafting, well beyond the stage when *Hoxb9* should be switched off in wing cells, before being fixed and assayed for *Hoxb9* expression. In all cases, *Hoxb9* transcripts were detected in the grafted flank cells but not in the surrounding wing tissue (Fig. 17c). When flank cells opposite somite 21 were transplanted to the anterior wing, expression was again detected in the graft in all cases (n=3; Fig. 17d). Thus, in contrast to limb bud cells, flank cells stably express *Hoxb9* and are unresponsive to direct application of SHH or to exposure to factors present in posterior limb buds.

Figure 17. Regulation of *Hoxb9* in the chick leg bud and flank

a. *Hoxb9* expression in the leg bud of a chick embryo 24 hours after application of a retinoic acid (0.1 mg/ml) bead to the anterior margin of the bud. b. *Hoxb9* expression in the leg bud of a chick embryo 24 hours after application of a SHH (16 mg/ml) bead to the anterior margin of the bud. c, d. *Hoxb9* expression in wing buds after transplantation of flank cells to the anterior (c) or posterior (d) margin of the wing. c. Flank cells from opposite somite 22 were transplanted to the posterior margin of the chick wing and assayed after 24 hours for *Hoxb9* expression. Note that expression persists in the grafted flank cells but has disappeared from surrounding posterior wing cells. d. Flank cells from opposite somite 21 were transplanted to the anterior margin of the chick wing and assayed after 24 hours for *Hoxb9* expression. Strong *Hoxb9* expression is detected in the grafted flank cells.



3. Discussion

3.1 Hox gene expression specifies limb position

The results reported in this chapter are consistent with the idea that early primary expression of *Hox* genes in lateral plate mesoderm along the body axis specifies positions where limbs develop. Further evidence for this role for *Hox* genes comes from mice lacking *Hoxb5*, in which forelimb position is altered (Rancourt *et al.* 1995). The anterior boundaries of *Hox* group 9 paralogues overlap in the region where the wing will form. Staggered boundaries of *Hox* gene expression are known to be important for specifying positional differences along the body axis, as in the distinct segment types in insects (Akam *et al.*, 1994), the chordate neural tube (Lumsden and Krumlauf, 1996) and the vertebrate axial skeleton (Krumlauf, 1994). FGF resets *Hox* expression boundaries in lateral plate mesoderm so that they come to lie in the flank. According to the new pattern of *Hox* gene expression, the same population of flank cells then forms either an additional wing or leg. The fact that an additional limb forms, rather than a shift in position of the nearby normal limb, suggests that position of the normal limb has already been specified by a ratchet-like mechanism which irreversibly commits cells. The cascade of gene expression set in train as a result could include the recently identified T-box genes, which are differentially expressed in forelimbs and hindlimbs and thus are candidates for specifying limb identity (Gibson-Brown *et al.*, 1996).

The observation that *Hox* gene expression is altered prior to activation of *Fgf-8* and *Shh* is reminiscent of the changes in gene expression that enable butterfly prolegs to develop in abdominal segments, when downregulation of *Ubx* and *abd-a* precedes activation of *Antennapedia* (*Antp*) and *Distal-less* (*Dll*) in the prospective limbs (Warren *et al.*, 1994). It may necessary to locally change the identity of cells from abdomen to thorax

first, so that leg-specific genes will operate in a thoracic context of Hox gene expression. This may also explain why in the chick, SHH fails to induce limb development in the flank when it can initiate ectopic transcription of *Fgf8*. Given the inability of SHH to alter *Hoxb9* expression in the flank, *Fgf8* is activated in a *flank* rather than a *limb* context of Hox gene expression.

3.2 The polarizing region pathway is independent of *Hoxb9*

Although positional identity and Hox gene expression is reset in the flank so that an additional limb forms, ectopic limbs have reversed polarity and *Shh* is expressed at the anterior of the ectopic buds (Chapter 3). Thus it appears that polarizing potential in the flank is not reset. Retinoic acid does not induce ectopic *Hoxb9* when applied to the anterior of the wing bud. This important difference between *Hoxb9* and *Hoxb8* suggests that *Hoxb9* is not involved in specification of the polarizing region. The possibility that *Hoxb9* may lie upstream of retinoic acid during normal limb development, however, can not be excluded by these experiments. If the latter suggestion is correct and *Hoxb9* is involved in positioning the polarizing region, then this information must be irreversibly specified when *Hoxb9* reaches the definitive anterior boundary, as movement of this boundary by FGF does not reset the gradient of polarizing potential.

3.3 *Hoxb9* expression is reduced by local signals in the limb bud

During later stages of limb development, lineage tracing indicates that the pattern of *Hoxb9* expression changes because cells in the posterior wing switch off the gene. Direct application of both SHH and retinoic acid to the anterior leg bud causes reduction in the level of *Hoxb9* expression, which suggests that these signals may play a role in the regulation of expression in

the leg. This finding may also explain the loss of *Hoxb9* expression from the posterior wing, if *Hoxb9* expression in the wing is also sensitive to retinoic acid and SHH. The differential response of *Hoxb9* in flank and limb cells exposed to SHH suggests that *Hox* gene expression in flank and limb are under different regulatory control. The position-specific changes in *Hoxb9* expression observed in ectopic limb buds induced by FGF suggests that these differences are eliminated and flank cells can respond to SHH after their positional identity is reprogrammed from *flank* to *limb*. Differential regulation of *Hox* genes in flank and limb may underlie the stability of normal limb position and identity when the flank is transformed by FGF.

3.4 Hox genes and the evolution of paired appendages

In light of these results, new pathways for paired fin and limb developmental evolution can be considered. *Hox* gene expression dynamics, the independence of *Hox* gene regulation in paraxial and lateral plate mesoderm, and the fact that morphological transformations can occur in one tissue without altering the other, raise the following possibilities: (a) that paired appendage evolution included a mechanism which staggered *Hox* gene expression along the lateral plate mesoderm. This is likely to have been achieved by modifying genes which regulate *Hox* gene expression, rather than the *Hox* genes themselves; and (b) that paired appendages originated without an obligatory reorganisation of the axial skeleton. Modular control of *Hox* genes, perhaps by tissue-specific regulatory genes, would enable decoupling of anatomical systems and freedom for variation to occur without inducing wholesale body plan transformations. This model can account for the idea that paired fins appear to have evolved before a regionalized axial skeleton (Carroll, 1988). Independent regulation of *Hox* gene expression would also allow the position of paired appendages to shift along the body axis without dramatic

reorganization of the axial skeleton (See Agar, 1907, Goodrich, 1930, Thorogood and Ferretti, 1993).

Prior to the evolutionary origin of vertebrates, *Hox* gene expression was central to regional specialization of the gut (Bienz, 1994, Roberts *et al.*, 1995). *Hox* gene expression is staggered in the tetrapod splanchnic mesoderm and is important for regional patterning of the developing gut (Boulet and Capecchi, 1996). Given that somatic and splanchnic mesoderm are both derived from lateral plate, one possibility is that staggered *Hox* boundaries in lateral plate mesoderm appeared concomitantly with gut regionalization. Molecular regionalization of the body wall would therefore have provided differential positional values along the body axis before evolutionary emergence of paired fins. Differential *Hox* expression could have allowed spatially restricted activation of outgrowth signals such as FGF (Caré *et al.*, 1996), and the resultant fins would have inherent differences in their positional identity at different loci along the body axis. The same signaling molecules could therefore operate in different contexts in anterior and posterior appendages, and the resultant differences in signal interpretation during development may explain morphological differences between anterior and posterior appendages. This is consistent with evidence from the fossil record which indicates that evolution of a stomach and pectoral fins was coordinated, and that pelvic and pectoral appendages evolved as morphologically distinct structures (Coates, 1994).

CHAPTER FIVE: Developmental Analysis of Limblessness and Axial Patterning in Python Embryos

1. Background

Development of forelimbs and hindlimbs can be induced in chick embryos by FGFs, and the identity of the limb is related to particular combinations of Hox gene expression in the lateral plate mesoderm along the main body axis (Chapters 3 and 4). In snakes, forelimbs and hindlimbs fail to develop and regional specialization of the axial skeleton has been lost, but the developmental basis for these changes is unknown. This chapter aims to investigate the changes that have occurred during evolution of snake development.

Number, pattern and identity of elements within the vertebral column can vary widely across vertebrates. A clear pattern of regionalization is usually evident, in particular among tetrapods (Gadow, 1933, Romer, 1966). In limbed reptiles, the pattern of vertebral identity is generally *cervical* vertebrae at the anterior, followed by *dorsal* (in higher vertebrates subdivided into rib-bearing *thoracic* and rib-less *lumbar*), *sacral* and *caudal* (Romer, 1956). Although *dorsal* vertebrae is the formal name for the vertebrae between the *cervical* and *sacral* series, to avoid confusing terminology, I will refer to *dorsal* vertebrae as *thoracic* in this thesis. Snakes have between 160 and 400 individual vertebrae, depending on the species, and classification of vertebral type other than "precaudal" versus "caudal" has proved to be a difficult and subjective task because of their apparent uniformity (Bellairs, 1969, Gadow, 1933, Gasc, 1976).

Hox genes are expressed in paraxial mesoderm of vertebrates with specific boundaries corresponding to morphological transitions (e.g., *Hoxc6* at the thoracic-cervical junction in frogs, chicks and mice) (Burke *et al.*, 1995,

Oliver *et al.*, 1988a). The pattern of Hox gene expression across vertebrates with different vertebral formulae correlates with morphological identity of the vertebrae rather than with vertebral number (Gaunt, 1994; Burke *et al.*, 1995). Gain and loss of function mutations often result in homeotic transformations, in which one type of vertebra is transformed into another. *Hoxc6* and *Hoxc8* are expressed in restricted domains corresponding to the thoracic region of the vertebral column in frogs, chicks and mice (Awgulewitsch and Jacobs, 1990, Jegalian and De Robertis, 1992, Kessel, 1992, Oliver *et al.*, 1988a). Overexpression of *Hoxc6* and *Hoxc8* each result in anterior transformation of lumbar vertebrae to rib-bearing thoracic vertebrae (Jegalian and De Robertis, 1992, Pollock, Jay, and Bieberich, 1992). *Hoxb5* is expressed in paraxial mesoderm with an anterior boundary at the first cervical vertebra (Wall *et al.*, 1992). Loss of function mutation in the *Hoxb5* gene causes anterior transformation of thoracic 1 to cervical 6 (Rancourt *et al.*, 1995).

The signaling molecules that maintain outgrowth and patterning of the limbs after limb initiation in mice and chicks are common to forelimbs and hindlimbs, and the structures that they specify are determined by the context of gene expression in which they operate. The common mechanisms of forelimb and hindlimb development are reflected by several mutations which effect development of both limbs (e.g., *Extra toes*, *Leg/less* and *Strong's Luxoid*) (Chan *et al.*, 1995, Masuya *et al.*, 1997, Singh *et al.*, 1991). A number of mutations, however, effect only forelimbs (e.g., *Wing/less*, *TBX3* /ulnar-mammary syndrome and *TBX5* /Holt-Oram syndrome), or only hindlimbs (e.g., *Rim4*), which indicates a level of independence in forelimb and hindlimb development (Bamshad *et al.*, 1997, Li *et al.*, 1997, Masuya *et al.*, 1995, Zwilling, 1956b). The ability of forelimbs and hindlimbs to undergo morphological changes without affecting one another has allowed

vertebrates to evolve specializations restricted to one set of limbs.

Modularity during limb development has allowed some vertebrates to lose one set of limbs, as whales have done with hindlimbs and several Australian skinks have done with forelimbs (Greer, 1989). Complete loss of limbs may be caused by failure to initiate limb budding, and this could be related to higher-order changes in the primary body axis, such as loss of regional specialization which may eliminate localized inductive interactions at forelimb and/or hindlimb levels. This hypothesis is supported by the observation that limblessness is often associated with elongation of the body and loss of clear regionalization of the axial skeleton in the region of the lost limb. Most modern snakes have lost both fore and hindlimbs, and determination of regional identity of the vertebrae is difficult (Romer, 1956). Pythons and boas have retained vestiges of hindlimbs, however, suggesting that limb budding is initiated posteriorly but the cellular interactions within the bud have been disrupted. Anteriorly, however, the limb initiation signal appears to have been lost. To understand the developmental basis of the changes that have occurred during evolution of the snake body plan, expression of Hox genes, FGF and several transcription factors involved in chick and mouse limb development was studied in embryonic pythons.

2. Results

Most of the results described in this chapter come from work done on Burmese and Indian pythons, *Python molurus molurus* and *Python molurus bivittatus*. Duration of development is fairly uniform within the species; eggs are laid two months after mating, and they hatch after another two months (Ross, 1990). A few specimens of spotted python were used for analysis of skeletal development and scanning electron microscopy. Although the taxonomic classification of the spotted python has not yet been resolved

(either *Python antaresia maculosa* or *Liasis maculosa*), the skeletal morphology of the limbs is indistinguishable from the *Molurus* group. All results in this chapter refer to *Python molurus* unless otherwise specified.

2.1 Segmental identity in the python axial skeleton

Pythons have over 300 vertebrae (Fig. 18a), and ribs are present on every segment with the exceptions of the atlas and the caudal vertebrae of the tail (Fig. 18b, d). The morphology of the ribs is approximately uniform between the atlas and the leg/cloacal level, where the ribs abruptly change from long movable structures, to short, forked ribs (lymphapophyses) which are fused to the vertebrae (Fig. 18c). These lymphapophyses contain dorsal and ventral processes which protect the lymph hearts. The transitional vertebra between the free ribs and the lymphapophyses may represent the vestige of a sacral vertebra (Fig. 18d; Gadow, 1933), although a distinct sacral vertebra is not present (Romer, 1956). Posterior to the forked lymphapophyses-bearing series, the vertebrae lack true ribs but have short transverse processes, and are typically referred to as the caudal or tail vertebrae (Fig. 18d). Presence of ribs on all vertebrae anterior to the caudal series suggests that snakes may have undergone anterior and posterior expansion of thoracic identity along the axial skeleton, resulting in what appear to be serial homologues, but are actually secondarily similar structures. The anterior vertebrae do not show any clear transition in regional identity which, in other vertebrates, would indicate forelimb position.

The relationship between *Hox* gene expression and segmental identity was investigated in the snake axial skeleton in order to determine whether these morphological changes are associated with altered patterns of *Hox* gene expression. Whole-mount antibody staining of *Python molurus* embryos at 1 day of incubation was performed with antibodies against

HOXC6, HOXC8 and HOXB5 (Oliver *et al.*, 1988a, Oliver *et al.*, 1988b, Shashikant *et al.*, 1995, Wall *et al.*, 1992). The restricted transverse band of HOXC8 expression seen in the chick thorax (Fig. 19a, b), was not seen in the python, but instead HOXC8 expression was found to extend posteriorly from the anterior limit of the vertebral column (Fig. 19e) throughout the trunk (Fig. 19f). A precise posterior limit of expression can not be determined, but HOXC8 is expressed throughout the lymphapophysis-bearing vertebrae and expression fades posterior to the leg bud in the tail. HOXC6 and HOXB5 expression was examined in the trunks of embryos which had the limbs and head removed for other experiments. HOXC6 expression was detected in a segmental pattern in somites along the entire trunk (Fig. 19g), which contrasts with the restricted thoracic pattern of expression seen in the chick embryo, where the anterior boundary of expression marks the level of the forelimb (Fig. 19c). HOXB5 is expressed in the somites and dorsal root ganglia along the entire trunk (Fig. 19h), which is similar to the expression pattern seen in the chick (Fig. 19d) and mouse (Wall *et al.*, 1992). Thus, both HOXC6 and HOXC8, which are expressed exclusively in the thoracic region of the chick axial skeleton, are expressed throughout the python trunk. HOXB5, which is expressed up to a cervical level in chicks, is also expressed throughout the python axial skeleton. Expansion of rib-bearing vertebrae along the python body axis is tightly correlated with expansion of Hox gene expression domains characteristic of thoracic identity.

Figure 18. Morphological pattern in the python axial skeleton

Alcian blue and Alizarin red stained skeletal preparation of a spotted python embryo at 24 days of incubation. Hindlimb vestiges have been removed to improve visibility of the vertebrae. Anterior is to the left in **b-d**.

- a. Lateral view of complete skeleton. **b.** High power ventral view of the anterior axial skeleton and base of skull. Note the absence of ribs on the atlas (at). White arrowhead indicates hypapophysis extending ventrally from vertebral body. **c.** Lateral view of posterior axial skeleton. Arrows indicate lymphapophyses in cloacal region. Note the morphology of the rib on the transitional vertebra (t) that separates the vertebrae with large, movable ribs (left) and the lymphapophyses-bearing vertebrae (right). **d.** Dorsal view of posterior axial skeleton, showing clear morphological regionalization. d = thoracic/"dorsal" vertebrae, t = transitional vertebra, arrows = lymphapophyses-bearing vertebrae, and c = caudal vertebrae.

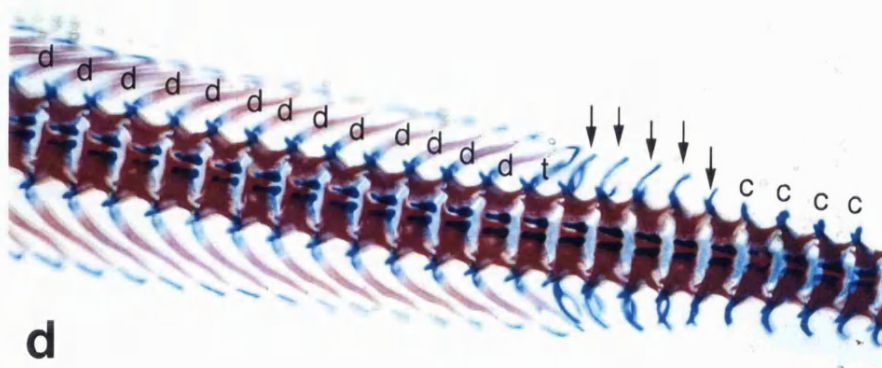
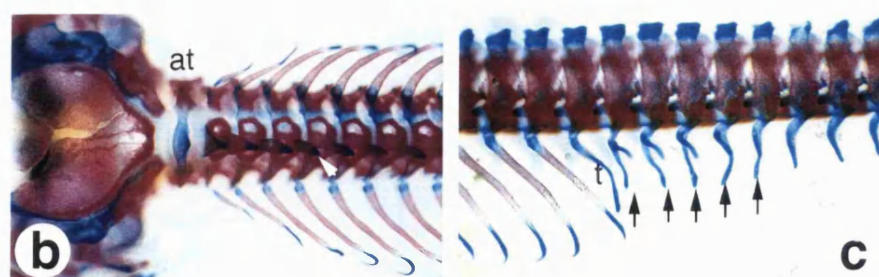
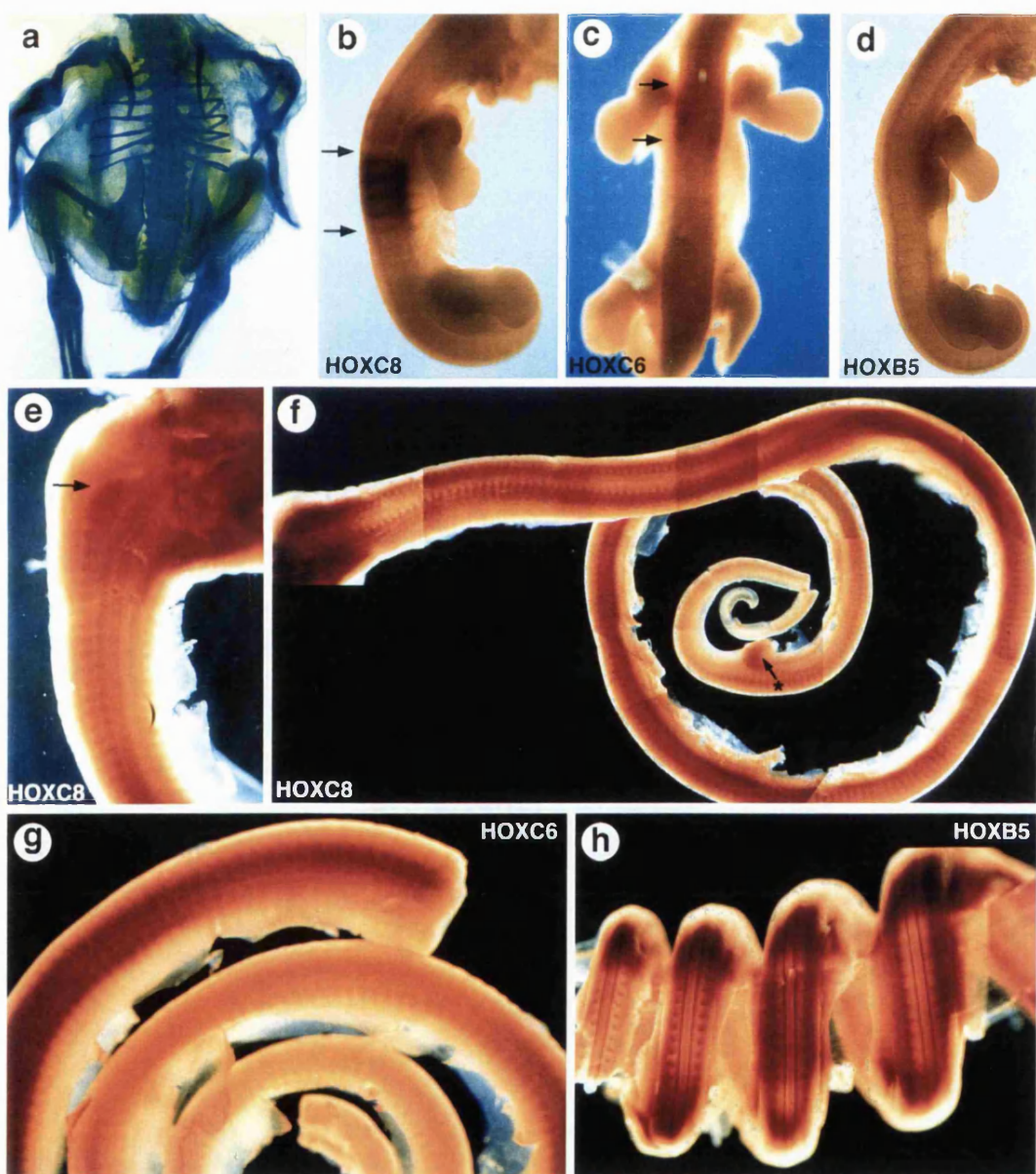
a**d**

Figure 19. Comparative *Hox* gene expression in python and chick embryos.

Whole mount antibody staining to show *Hox* gene expression patterns in stage 25 chick embryos and *Python molurus* embryos at 1 day of incubation. Anterior is at the top in **a-e** and **g**, left in **f**, and right in **h**. **a.** Skeletal preparation of a 10 day chick embryo to show the pattern of regionalization of the axial skeleton and position of the limbs. **b-d.** Expression of HOXC8 (**b**), HOXC6 (**c**) and HOXB5 (**d**) in stage 25 chick embryos. Arrows indicate anterior and posterior expression boundaries. **e.** Lateral view of anterior trunk and head of python embryo stained with HOXC8 antibody. Note expression extends to the anterior limit of the axial skeleton (arrow). **f.** Low power view of the embryo shown in panel **e**. Expression of HOXC8 is detected posterior to the anterior boundary, extending throughout the entire trunk and posterior to the leg bud (arrow with *). Expression fades in the tail. **g.** HOXC6 expression in a python embryo. Expression is detected throughout the entire trunk posterior to the head (head removed from this specimen), in a similar pattern to HOXC8. **h.** HOXB5 expression in a python embryo. HOXB5 expression is detected throughout the python trunk.



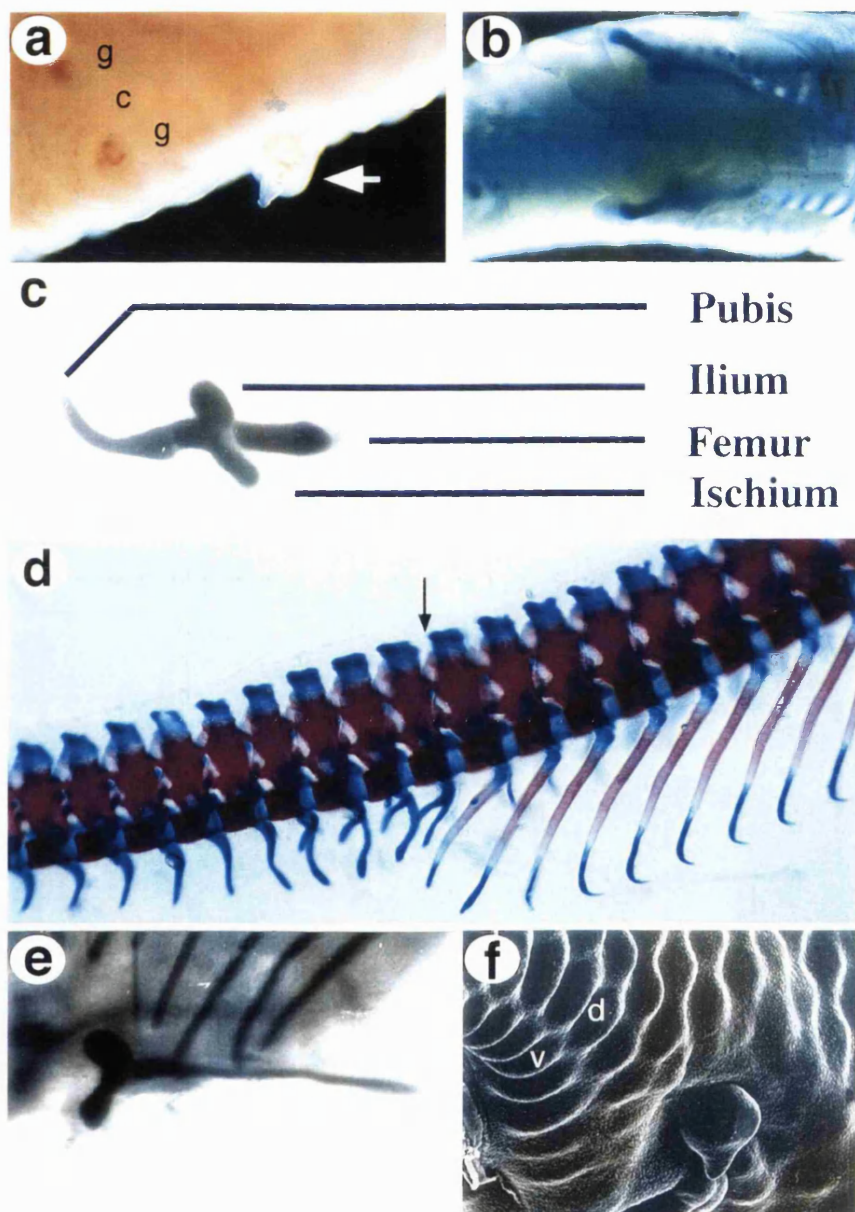
2.2 Morphology of python limbs

Mature pythons and boas possess paired "spurs", which are vestiges of the hindlimbs, situated ventrally on either side of the cloaca (Fig. 20a) (Bellairs, 1969, Raynaud, 1985). By 14 days of incubation, the skeleton of the Burmese python has formed in cartilage and can be visualized by staining with Alcian green. At this stage of development, all 3 elements of the pelvic girdle and the femur are visible (Fig. 20b). At 35 days of incubation, limb morphology has not changed significantly, although the terminal claw is visible and the pubis is considerably longer than the other elements (Fig. 20c). The limb is positioned along the body axis at the transition between rib-bearing thoracic vertebrae and lymphapophysis-bearing vertebrae, one of the only distinguishable morphological transitions in the axial skeleton (Fig. 20d, e, and see below). Interestingly, the dorsoventral position of the limb corresponds to the junction between dorsal body scale buds and wider ventral (belly) scale buds (Fig. 20f). There is no sign of forelimb buds, nor is there any evidence of cartilaginous limb rudiments anteriorly in the trunk.

Figure 20. Morphological pattern in python limbs

Anterior is to the right in all panels except **c**, where anterior is to the left.

- a.** Ventral view of a spotted python embryo at 24 days of incubation. The left hindlimb vestige (arrow) is visible at the level of the cloaca (c) and paired genital tubercles (g).
- b.** Ventral view of a Burmese python embryo at 14 days of incubation stained with Alcian green to reveal the skeletal pattern. The pelvis is visible within the body wall and the short femora can be seen protruding from the body wall.
- c.** Skeletal preparation of the hindlimb and associated pelvis dissected from the embryo shown in **b**. The femur and all three elements of the pelvic girdle are present (pubis, ilium and ischium).
- d.** Skeletal preparation showing the cloacal region of a spotted python embryo at 24 days of incubation. Arrow indicates the position of the hindlimb relative to the axial skeleton.
- e.** Skeletal preparation of the embryo shown in **a**. Note the presence of a terminal claw distal to the femur.
- f.** Scanning electron micrograph of spotted python embryo at 24 days of incubation. Note the hindlimb is positioned at the junction between the morphologically distinct dorsal scales (d) and ventral belly scales (v).



2.3 Early development of the python hindlimb bud

The presence of a complete pelvic girdle and a truncated femur in the Burmese python suggests that the earliest events in hindlimb development, specification of the position of the hindlimb with respect to dosoventral and anteroposterior axes, and initiation of limb development, have been maintained in pythons, but subsequent outgrowth of the hindlimb appears to be interrupted. Burmese python embryos have well-developed limb buds at the time of oviposition. Transverse sections of limb buds of an embryo at 1 day after laying indicate that the ectoderm has uniform thickness dorsoventrally, and an apical ridge could not be detected. Scanning electron microscopy indicates that at 4 days of incubation, the limb bud is well-developed (Fig. 21a), but no apical ridge is visible (Fig. 21b). At 5 days of incubation, the shape of the limb bud is altered, and the apex is slightly puckered and appears to be degenerating (Fig. 21c).

In order to determine the pattern of cell death, limb buds of python embryos between 1 and 5 days of incubation were stained with Nile blue sulphate. At day 1, although there was no apparent morphological ridge, a clear stripe of cell death was detected along the apex of the limb bud (Fig. 22a,b) in a pattern resembling that seen in the apical ridge of a stage 20 chick embryo . At day 5, the stripe of cell death was surprisingly similar to that observed at E1, with a clear pattern of punctate staining along the apex of the limb bud (Fig. 22c,d). Areas of the apex that appeared to be flat in SEM did not show increased uptake of Nile blue, but rather staining appeared uniform along the apex (compare Fig. 21c with Fig. 22c,d). A second discrete patch of staining was observed at the junction of the ventral surface of the limb bud and the body wall (Fig. 22. c,d). These results indicate that lack of an apical ectodermal ridge in the limb buds of the Burmese python is consistent with the condition described for other limbless

reptiles (Rahmani, 1974, Raynaud, 1977, Raynaud, 1985, Raynaud, 1990), although comparison with chick limbs indicates that lack of a ridge in pythons is not associated with a high level of cell death.

Figure 21. Scanning electron micrographs of python limb buds

- a.** Distal view of the right limb bud and trunk of a Burmese python embryo at 4 days of incubation.
- b.** High power view of the limb bud of a Burmese python embryo at 4 days of incubation. The distal tip of the bud lacks an apical ectodermal ridge.
- c.** Distal view of the limb bud of a Burmese python embryo at 5 days of incubation.

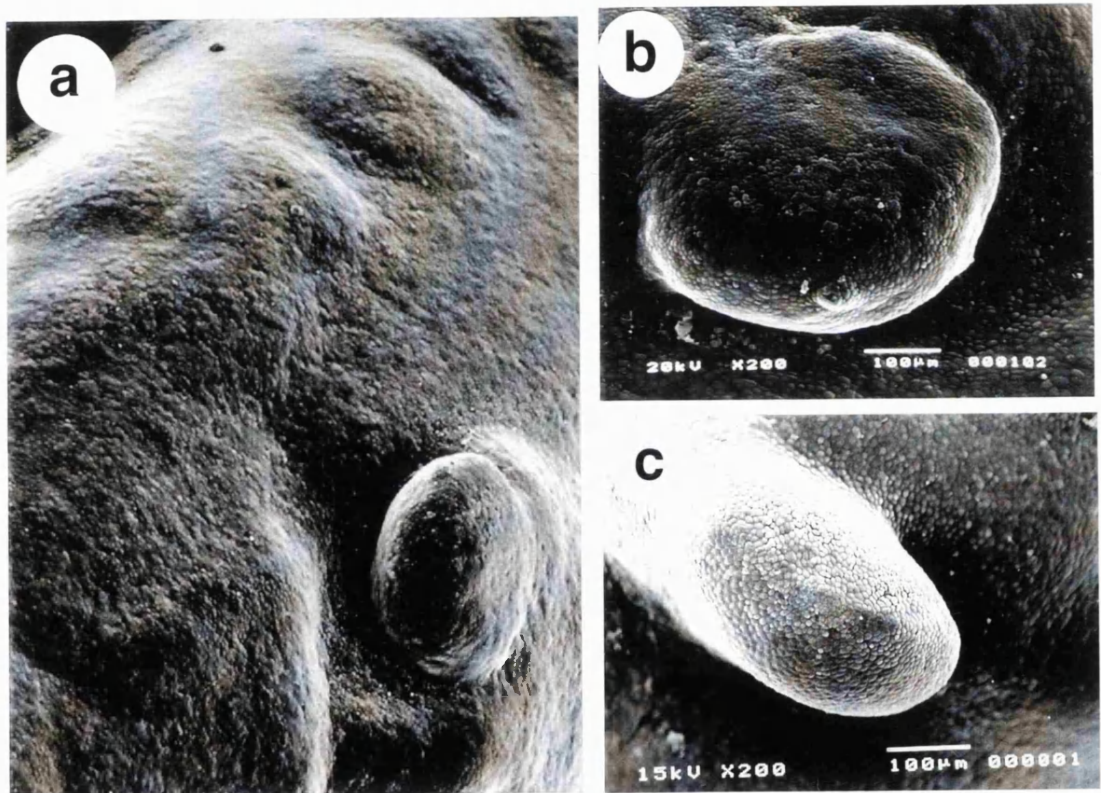
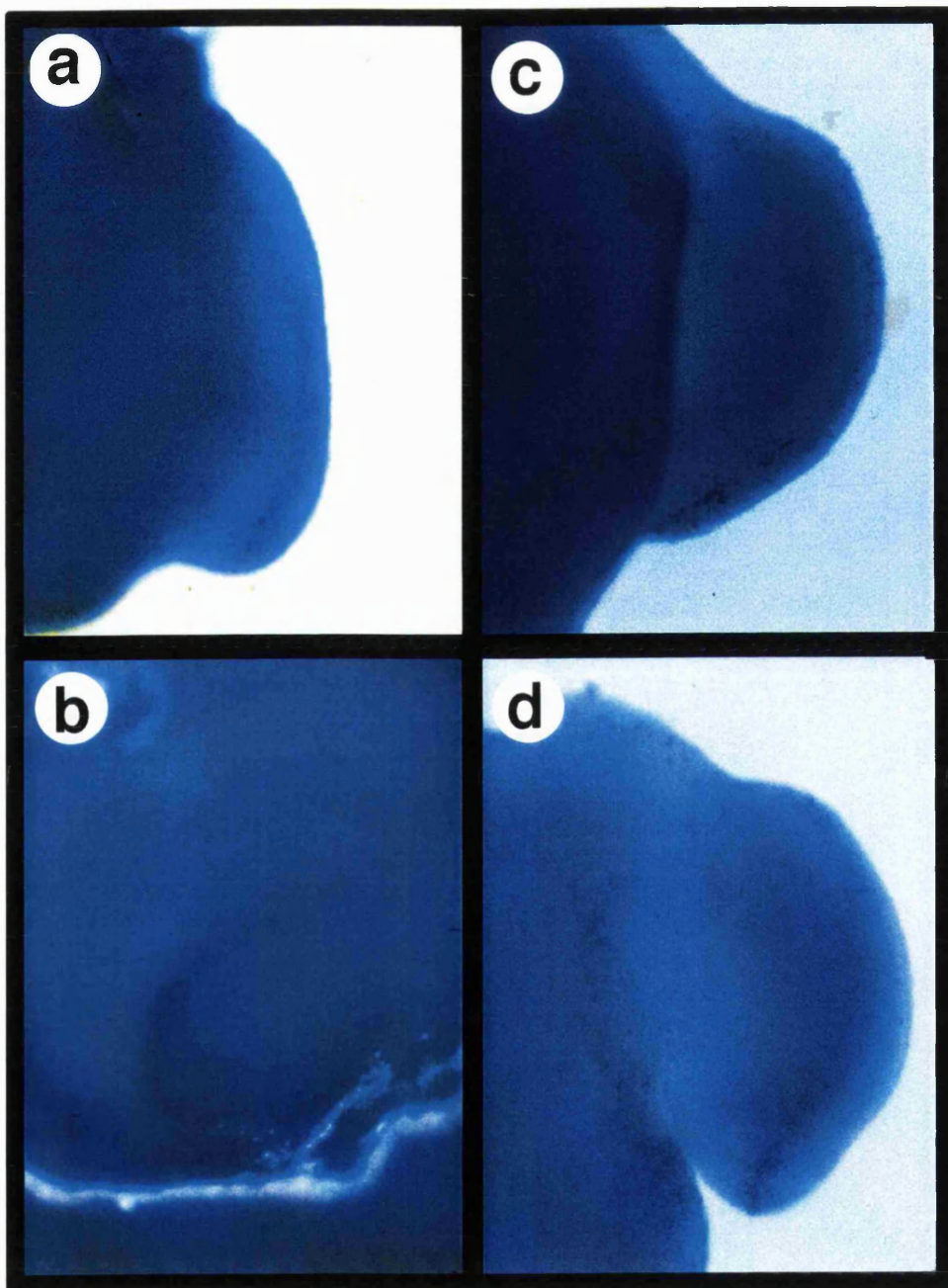


Figure 22. Cell death in python limb buds

Limb buds of Burmese pythons at 1 (**a, b**) and 5 (**c, d**) days of incubation stained with Nile blue sulphate to show the pattern of cell death. **a.** At 1 day of incubation, a thin stripe of dark, punctate staining is visible along the apex of the bud (**a.** ventral-distal view, **b.** apical view). **c, d.** At 5 days of incubation, a thin stripe of dark punctate staining, similar to that seen at 1 day, is visible along the apex of the bud (**c.** ventral view, **d.** apical view). Note staining at junction of ventral (left) aspect of the limb bud and the body wall in **d.**



2.4 Gene expression in the python limb ectoderm

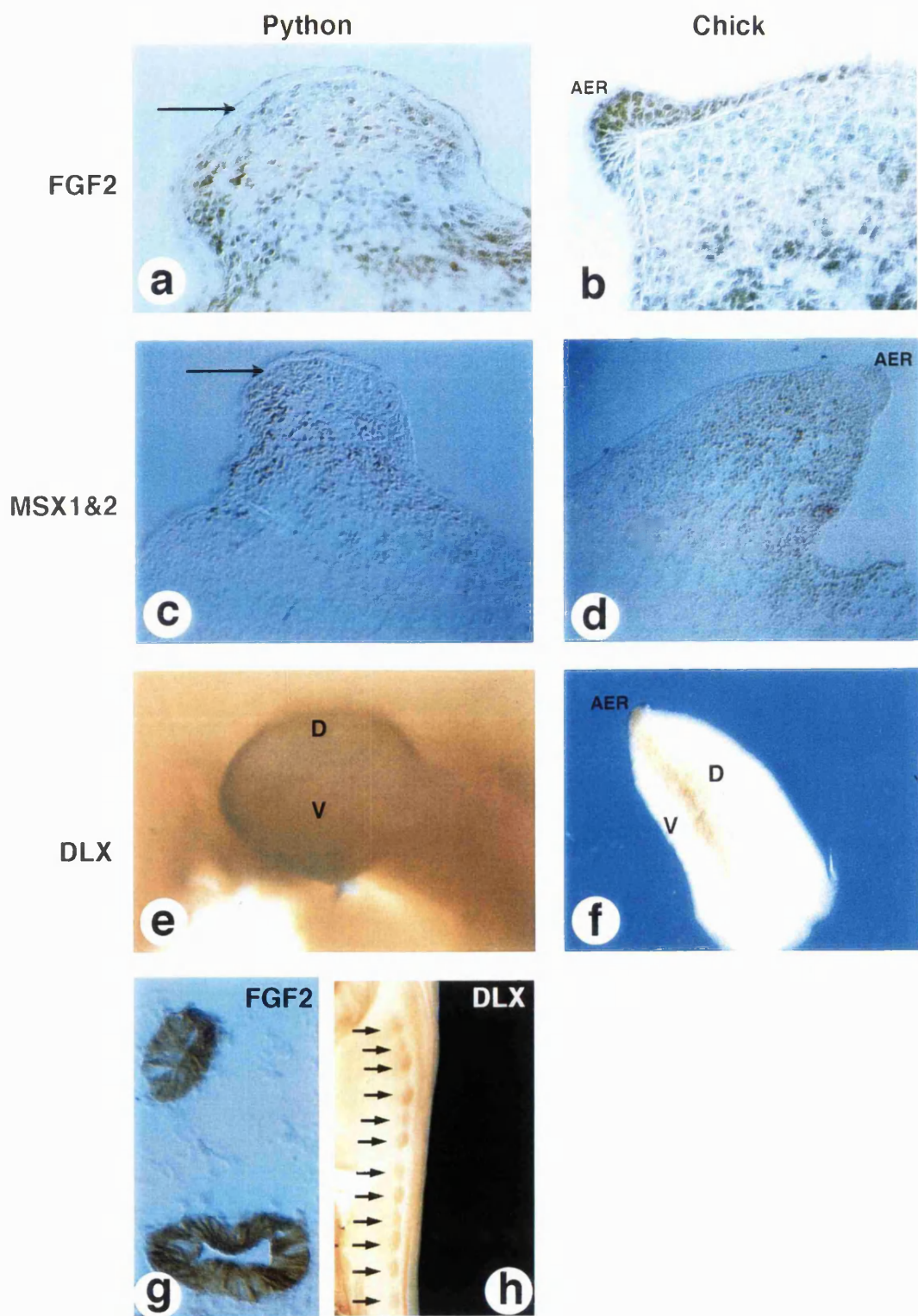
Absence of a morphologically distinct apical ridge suggested that pythons lack the specialized epithelium required for maintenance of limb outgrowth. To determine whether python limb bud ectoderm might nevertheless express genes normally associated with an apical ridge, expression of DLX, FGF2, and MSX genes was examined by staining embryos with antibodies against these proteins. The expression profile and specificity of these antibodies has been well-characterized in a variety of species (Dono and Zeller, 1994, Liem *et al.*, 1995, Panganiban *et al.*, 1995), and this approach allows direct comparison with chick embryos. In the chick embryo, FGF2 is expressed at high levels in limb bud ectoderm and at lower levels in the mesenchyme (Fig. 23b; (Dono and Zeller, 1994, Savage *et al.*, 1993), and functional assays have shown that FGF2 can substitute for the apical ridge (Fallon *et al.*, 1994). In the python limb bud, FGF2 is expressed in limb bud mesenchyme, but limb ectoderm, which appears to have a uniform thickness around the entire limb bud, was negative for FGF2 (Fig. 23a). Strong FGF2 expression was also detected in the developing kidney of the python embryo (Fig. 23g), as Dono and Zeller (1994) described for the chick embryo.

In mouse and chick embryos, *Msx2* is expressed in the apical ectodermal ridge and in anterior limb bud mesenchyme (Coelho *et al.*, 1991, Davidson *et al.*, 1991), and *Msx1* is expressed in a distal to proximal gradient in the limb mesenchyme and weakly in the apical ridge (Davidson *et al.*, 1991, Hill *et al.*, 1989). Mesenchymal expression of *Msx1* is maintained by the apical ridge and can be rescued by FGF after ridge removal (Fallon *et al.*, 1994, Vogel, Roberts, and Niswander, 1995). In chick embryos, using the monoclonal antibody 4G1, which recognizes both MSX1 and MSX2, nuclear expression was observed in the apical ridge, and in the

limb mesenchyme in a distal to proximal gradient of expression (Fig. 23d). This pattern of protein distribution is consistent with mRNA distribution described above. In python limb buds, MSX protein could not be detected in the limb ectoderm, but surprisingly, expression was detected in the mesenchyme in a distal to proximal gradient (Fig. 23c). Although it is not possible to distinguish between MSX1 and MSX2 expression in the mesenchymal domain, the lack of ectodermal staining indicates that neither MSX1 nor MSX2 are expressed in python limb ectoderm. Members of the *Dlx* family are also expressed in the apical ridge of fish and tetrapods (Fig. 23f) (Akimenko *et al.*, 1994, Bulfone *et al.*, 1993, Dolle, Price, and Duboule, 1992, Ferrari *et al.*, 1995). Using a *Dll* antibody which has been shown to detect *Dll* expression in several arthropods and DLX in the chick limb and zebrafish fin (Panganiban *et al.*, 1995), DLX expression was examined in python embryos. DLX expression was not detected in the python limb bud (Fig. 23e), although strong expression was detected in the developing teeth and scale buds at later stages (Fig. 23h). Control experiments in which the primary antibodies were omitted showed no staining. Thus, several of the transcription factors and growth factors that characterize the apical ridge are absent from the python limb bud ectoderm. These results show that the python limb bud ectoderm lacks morphological and molecular specializations that are characteristic of an apical ectodermal ridge. This suggests that limblessness results from failure to develop a functional apical ridge.

Figure 23. Gene expression in limb bud ectoderm

Antibody staining of python limb buds at 1 day of incubation (**a, c, e**) and stage 20 chick leg buds (**b, d, f**) with antibodies against FGF2, MSX, and DLX. **a.** FGF2 expression is present in python limb bud mesenchyme but could not be detected in the ectoderm (arrow). **b.** FGF2 expression is present in chick limb bud mesenchyme and ectoderm, with strong expression in the apical ectodermal ridge (AER). **c.** MSX expression is present in python limb bud mesenchyme in a proximal to distal gradient but could not be detected in the ectoderm (arrow). **d.** MSX expression is present in chick limb bud mesenchyme in a proximal to distal gradient, and is present in the apical ectodermal ridge (AER). **e.** DLX expression could not be detected in the python limb. As a control, python maxilla was stained with the DLX antibody (**h**), and strong expression was detected in the tooth buds (arrows). **f.** DLX expression was detected in the apical ectodermal ridge (AER) of the chick leg bud. **g.** FGF2 was detected in the python kidney, a known site of expression in the chick (Dono and Zeller, 1994).



2.5 Polarizing activity in python limbs and flank

Polarizing activity and *Shh* expression in chick limbs are maintained by the apical ridge (Vogel and Tickle, 1993; Laufer *et al.*, 1994; Niswander *et al.*, 1994). Therefore, given the lack of an apical ridge in python embryos, one might expect that the underlying mesenchyme of the limb would not express *Shh* or have polarizing activity. *Shh* expression was examined using an antibody against a small region of the N-terminal peptide, which recognizes the full-length and amino peptide of SHH (Bumcrot, Takada, and McMahon, 1995, Marti *et al.*, 1995b). In chick limb, this antibody detects SHH in close association with *Shh* mRNA in the polarizing region (Fig. 24b) (Marti *et al.*, 1995b). In python embryos at 2 days of incubation, SHH expression was detected in the floor plate of the neural tube and in the notochord, but SHH could not be detected in the limb buds (Fig. 24a). In order to determine whether python limb bud mesenchyme has polarizing activity, python posterior limb bud mesenchyme was transplanted under the apical ridge at the anterior margin of a stage 20 chick wing bud, and the skeletal pattern was examined after 10 days. This resulted in a digit pattern of **2-2-2-3-4**, indicating that python limb bud has polarizing activity (Fig. 24c). Python anterior limb mesenchyme cells were also grafted under the anterior apical ridge of the chick wing bud. Surprisingly, anterior cells were also found to have polarizing activity, inducing a digit pattern of **2-2-3-4** in the chick wing (Fig. 24d). Thus, although pythons do not express SHH, they have retained polarizing activity in the limb, but this activity appears to be weak and not posteriorly restricted. Moreover, the ability of python limb bud cells to induce digits in the chick indicates conservation of polarizing signals during evolution.

To determine whether the snake flank has potential polarizing

activity, flank tissue was taken from 3 different positions along the body axis and transplanted to the anterior margin of the chick limb. Given the difficulty in obtaining accurate somite counts, the coiling pattern of the embryo (3 coils posterior to the head) was used as a guide for determining axial level. The leg bud develops on the third coil. Flank tissue taken from anterior to the first coil as well as within the first coil had no effect on chick limb development. Flank cells from coil 2, however, were found to have polarizing activity. The chick embryo in which coil 2 flank cells were grafted died before digit identity could be determined, but the autopod showed a clear anterior duplication. This indicates that, although forelimb development has been completely lost in pythons, polarizing activity has been retained in the flank lateral plate mesoderm anterior to the leg.

2.6 Python SHH expression can be rescued by a chick apical ridge.

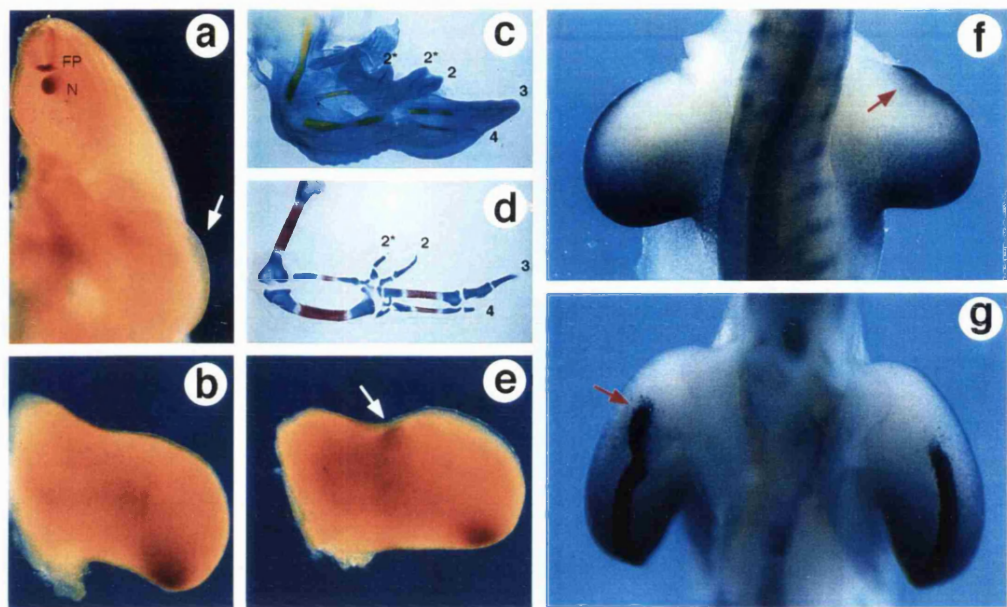
The polarizing activity of python mesenchyme could be due to activation of *Shh* when the cells are grafted to the chick limb bud. According to this idea, python SHH would then induce additional digits in the chick limb. This was tested by transplanting cells from the posterior margin of the python limb bud under the anterior apical ridge of the chick wing, and examining SHH expression after 24 hours. Remarkably, SHH was activated in the graft of python posterior limb mesenchyme (Fig. 24e). In order to determine whether chick cells are indeed responding to python SHH, expression of *Ptc* was examined following grafts of python posterior limb mesenchyme to the chick limb. Ectopic *Ptc* expression was detected anteriorly in chick limb cells around the python graft by 19.5 hours after transplantation (Fig. 24f). Thus, python limb bud mesenchyme has polarizing activity and potential to express SHH. This potential can be activated by exposure to chick apical ridge signals, and SHH produced by

the graft subsequently activates the SHH transduction pathway in neighboring chick cells.

Figure 24. Polarizing activity in python limb buds

Anterior is at the top in all panels

a. Python embryo at 2 days of incubation stained with an antibody against SHH. SHH expression (dark brown) could be detected in the floor plate (FP) and notochord (N), but could not be detected in the limb bud (arrow). b. SHH expression in the polarizing region of a chick wing bud. c. Wing of a ten day chick embryo with a duplicated pattern of digits that developed after transplantation of python posterior limb bud mesenchyme to the anterior margin of the wing bud at stage 20. Two additional digit 2s were specified anterior to the normal digits. (* = duplicated digits). d. Wing of a ten day chick embryo with a duplicated pattern of digits that developed after transplantation of python anterior limb bud mesenchyme to the anterior margin of the wing bud at stage 20. A single duplicated digit 2 is present anterior to the normal digits. e. SHH expression in a chick wing bud 24 hours after python posterior limb mesenchyme was grafted anteriorly under the apical ridge. SHH expression was detected in the graft of python cells (arrow) and in the chick polarizing region. f, g. Double *in situ* hybridization showing expression of chick *Ptc* and *Fgf8* 24 hours after transplantation of python posterior limb mesenchyme to the anterior margin of the chick right wing bud. Red arrow in f (dorsal view) indicates ectopic expression of chick *Ptc* in anterior mesenchyme around the grafted python cells. Red arrow in g (ventral view) indicates anteriorly extended domain of *Fgf8* in the chick ectoderm overlying the python mesenchyme cells (compare anterior limit of *Fgf8* expression in the limb containing the graft (left) with the contralateral limb (right)).



2.7 Failure of apical ridge formation in python limb buds

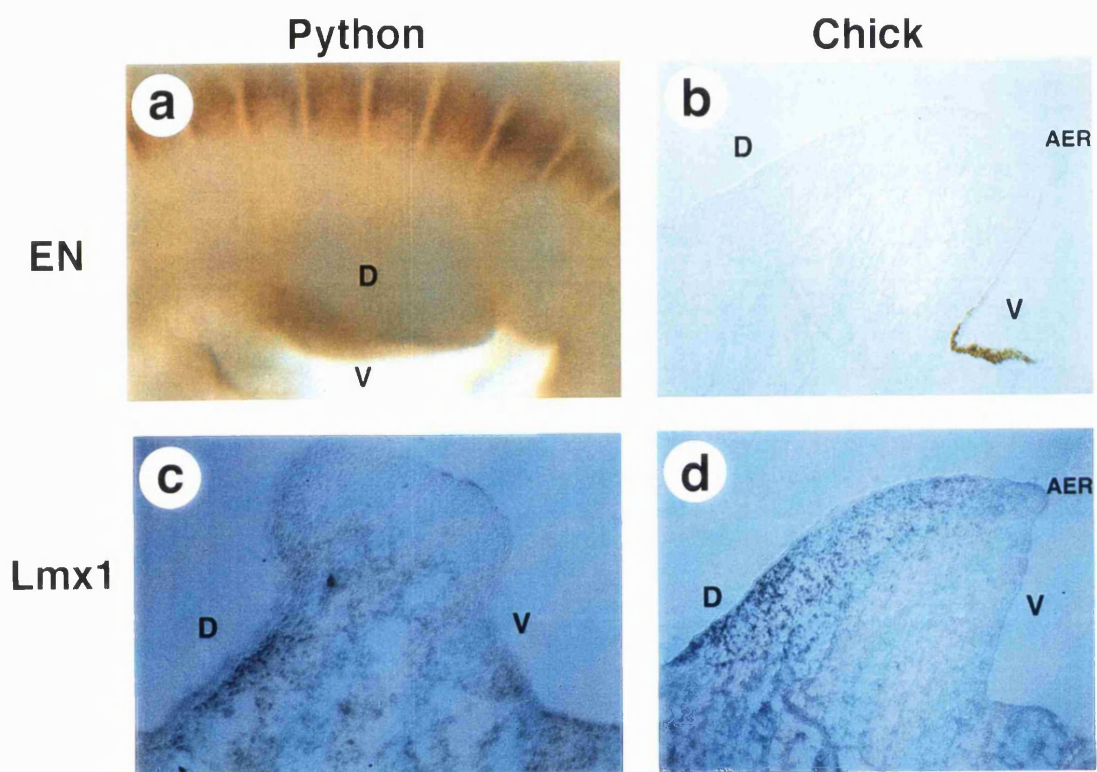
Failure of apical ridge formation in python limb buds could be due to either defective mesenchyme being unable to induce ridge formation in the ectoderm, or defective ectoderm being unable to respond to inductive signals from the mesenchyme. In chick embryos, transplantation of posterior mesenchyme to the anterior margin of the limb bud maintains the anterior part of the apical ridge which continues to express *Fgf8* (Ohuchi *et al.*, 1997). In order to determine whether python limb mesenchyme can maintain anterior ridge, posterior limb mesenchyme was transplanted from a 1 day python embryo to the anterior margin of a stage 20 chick limb, and expression of chick *Fgf8* gene was examined to determine the extent of the apical ridge. By 19.5 hours after transplantation, the python graft had maintained the *Fgf8* domain anteriorly in the chick limb (Fig. 24g), indicating that python limb mesenchyme can maintain an apical ridge. The ability of python limb mesenchyme to maintain the apical ridge in anterior ectoderm of the chick limb suggests that absence of an apical ridge in python limbs is due to defective ectoderm.

The molecular nature of ridge induction and maintenance is not yet understood but recent work has shown that dorsoventral compartmentalization of the limb ectoderm initially positions the ridge at the apex of the bud (See Chapter 1) (Grieshammer *et al.*, 1996, Laufer *et al.*, 1997, Loomis *et al.*, 1996, Noramly *et al.*, 1996, Rodriguez-Esteban *et al.*, 1997, Ros *et al.*, 1996). *Limbless* mutants lack *En1* in the ventral limb ectoderm, and *R-fng* and *Wnt7a* are expressed throughout the limb ectoderm, rather than being restricted to dorsal ectoderm. WNT7a signaling activates *Lmx1* expression throughout the dorsal mesenchyme of *limbless* mutants. In order to determine whether lack of dorsoventral compartmentalization of the ectoderm may underlie failure of apical ridge

formation in python limb ectoderm, dorsoventral polarity of the python limb bud was investigated using antibodies raised against the mouse EN protein (Davis *et al.*, 1991) and the chick LMX1 protein (Riddle *et al.*, 1995). In python limb buds, at 2 days after laying, EN expression was detected in the entire ventral part of the limb bud ectoderm, with a sharp boundary of expression running along the apex of the bud (Fig. 25a). LMX1 is expressed in dorsal limb mesenchyme within 7-10 cell diameters of the dorsal ectoderm (Fig. 25c). Strong nuclear staining can be seen proximally, but the expression domain is much weaker distally. Chick limb buds were stained with the same antibodies as controls. In the chick limb buds, EN expression was restricted to the ventral ectoderm and LMX expression was restricted to the dorsal mesenchyme (Fig. 25b,d). These results indicate that python leg buds have normal dorsoventral polarity.

Figure 25. Dorsoventral polarity in python limb buds.

Antibody staining to compare expression of EN and LMX1 in python limb buds at 1 day of incubation and chick limb buds at stage 20. **a, b.** Expression of EN is detected in the ventral ectoderm of the python limb bud (**a**) and the chick limb bud (**b**). EN expression is also seen in the python somites (**c**). Expression of LMX1 is detected in the dorsal mesenchyme of the python limb bud (**c**) and the chick limb bud (**d**). D = dorsal, V = ventral.



3. Discussion

The results presented in this chapter indicate that loss of regional specialization along the python body axis is associated with loss of regionalized Hox gene expression. The finding that anterior boundaries of Hox expression have been transposed to the anterior limit of the trunk suggests that failure to initiate forelimb development may be due to elimination of the regional specialization that is generated by staggered boundaries of Hox expression. The results also suggest that a deficiency in the hindlimb ectoderm is the basis for limblessness. The initial events of python leg development appear to be in place, but the transition between limb initiation and maintenance of limb outgrowth is disrupted by failure to form a functional apical ridge. The patterns of gene expression and the ability of python limb bud mesenchyme to respond to chick ridge signals by expressing SHH, and to signal back to chick cells, indicate that signaling pathways involved in vertebrate limb development have been conserved in pythons.

3.1 Hox gene expression and regionalization of the python body axis

The coordinated transposition of vertebral identity and Hox gene expression boundaries along the python body axis strongly suggests that the axial skeleton has been modified in snake evolution by changes in the upstream regulatory elements that control Hox gene expression. Accordingly, the anterior and posterior boundaries of *Hoxc6* and *Hoxc8* expression have been anteroposteriorly expanded along the paraxial mesoderm, and a thoracic positional value has been assigned to all somites within the domain. The differences seen within the rib bearing vertebrae, such as size, shape, presence of ventral hypapophyses at the anterior and posterior ends of the column, and presence of free ribs vs. lymphapophyses,

may be generated by different combinations of other Hox genes or differences in level of Hox gene expression (Pollock, Jay, and Bieberich, 1992).

The compete absence of forelimb development in pythons is associated with loss of clear regionalization of the axial skeleton, whereas, the hindlimb develops in a region of morphological specialization. In many tetrapod vertebrates, the forelimb forms opposite the cervical-thoracic transition and anterior boundary of *Hoxc6* in the paraxial mesoderm (Gaunt, 1994; Burke *et al.*, 1995). Although Hox gene expression in paraxial and lateral plate mesoderm is clearly under independent regulation (see chapter 4), specification of limb position in the neural tube and lateral plate mesoderm must be aligned, and the possibility of mediolateral signaling during limb induction has not been excluded (reviewed in chapter 1). It is therefore tempting to speculate that during evolution of a more uniform body plan, in particular anterior to the cloaca, loss of staggered Hox gene expression boundaries may have eliminated forelimb inductive signals (or responses) that were localized to the pectoral position. The position of the hindlimb buds and cloacal opening (lateral plate mesoderm) and the thoracic-sacral transition (paraxial mesoderm) at the same axial level suggests the presence of a more posterior Hox expression boundary in both tissues.

The uniform pattern of vertebrae in snakes is reminiscent of segmental identity in the trunk of myriapods. Grenier *et al.* have recently examined Hox gene expression in the centipede, which has 22 limb-bearing trunk segments posterior to the head (Grenier *et al.*, 1997). In insects *Ubx/abd-A* expression is associated with limblessness in abdominal segments (Vachon *et al.*, 1992), however in centipedes *Ubx/abd-A*

expression is detected in almost the entire trunk (Grenier *et al.*, 1997). Thus, in both centipedes and snakes, uniform Hox gene expression is associated with uniformity of segmental identity.

3.2 Dorsoventral position of the hindlimb

Position of the limb with respect to the dorsoventral axis corresponds with the transition from dorsal scales to wider ventral "belly" scales in the ectoderm. In chicks, the entire trunk ectoderm is compartmentalized (Altabef *et al.*, 1997). Dorsoventral position of the chick limb appears to be under the control of ectodermal factors (Michaud, Lapointe, and Le Douarin, 1997, Tanaka *et al.*, 1997). Thus, scale identity in pythons may reflect the dorsoventral polarity of the ectoderm. According to this idea, scales that form in the dorsal ectoderm have a different morphology than the scales that form in the ventral ectoderm due to different positional values of dorsal and ventral ectoderm. The fact that the junction between dorsal and ventral scales corresponds to the position at which the limb bud arises suggests that limb position and scale identity may be coordinated by factors that control dorsoventral polarity of the ectoderm.

3.3 Failure of hindlimb development

It is striking that the python limb bud has a normal tetrapod pattern of dorsoventral polarity at the molecular level, yet the apical ridge does not form. The pattern contrasts with that seen in *limbless* mutants, which fail to form a ridge because the dorsoventral compartmentalization of the limb ectoderm is lost and the entire limb is dorsalized. During normal ridge induction, the limb bud mesenchyme induces ridge formation by signaling to the overlying ectoderm, and dorsoventrally polarized factors in the limb ectoderm position the ridge by restricting to the dorsal-ventral junction (apex) the competence to respond to the inductive signals. The dorsoventrally

restricted pattern of LMX and EN expression in the python limb suggests that python *R-fng*, if expressed at all, is restricted to the dorsal ectoderm. These results, together with the ability of python limb mesenchyme to maintain ridge formation in the chick, suggest that python limblessness is due to an ectodermal defect that lies downstream of both dorsoventral compartmentalization of the ectoderm (*Wnt7a*, *R-fng* and *En1*) and mesenchymal signaling and probably disrupts interpretation of mesenchymal signals or physical assembly of the ridge.

Transplantation experiments show that python limb mesenchyme is competent to express SHH, but does not normally do so. When python limb cells are placed under a functional apical ridge, this competence is realized and *Shh* is activated in the python cells. SHH protein produced by python cells can be detected by an antibody against the N-terminal region of the mouse SHH peptide, and can induce expression of chicken *ptc* and establish a feedback loop in the chick limb, indicating strong evolutionary conservation of the python *Shh* gene. Moreover, the ability of python limb mesenchyme to maintain the chick apical ridge and associated *Fgf8* expression anteriorly indicates that python limb mesenchyme has retained the ability to maintain the apical ridge, and suggests that the defect may be an inability of python limb ectoderm to respond to mesenchymal inductive signals. In the absence of an apical ridge, *Shh* is not induced in cells with polarizing potential, and the positive feedback loop needed to coordinate outgrowth and patterning (Niswander *et al.*, 1994; Laufer *et al.*, 1994) is not established. The extent of development seen in the python limb approximates that seen in the *Shh* knockout mouse, in which the girdle and proximal part of the femur develop (Chiang *et al.*, 1996). The results of the python experiments described here together with the *Shh* knockout support the idea that *Shh* is not required for development of proximal limb elements.

Polarizing activity in the python leg bud does not appear to be restricted to the posterior; weak polarizing activity is also found anteriorly. The mechanisms involved in restricting polarizing activity in tetrapods would have been released from selective pressure once distal structures had been lost in ancestral snakes. Presence of polarized pentadactyl limbs in the marine mosasaurs (Carroll, 1988), the closest relatives of snakes (Caldwell and Lee, 1997), suggests that anterior polarizing activity in the python does not reflect a polydactylous ancestry, but is more likely a consequence of more recent changes that occurred after the autopod was lost.

Python flank cells have potential polarizing activity which can be activated by transplantation under the apical ridge of a chick limb bud. In chick embryos, the anterior limit of polarizing activity marks the posterior margin of the prospective forelimb bud (Hornbruch and Wolpert, 1991). The anterior limit of potential polarizing activity in the python embryo may be between the first and second coils of the trunk, suggesting that the primitive forelimb may have formed at this position. If polarizing activity in the flank was no longer stabilized after the forelimb was lost, however, then the original boundary may have been altered. Although the entire trunk anterior to the leg bud has been transformed towards thorax (flank), the anterior limit of polarizing potential may be restricted to a more posterior position. A similar dissociation between regional identity and polarizing potential is seen when extra limbs are induced; flank cells are anteriorized towards a wing identity, but the distribution of polarizing potential in the flank is unaffected.

The apparent weakness of python polarizing activity appears to be within the normal range for limbed reptiles. Fallon and Crosby (1977) and

Honig (1984) transplanted alligator, turtle, lizard and snapping turtle polarizing region cells to chick limb buds and found that while they all had polarizing activity, none could induce a full duplication in the chick. Honig (1984) suggested that this could be due to temperature differences between chick and reptile, although it is possible that reptile limbs may be polarized by relatively weaker signals.

3.4 Rescuing snake limb development

The results presented in this chapter raise the question of whether limb development could be rescued in modern snakes if missing factor(s) could be restored. In the python hindlimb, initiation of limb budding appears to be normal, but establishment of the positive feedback loop between the apical ridge and polarizing region is disrupted by an ectodermal defect that prevents cells from responding to inductive signals. FGFs can rescue limb development in *limb/less* and *wing/less* mutants which fail to form a ridge. My own preliminary experiments have shown that FGF2 can induce outgrowth of the python genital tubercle, and Raynaud and colleagues have shown that addition of FGF2 can delay involution of slow worm limb buds in organ culture (Raynaud *et al.*, 1995). The presence of polarizing potential in python limb buds suggests that application of FGF may be sufficient to rescue limb development in the python. In the context of the python limb bud, FGF would act as a substitute for a defective ectoderm which is unable to send, and possibly to receive, signals involved in the positive feedback loop described by Niswander *et al.* (1994) and Laufer *et al.* (1994). Based on the pattern of gene expression, one would predict that the limb would have a normal dorsoventral polarity, perhaps with duplicated digits arising from the weak anterior polarizing potential. This experiment should also have important phylogenetic significance, because if pythons are in fact descendants of mosasauroids, then the ankle of the snake leg should have a

separate astragalus and calcaneum, a condition found in the hindlimb of mosasaurs but none of the other squamates (Caldwell and Lee, 1997).

3.5 Evolution of the snake body plan

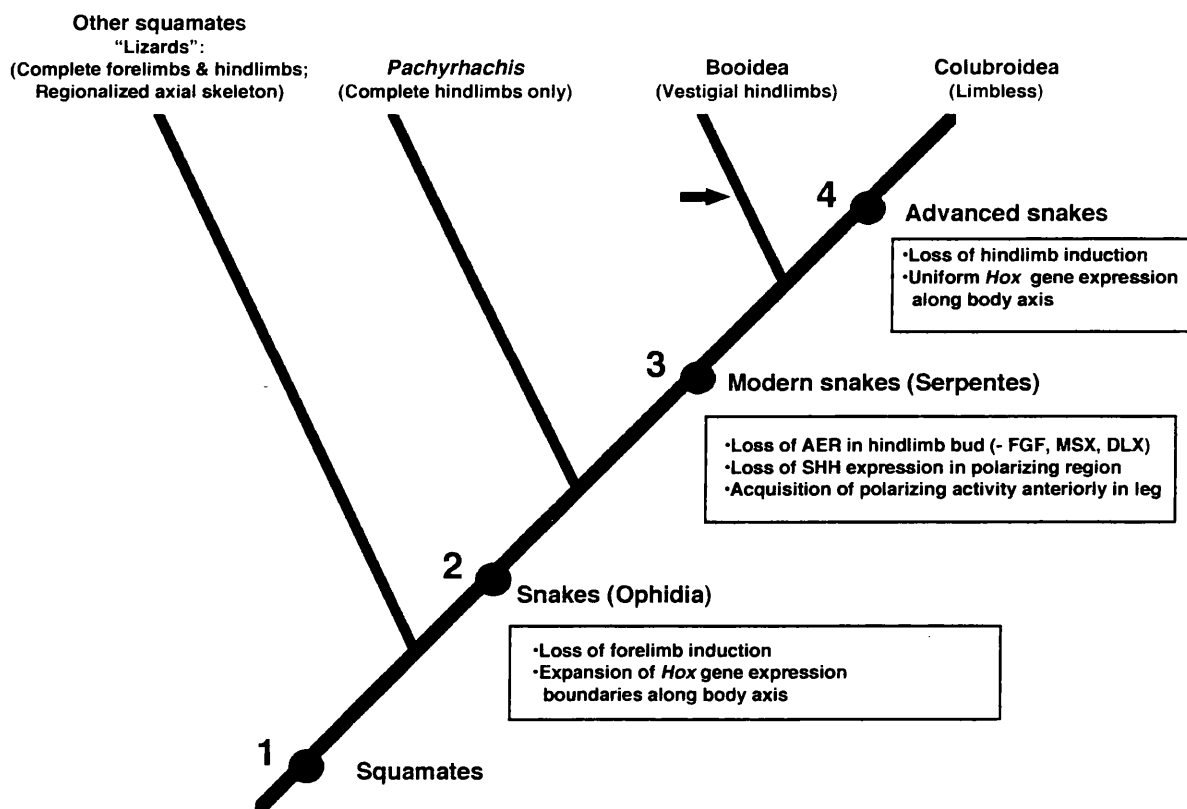
The results presented in this chapter have implications for understanding the developmental mechanisms that underlie key changes in evolution of the snake body plan. Snakes evolved from tetrapod lizards, which have complete forelimbs and hindlimbs and a clearly regionalized axial skeleton as a primitive condition (Fig. 26, node 1; Romer, 1956). Recent work has shown that the closest relatives of snakes are marine mosasaurs (Caldwell and Lee, 1997). The most primitive snake known, *Pachyrhachis problematicus*, supports the link between mosasaurs and snakes, and shows that most of the morphological features of modern snakes, including loss of the pectoral girdle and forelimb, elongation of the trunk and loss of a clearly regionalized vertebral column, were in place by the mid-Cretaceous (~100 MYA; Carroll, 1987; Caldwell and Lee, 1997). Together with the results presented in this chapter, this suggests that loss of pectoral limb initiation signals (i.e., FGF), and expansion of Hox gene expression along the main body axis had already occurred in the *Pachyrhachis* lineage (Fig. 26, node 2). Changes in hindlimb bud ectoderm that resulted in loss of apical ridge formation and loss of *Shh* expression appear to have occurred after the divergence of the *Pachyrhachis* lineage and prior to the divergence of the lineage leading to pythons and boas (Fig. 26, node 3), because the *Pachyrhachis* hindlimb was complete from the well-developed pelvic girdle to the tarsals and possibly digits (Caldwell and Lee, 1997; M. Caldwell, pers. comm.). The presence of polarized, pentadactyl limbs in mosasaurs (Carroll, 1988) supports the proposed position of this event in figure 26. If anterior polarizing activity had been acquired earlier, then one would expect to find polydactyly in the mosasaur

lineage.

The postcranial skeleton of pythons and boas (Booidea) differs than that of advanced snakes (Colubroidea). Pythons posses vestigial hindlimbs, and hypapophyses are found only on the first 64 vertebrae, whereas colubrids are completely limbless and all of the vertebrae contain hypapophyses. Based on the results reported in this chapter, one can predict that the transition from a boid-like body plan to the colubrid body plan must have involved loss of hindlimb bud initiation and further expansion of Hox gene expression domains along the primary body axis (Fig. 26, node 4). Examination of expression patterns of genes that characterize the early limb and the patterns of Hox gene expression in extant colubrids will further test these hypotheses.

Figure 26. Developmental model for evolution of the snake body plan

Phylogenetic relationships among these taxa based on the work of Caldwell and Lee (Caldwell and Lee, 1997) and Rieppel (Rieppel, 1988). Tree shows evolutionary relationships among the following (in bold: the primitive snake *Pachyrhachis problematicus*, which lacks forelimbs, has complete or near-complete hindlimbs and a large number of similar vertebrae which nonetheless have identifiable regional differences; **Booidea** (including pythons and boids) which lack forelimbs, have vestigial hindlimbs and a large number of morphologically uniform vertebrae with few or equivocal regional differences; **Colubroidea** (advanced snakes) which lack both forelimbs and hindlimbs and have a large number of near-identical vertebrae; and all other **squamates** which have complete forelimbs and hindlimbs and a clearly regionalized axial skeleton as a primitive condition. Node **1** indicates the origin of squamates, node **2** indicates the origin of snakes, node **3** indicates the origin of modern snakes, and node **4** indicates the origin of advanced snakes. Boxes located between nodes **1**, **2**, **3**, and **4** contain proposed developmental events associated with evolutionary changes to the snake body plan. Justification for each of the proposed events is contained within the main text of this chapter (section 3.5). In this scheme, it is assumed that the primitive condition at node 1 is a morphologically regionalized axial skeleton and complete, normally polarized forelimbs and hindlimbs. Arrow indicates the lineage to which pythons belong.



CHAPTER SIX: General Discussion

1. FGF as limb initiation signal

In this thesis, I have shown that fibroblast growth factors can induce formation of complete additional limbs when applied to the flank of pre-limb bud stage chick embryos. This work, which was published in 1995 (Cohn *et al.*, 1995), suggested that a member of the FGF family could be the endogenous limb initiation signal, and it now appears that the newest member of the FGF family, FGF10, may be this signal (See chapter 3).

2. Positioning FGF along the body axis

The position in which *Fgf10* is expressed along the primary body axis could determine the position at which limbs form. In chapter 4, I showed that FGF application reprograms the pattern of *Hox* gene expression in the flank to reproduce a wing or leg expression pattern *before* a new domain of *Fgf8* expression is induced, suggesting that the early primary pattern of *Hox* gene expression in lateral plate mesoderm along the primary body axis specifies the positions where limbs develop. An attractive hypothesis is that local expression of *Fgf* in the lateral plate may be under the control of *Hox* genes. This idea is supported by the recent finding that HOXB7 directly activates bFGF expression in melanoma cell lines and primary cultures (Caré *et al.*, 1996). The FGF2 promoter region contains at least 5 homeoprotein binding sites, and *in vitro* assays show that HOXB7 protein induces a dose-dependent increase in bFGF promoter activity. Moreover, blocking HOXB7 activity with antisense oligonucleotides inhibits bFGF expression and cell proliferation in melanoma cell lines (Caré *et al.*, 1996). Thus, it appears that at least one *Hox* gene can directly activate transcription of bFGF. Disruption and overexpression of multiple *Hox* genes in lateral plate mesoderm should indicate whether *Hox* genes are involved in activation of

FGF during limb induction. All 4 paralogues of the *Hox9* group have been knocked-out individually and two double mutants have been generated (Chen and Capecchi, 1997, Fromental-Ramain *et al.*, 1996, Suemori, Takahashi, and Noguchi, 1995), but none of these experiments have informed the problem of limb initiation. Although limb phenotypes have been observed in some mutants (Fromental-Ramain *et al.*, 1996), none have developed changes in limb position. Interpretation of these results is complicated by the ability of *Hox* genes to act synergistically (Chen and Capecchi, 1997) and the discovery that loss of function of a single *Hox* gene can have a collateral effects on expression of other *Hox* genes. For example, mice with mutations in *Hoxc9* were found to have extended domains of *Hoxc8* expression (Suemori *et al.*, 1995). Generation of quadruple mutants to knock-out entire parologue groups should be informative, and monitoring the responses of other *Hox* genes should be an important component of these studies.

How is FGF maintained at limb levels? *Fgf10* is expressed in lateral plate mesoderm of the limbs and flank through stage 12, after which expression is downregulated in the flank but maintained in the limbs (Ohuchi, 1997). In *Xenopus*, e β FGF is activated by *Xbra*, and e β FGF feeds back to maintain continued expression of *Xbra* (Schulte-Merker and Smith, 1995). *Xbra* is a *Xenopus* homologue of the *Brachyury* or *T* gene, and recent work has identified a family of genes, *Tbx*, which contain a region homologous to the DNA-binding region of the *T* gene, known a T-box (Gibson-Brown *et al.*, 1996). Interestingly, *Tbx5* and *Tbx4* are expressed in the forelimb and hindlimb, respectively, from stage 13 (Ohuchi *et al.*, 1997). Thus, based on the e β FGF - *Xbra* positive feedback loop in frogs, it is possible that *Tbx* expression in the limbs could maintain expression of *Fgf10* in the limbs when it is downregulated in the flank, and FGF could, in turn, feedback

to maintain expression of *Tbx* in the limbs. If this is correct, then loss of function mutations (or compound mutations) in *Tbx* genes may result in loss or truncation of the limbs.

3. Reprograming Hox expression in the flank

The ability of FGF to transform positional identity and *Hox* gene expression in chick lateral plate mesoderm is similar to the role proposed for FGF in patterning the a-p axis in *Xenopus* (Doniach, 1995, Isaacs, Pownall, and Slack, 1994, Pownall *et al.*, 1996, Ruiz i Altaba and Melton, 1989). Experiments in *Xenopus* have shown that FGF acts as a posteriorizing factor during mesoderm induction and at gastrula and neurula stages by induction of posterior *Hox* genes (including *Hoxb9*) via *Xcad* (a *caudal* [cdx] homologue) (Pownall *et al.*, 1996). How does FGF induce a differential response of *Hox* genes in chick lateral plate mesoderm according to position? The elapsed time between FGF application and the earliest changes in *Hox* expression suggests that regulation of *Hox* gene expression patterns by FGF is unlikely to be a direct effect. Instead FGF may interfere with systems which regulate expression of *Hox* genes. After *Hox* gene expression has been initiated, patterns are stabilized by regulatory proteins belonging to the *Trithorax* group (trxG) or *Polycomb* group (PcG). *Trithorax* and *Polycomb* (in *Drosophila*), and their homologues in vertebrates, act by respectively maintaining the "on" state in *Hox* genes that have been transcriptionally activated, or the "off" state in *Hox* genes that have been repressed (Simon, 1995). In heterozygous mutants for the *Mixed-lineage leukaemia* (*Mll*) gene, a mouse homologue of trithorax, *Hox* gene expression is not maintained and both anterior and posterior homeotic transformations are observed in the vertebral column (Yu *et al.*, 1995). This is reminiscent of the ability of FGF to induce changes in *Hox* gene expression that lead to bidirectional transformations of cell fate in flank

lateral plate mesoderm (i.e., anterior to wing and posterior to leg). If FGF locally interferes with such regulatory genes in lateral plate mesoderm, this could explain how a single factor induces limbs of different types according to where it is applied. The mechanism by which FGF acts on Hox gene expression needs to be explored further, and it will be interesting to determine how chick homologues of *trxG*, *PcG* and *Cdx* genes respond to FGF application to different positions along the body axis.

4. Implications for co-ordinating axial patterning

The ability of FGF to alter *Hox9* gene expression exclusively in lateral plate mesoderm, even when FGF beads are placed directly in the paraxial mesoderm, indicates that Hox gene expression can be independently regulated in the neural tube, paraxial and lateral plate mesoderm. Although modularity has clear evolutionary advantages, the positional relationship of the brachial and sacral plexus and the fore-and hindlimbs must be co-ordinated for the limbs to be properly wired and functional. The nature of this relationship remains to be determined, but the results presented in this thesis suggest that the tissues are linked by a mechanism that does not involve coregulation of Hox gene expression. The observations of Oliver *et al.* (1989) and Burke *et al* (1995) -- that forelimbs develop in lateral plate mesoderm opposite the anterior boundary of *Hoxc6* expression in paraxial mesoderm -- may reflect the presence of secondary signals induced by Hox genes which act to coordinate axial patterning in different tissues. Complete loss of the forelimb in pythons may be due to anterior extension of *Hoxc6* (and possibly *Hox9*) expression boundaries, which cause uniformity of pattern along the body axis and may eliminate specialized signaling regions that normally act to induce limb initiation.

5. Evolution of body plans

The observation that *Hox* gene expression is uniform in the morphologically uniform vertebrae of pythons indicates that changes in *Hox* regulation have occurred in snake evolution. Comparative analyses of *Hox* gene expression in insects and crustacea have revealed that evolutionary diversification of the arthropods has involved changes upstream of the *Hox* genes (Averof and Patel, 1997) and downstream of the *Hox* genes (Warren *et al.*, 1994). My analysis of *Hox* gene expression in pythons, taken together with the chick and mouse comparison of Gaunt (1994) and Burke *et al.* (1995), provides strong evidence that modification upstream of the *Hox* genes is a viable route for evolutionary diversification of vertebrates.

These results raise several further questions that will need to be resolved by cloning and studying the expression patterns of python *Hox* genes. Differential *Hox* gene expression in paraxial mesoderm is involved in patterning the vertebrate hindbrain (Itasaki *et al.*, 1996), which controls the pattern of cranial nerves. The pattern of *Hox* gene expression in the python paraxial mesoderm begs the question of how hindbrain patterning is achieved in snakes. This should be clarified by examining expression of more anterior *Hox* genes, in particular the *Hox1*, *Hox2* and *Hox4* parologue groups.

Another key question emerging from this work and the work of Aparicio *et al.* (1997) deals with organization of the snake *Hox* complex. The *Hox* complex of the pufferfish *Fugu* is now known to have undergone extensive evolution, involving loss of up to 11 *Hox* genes (and a possible gain of 1) (Aparicio *et al.*, 1997). *Fugu* has an extremely derived body plan which includes loss of the pelvic fins and ribs. Snakes have dispensed with much of the postcranial specialization seen in other vertebrates (although

the head is highly specialized) in evolution of a generalized, uniform body plan. It will be interesting to determine to what extent these morphological changes are rooted in genomic changes, in contrast to the regulatory changes demonstrated in this thesis. Finally, the experimental analysis of the python hindlimb bud strongly suggests that application of FGF should rescue python limb development .

REFERENCES

- Abraham, J. A., A. Mergia, J. L. Whang, A. Tumolo, J. Friedman, K. A. Hjerrild, D. Gospodarowicz, and J. C. Fiddes. (1986). Nucleotide sequence of a bovine clone encoding the angiogenic protein, basic fibroblast growth factor. *Science* 233 : 545-8.
- Abud, H. E., J. A. Skinner, F. J. McDonald, M. T. Bedford, P. Lonai, and J. K. Heath. (1996). Ectopic expression of Fgf-4 in chimeric mouse embryos induces the expression of early markers of limb development in the lateral ridge. *Dev Genet* 19 : 51-65.
- Agar, W. E. (1907). The development of the anterior mesoderm, and paired fins with their nerves, in *Lepidosiren* and *Protopterus*. *Trans. Roy. Soc. Edin.* 45 : 611-640.
- Akam, M., M. Averof, J. Castelli-Gair, R. Dawes, F. Falciani, and D. Ferrier. (1994). The evolving role of Hox genes in arthropods. *Development Supplement* : 209-215.
- Akimenko, A.-M., S. Johnson, M. Westerfield, and M. Ekker. (1995). Differential induction of four *msx* homeobox genes during fin development and regeneration in zebrafish. *Development* 121 : 347-357.
- Akimenko, M.-A., and M. Ekker. (1995). Anterior duplication of the *Sonic hedgehog* expression protein in the pectoral fin buds of zebrafish treated with retinoic acid. *Dev. Biol.* 170 : 243-247.
- Akimenko, M. A., M. Ekker, J. Wegner, W. Lin, and M. Westerfield. (1994). Combinatorial expression of three zebrafish genes related to distal-less: part of a homeobox gene code for the head. *J Neurosci* 14 : 3475-86.
- Altabef, M., J. D. W. Clarke, and C. Tickle. (1997). Dorso-ventral ectodermal compartments and origin of apical ectodermal ridge in developing chick limb. *Development* : In press.
- Aparicio, S., Hawkem K., A. Cottage, Y. Mikawa, L. Zuo, B. Venkatesh, E. Chen, R. Krumlauf, and S. Brenner. (1997). Organization of the *Fugu rubripes* Hox clusters: evidence for continuing evolution of vertebrate complexes. *Nature Genetics* : 79-83.
- Averof, M., and N. H. Patel. (1997). Crustacean appendage evolution associated with changes in Hox gene expresion. *Nature* 388 : 682-686.
- Awgulewitsch, A., and D. Jacobs. (1990). Differential expression of Hox 3.1 protein in subregions of the embryonic and adult spinal cord. *Development* 108 : 411-20.
- Balinsky, B. I. (1925). Transplantation des ohrblaschens bei Triton. *Wilhelm Roux Arch. fur EntwMech. Orgs* 143 : 718-731.

- Balinsky, B. I. (1933). Das extremitatenseitenfeld, seine ausdehnung und beschaffenheit. Roux Arch 130 : 704-747.
- Balinsky, B. I. (1965). An Introduction to Embryology. Second ed. London: W. B. Saunders.
- Bamshad, M., R. C. Lin, D. J. Law, W. C. Watkins, P. A. Krakowiak, M. E. Moore, P. Franceschini, Lala. R., L. B. Holmes, T. C. Gebhur, B. G. Bruneau, A. Schinzel, J. G. Seidman, C. E. Seidman, and L. B. Jorde. (1997). Mutations in human TBX3 alter limb, apocrine and genital development in ulnar-mammary syndrome. Nature Genetics 16 : 311-315.
- Basler, K., and G. Struhl. (1994). Compartment boundaries and the control of Drosophila limb pattern by hedgehog protein. Nature 368 : 208-14.
- Bateson, W. (1894). Materials for the study of variation. London: Macmillan.
- Beddington, R. S. P., and J. C. Smith. (1993). Control of vertebrate gastrulation: inducing signals and responding genes. Curr Opin Genet Devel 3 : 655-661.
- Bellairs, A. (1969). The Life of Reptiles. London: Weidenfeld and Nicolson.
- Bernfield, M., M. T. Hinkes, and R. L. Gallo. (1993). Developmental expression of the syndecans: possible function and regulation. Development Supplement : 205-12.
- Biencz, M. (1994). Homeotic genes and positional signalling in the Drosophila viscera. Trends Genet 10 : 22-6.
- Bitgood, M. J., and A. P. McMahon. (1995). *Hedgehog* and *Bmp* genes are coexpressed at many diverse sites of cell-cell interaction in the mouse embryo. Dev. Biol. 172 : 126-138.
- Blair, S. S. (1995). Compartments and appendage development in Drosophila. Bioessays 17 : 299-309.
- Boulet, A. M., and M. R. Capecchi. (1996). Targeted disruption of Hoxc-4 causes esophageal defects and vertebral transformations. Dev. Biol. 177 : 232-249.
- Bueno, D., J. Skinner, H. Abud, and J. K. Heath. (1996). Spatial and temporal relationships between Shh, Fgf4, and Fgf8 gene expression at diverse signalling centers during mouse development. Dev Dyn 207 : 291-9.
- Bulfone, A., L. Puelles, M. H. Porteus, M. A. Frohman, G. R. Martin, and J. L. Rubenstein. (1993). Spatially restricted expression of Dlx-1, Dlx-2 (Tes-1), Gbx-2, and Wnt-3 in the embryonic day 12.5 mouse forebrain defines potential transverse and longitudinal segmental boundaries. J Neurosci 13 : 3155-72.
- Bumcrot, D. A., R. Takada, and A. P. McMahon. (1995). Proteolytic processing yields two secreted forms of sonic hedgehog. Mol Cell Biol 15 :

2294-303.

Burke, A. C., C. E. Nelson, B. A. Morgan, and C. Tabin. (1995). Hox genes and the evolution of vertebrate axial morphology. *Development* 121 : 333-46.

Burke, R., and K. Basler. (1996). Hedgehog-dependent patterning in the *Drosophila* eye can occur in the absence of Dpp signaling. *Dev Biol* 179 : 360-8.

Caldwell, M. W., and M. S. Lee. (1997). A snake with legs from the marine Cretaceous of the Middle East. *Nature* 386 : 705-709.

Caré, A., A. Silvani, E. Meccia, G. Mattia, A. Stoppacciaro, G. Parmiani, C. Peschle, and M. P. Colombo. (1996). HOXB7 constitutively activates basic fibroblast growth factor in melanomas. *Mol Cell Biol* 16 : 4842-51.

Carrington, J. L., and J. F. Fallon. (1984). The stages of flank ectoderm capable of responding to ridge induction in the chick embryo. *J Embryol Exp Morphol* 84 : 19-34.

Carroll, R. (1988). *Vertebrate Paleontology and Evolution*. New York: Freeman.

Carroll, S. B. (1995). Hox genes and the evolution of arthropods and chordates. *Nature* 376 : 479-485.

Chan, D. C., E. Laufer, C. Tabin, and P. Leder. (1995). Polydactylous limbs in Strong's Luxoid mice result from ectopic polarizing activity. *Development* 121 : 1971-8.

Charite, J., W. de Graaff, S. Shen, and J. Deschamps. (1994). Ectopic expression of Hoxb-8 causes duplication of the ZPA in the forelimb and homeotic transformation of axial structures. *Cell* 78 : 589-601.

Chaube, S. (1959). On axiation and symmetry in transplanted wing of the chick. *J. Exp. Zool.* 140 : 29-77.

Chen, F., and M. R. Capecchi. (1997). Targeted mutations in Hoxa-9 and Hoxb-9 reveal synergistic interactions. *Dev Biol* 181 : 186-96.

Chevallier, A., M. Kieny, and A. Mauger. (1978). Limb-somite relationship: effect of removal of somitic mesoderm on the wing musculature. *J Embryol Exp Morphol* 43 : 263-78.

Chiang, C., Y. Litingtung, E. Lee, K. E. Young, J. L. Corden, H. Westphal, and P. A. Beachy. (1996). Cyclopia and defective axial patterning in mice lacking Sonic hedgehog gene function. *Nature* 383 : 407-13.

Christian, J. L., D. J. Olson, and R. T. Moon. (1992). Xwnt-8 modifies the character of mesoderm induced by bFGF in isolated *Xenopus* ectoderm. *Embo J* 11 : 33-41.

Christiansen, J. H., C. L. Dennis, C. A. Wicking, S. J. Monkley, D. G. Wilkinson, and B. J. Wainwright. (1995). Murine Wnt-11 and Wnt-12 have temporally and spatially restricted expression patterns during embryonic development. *Mech Dev* 51 : 341-50.

Coates, M. I. (1994). The origin of vertebrate limbs. *Development Supplement* : 169-180.

Coelho, C. N., L. Sumoy, B. J. Rodgers, D. R. Davidson, R. E. Hill, W. B. Upholt, and R. A. Kosher. (1991). Expression of the chicken homeobox-containing gene GHox-8 during embryonic chick limb development. *Mech Dev* 34 : 143-54.

Cohn, M. J., J. C. Izpisúa-Belmonte, H. Abud, J. K. Heath, and C. Tickle. (1995). Fibroblast growth factors induce additional limb development from the flank of chick embryos. *Cell* 80 : 739-46.

Condie, B. G., and M. R. Capecchi. (1994). Mice with targeted disruptions in the paralogous genes Hoxa-3 and Hoxd-3 reveal synergistic interactions. *Nature* 370 : 304-7.

Conlon, R. A. (1995). Retinoic acid and pattern formation in vertebrates. *Trends in Genetics* 11 : 314-419.

Crossley, P. H., and G. R. Martin. (1995). The mouse Fgf8 gene encodes a family of polypeptides and is expressed in regions that direct outgrowth and patterning in the developing embryo. *Development* 121 : 439-51.

Crossley, P. H., G. Minowada, C. A. MacArthur, and G. R. Martin. (1996). Roles for FGF8 in the induction, initiation, and maintenance of chick limb development. *Cell* 84 : 127-36.

Davidson, D. R., A. Crawley, R. E. Hill, and C. Tickle. (1991). Position-dependent expression of two related homeobox genes in developing vertebrate limbs. *Nature* 352 : 429-31.

Davis, A. P., D. P. Witte, H. Li Hsieh, S. S. Potter, and M. R. Capecchi. (1995). Absence of radius and ulna in mice lacking Hoxa-11 and Hoxd-11. *Nature* 375 : 791-5.

Davis, C. A., D. P. Holmyard, K. J. Millen, and A. L. Joyner. (1991). Examining pattern formation in mouse, chicken and frog embryos with an En-specific antiserum. *Development* 111 : 287-98.

De Robertis, E. M. (1994). The homeobox in cell differentiation and evolution. In *Guidebook to the Homeobox Genes*. Edited by D. Duboule. 13-23. Oxford: Oxford University Press.

Dealy, C. N., A. Roth, D. Ferrari, A. M. Brown, and R. A. Kosher. (1993). Wnt-5a and Wnt-7a are expressed in the developing chick limb bud in a manner suggesting roles in pattern formation along the proximodistal and dorsoventral axes. *Mech Dev* 43 : 175-86.

Dhouailly, D., and M. Kieny. (1972). The capacity of the flank somatic mesoderm of early bird embryos to participate in limb development. *Dev. Biol.* 28 : 162-175.

Dolle, P., A. Dierich, M. LeMeur, T. Schimmang, B. Schuhbaur, P. Chambon, and D. Duboule. (1993). Disruption of the Hoxd-13 gene induces localized heterochrony leading to mice with neotenic limbs. *Cell* 75 : 431-41.

Dolle, P., J. C. Izpisúa-Belmonte, J. M. Brown, C. Tickle, and D. Duboule. (1991). HOX-4 genes and the morphogenesis of mammalian genitalia. *Genes Dev* 5 : 1767-7.

Dolle, P., M. Price, and D. Duboule. (1992). Expression of the murine Dlx-1 homeobox gene during facial, ocular and limb development. *Differentiation* 49 : 93-9.

Dolle, P., E. Ruberte, P. Kastner, M. Petkovich, C. M. Stoner, L. J. Gudas, and P. Chambon. (1989). Differential expression of genes encoding α , β and γ retinoic acid receptors and CRABP in the developing limbs of the mouse. *Nature* 342 : 702-705.

Doniach, T. (1995). Basic FGF as an inducer of anteroposterior neural pattern. *Cell* 83 : 1067-70.

Dono, R., and R. Zeller. (1994). Cell-type-specific nuclear translocation of fibroblast growth factor-2 isoforms during chicken kidney and limb morphogenesis. *Dev Biol* 163 : 316-30.

Duboule, D. (1995). Vertebrate Hox genes and proliferation: an alternative pathway to homeosis? *Curr Opin Genet Dev* 5 : 525-8.

Dudley, A. T., K. M. Lyons, and E. J. Robertson. (1995). A requirement for bone morphogenetic protein-7 during development of the mammalian kidney and eye. *Genes Dev.* 9 : 2795-2807.

Duprez, D. M., K. Kostakopoulou, P. Francis-West, C. Tickle, and P. M. Brickell. (1996). Activation of Fgf-4 and HoxD gene expression by BMP-2 expressing cells in the developing chick limb. *Development* 122 : 1821-8.

Eisenberg, L. M., P. W. Ingham, and A. M. Brown. (1992). Cloning and characterization of a novel Drosophila Wnt gene, Dwnt-5, a putative downstream target of the homeobox gene distal-less. *Dev Biol* 154 : 73-83.

Epstein, D. J., E. Marti, M. P. Scott, and A. P. McMahon. (1996). Antagonizing cAMP-dependent protein kinase A in the dorsal CNS activates a conserved Sonic hedgehog signaling pathway. *Development* 122 : 2885-94.

Fallon, J. F., and G. M. Crosby. (1977). Polarising zone activity in limb buds of amniotes. In *Vertebrate Limb and Somite Morphogenesis*. Edited by D. A. Ede, J. R. Hinchliffe and M. Balls. 55-70. Cambridge: Cambridge University Press.

Fallon, J. F., J. M. Frederick, J. L. Carrington, M. E. Lanser, and B. K.

Simandl. (1983). Studies on a *limbless* mutant in the chick embryo. In Limb Development and Regeneration. Edited by J. F. Fallon and A. I. Caplan. New York: Alan R. Liss.

Fallon, J. F., A. Lopez-Martinez, M. A. Ros, M. P. Savage, B. B. Olwin, and B. K. Simandl. (1994). FGF-2: Apical ectodermal ridge growth signal for chick limb development. *Science* 264 : 104-107.

Fan, C. M., and M. Tessier-Lavigne. (1994). Patterning of mammalian somites by surface ectoderm and notochord: evidence for sclerotome induction by a hedgehog homolog. *Cell* 79 : 1175-86.

Fawcett, D., P. Pasceri, R. Fraser, M. Colbert, J. Rossant, and V. Giguere. (1995). Postaxial polydactyly in forelimbs of CRABP-II mutant mice. *Development* 121 : 671-9.

Ferrari, D., L. Sumoy, J. Gannon, H. Sun, A. M. Brown, W. B. Upholt, and R. A. Kosher. (1995). The expression pattern of the Distal-less homeobox-containing gene Dlx-5 in the developing chick limb bud suggests its involvement in apical ectodermal ridge activity, pattern formation, and cartilage differentiation. *Mech Dev* 52 : 257-64.

Francis, P. H., M. K. Richardson, P. M. Brickell, and C. Tickle. (1994). Bone morphogenetic proteins and a signalling pathway that controls patterning in the developing chick limb. *Development* 120 : 209-18.

Francis-West, P., K. E. Robertson, D. A. Ede, C. Rodriguez, J. C. Izpisúa-Belmonte, B. Houston, D. W. Burt, C. Gribbin, P. M. Brickell, and C. Tickle. (1995). Expression of genes encoding bone morphogenetic proteins and sonic hedgehog in talpid (ta3) limb buds: their relationships in the signalling cascade involved in limb patterning. *Dev Dyn* 203 : 187-97.

Fromental-Ramain, C., X. Warot, N. Messadecq, M. LeMeur, P. Dolle, and P. Chambon. (1996). Hoxa-13 and Hoxd-13 play a crucial role in the patterning of the limb autopod. *Development* 122 : 2997-3011.

Fromental-Ramain, C., X. Warot, S. Lakkaraju, B. Favier, H. Haack, C. Birling, A. Dierich, P. Dolle, and P. Chambon. (1996). Specific and redundant functions of the paralogous *Hoxa-9* and *Hoxd-9* genes in forelimb and axial skeleton patterning. *Development* 122 : 461-472.

Gadow, H. F. (1933). The Evolution of the Vertebral Column. Cambridge: Cambridge University Press.

Garcia-Fernandez, J., and P. W. Holland. (1994). Archetypal organization of the amphioxus Hox gene cluster. *Nature* 370 : 563-6.

Gardiner, D. M., B. Blumberg, Y. Komine, and S. V. Bryant. (1995). Regulation of HoxA expression in developing and regenerating axolotl limbs. *Development* 121 : 1731-41.

Gasc, J. P. (1976). Snake vertebrae- a mechanism or merely a taxonomist's toy? In Morphology and Biology of Reptiles. Edited by A. Bellairs and C. B.

Cox. 177-190.

Gaunt, S. J. (1994). Conservation in the Hox code during morphological evolution. *Int. J. Dev. Biol.* 38 : 549-552.

Geduspan, J. S., and J. A. MacCabe. (1989). Transfer of dorsoventral information from mesoderm to ectoderm at the onset of limb development. *Anat Rec* 224 : 79-87.

Geduspan, J. S., and M. Solursh. (1992a). Cellular contribution of the different regions of the somatopleure to the developing limb. *Dev Dyn* 195 : 177-187.

Geduspan, J. S., and M. Solursh. (1992b). A growth-promoting influence from the mesonephros during limb outgrowth. *Dev Biol* 151 : 242-250.

Gibson-Brown, J. J., S. I. Agulnik, D. L. Chapman, M. Alexiou, N. Garvey, L. M. Silver, and V. E. Papaioannou. (1996). Evidence of a role for T-Box genes in the evolution of limb morphogenesis and specification of forelimb/hindlimb identity. *Mech. Dev.* 56 : 93-101.

Goodrich, E. S. (1930). *Studies on the Structure and Development of Vertebrates*. London: Macmillan.

Green, P. J., F. S. Walsh, and P. Doherty. (1996). Promiscuity of fibroblast growth factor receptors. *Bioessays* 18 : 639-646.

Greer, A. E. (1989). *The Biology and Evolution of Australian Lizards*. Chipping Norton, NSW: Surrey Beatty and Sons.

Grenier, J. K., T. L. Garber, R. Warren, P. M. Whitington, and S. Carroll. (1997). Evolution of the entire arthropod *Hox* gene set predated the origin and radiation of the onychophoran/arthropod clade. *Curr Biol* 7 : 547-553.

Grieshammer, U., G. Minowada, J. M. Pisenti, U. K. Abbott, and G. R. Martin. (1996). The chick limbless mutation causes abnormalities in limb bud dorsal-ventral patterning: implications for the mechanism of apical ridge formation. *Development* 122 : 3851-61.

Hamburger, V., and H. Hamilton. (1951). A series of normal stages in the development of the chick embryo. *J. Morphol.* 88 : 49-92.

Hammerschmidt, M., A. Brook, and A. P. McMahon. (1997). The world according to hedgehog. *Trends Genet* 13 : 14-21.

Hatta, K., R. Bremiller, M. Westerfield, and C. Kimmel. (1991). Diversity of expression of *engrailed*-like antigens in zebrafish. *Development* 112 : 821-832.

Hayamizu, T. F., and S. V. Bryant. (1992). Retinoic acid respecifies limb bud cells in vitro. *J Exp Zool* 263 : 423-429.

Hebert, J. M., T. Rosenquist, J. Gotz, and G. R. Martin. (1994). FGF5 as a

regulator of the hair growth cycle: evidence from targeted and spontaneous mutations. *Cell* 78 : 1017-25.

Heikinheimo, M., A. Lawshe, G. M. Shackleford, D. B. Wilson, and C. A. MacArthur. (1994). Fgf-8 expression in the post-gastrulation mouse suggests roles in the development of the face, limbs and central nervous system. *Mech Dev* 48 : 129-38.

Hill, R. E., P. F. Jones, A. R. Rees, C. M. Sime, M. J. Justice, N. G. Copeland, N. A. Jenkins, E. Graham, and D. R. Davidson. (1989). A new family of mouse homeo box-containing genes: molecular structure, chromosomal location, and developmental expression of Hox-7.1. *Genes Dev* 3 : 26-37.

Hinchliffe, J. R. (1985). 'One, two, three' or 'Two, three, four': An embryologist's view of the homologies of the digits and carpus of modern birds. In *Beginnings of Birds*. Edited by M. K. Hecht, J. H. Ostrom, G. Viohl and P. Wellnhofer. 141-147. Eichstatt: Jura-Museums.

Hinchliffe, J. R., and A. Sansom. (1985). The distribution of the polarizing zone (ZPA) in the legbud of the chick embryo. *J Embryol Exp Morphol* 86 : 169-75.

Holland, P. W. H., and J. Garcia-Fernandez. (1996). Hox genes and chordate evolution. *Dev Biol* 173 : 382-95.

Honig, L. S. (1984). Pattern formation during development of the amniote limb. In *The structure, development and evolution of reptiles*. Edited by M. W. J. Ferguson. 197-222. London: Academic Press.

Honig, L. S., and D. Summerbell. (1985). Maps of strength of positional signalling activity in the developing chick wing bud. *J Embryol Exp Morphol* 87 : 163-74.

Horan, G. S. B., R. Ramírez-Solis, M. S. Featherstone, D. J. Wolgemuth, A. Bradley, and R. R. Behringer. (1995). Compound mutants for the paralogous Hoxa-4, Hoxb-4 and Hoxd-4 genes show more complete homeotic transformations and a dose-dependent increase in the number of vertebrae transformed. *Genes Dev* 9 : 1667-1677.

Hornbruch, A., and L. Wolpert. (1986). Positional signalling by Hensen's node when grafted to the chick limb bud. *J Embryol Exp Morphol* 94 : 257-65.

Hornbruch, A., and L. Wolpert. (1991). The spatial and temporal distribution of polarizing activity in the flank of the pre-limb-bud stages in the chick embryo. *Development* 111 : 725-31.

Isaacs, H. V., M. E. Pownall, and J. M. Slack. (1994). eFGF regulates Xbra expression during *Xenopus* gastrulation. *Embo J* 13 : 4469-81.

Itasaki, N., J. Sharpe, A. Morrison, and R. Krumlauf. (1996). Reprogramming Hox expression in the vertebrate hindbrain: influence of paraxial mesoderm and rhombomere transposition. *Neuron* 16 : 487-500.

Harrison, R. G. (1969). *Organization and Development of the Embryo*. New Haven: Yale University Press.

Izpisúa-Belmonte, J. C., J. M. Brown, A. Crawley, D. Duboule, and C. Tickle. (1992). Hox-4 gene expression in mouse/chicken heterospecific grafts of signalling regions to limb buds reveals similarities in patterning mechanisms. *Development* 115 : 553-60.

Izpisúa-Belmonte, J. C., and D. Duboule. (1992). Homeobox genes and pattern formation in the vertebrate limb. *Dev Biol* 152 : 26-36.

Izpisúa-Belmonte, J. C., C. Tickle, P. Dolle, L. Wolpert, and D. Duboule. (1991). Expression of the homeobox Hox-4 genes and the specification of position in chick wing development. *Nature* 350 : 585-9.

Jackson, A., S. Friedman, X. Zhan, K. A. Engleka, R. Forough, and T. Maciag. (1992). Heat shock induces the release of fibroblast growth factor 1 from NIH 3T3 cells. *Proc Natl Acad Sci U S A* 89 : 10691-5.

Jegalian, B. G., and E. M. De Robertis. (1992). Homeotic transformations in the mouse induced by overexpression of a human *Hox3.3* transgene. *Cell* 71 : 901-910.

Johnson, D. E., P. L. Lee, J. Lu, and L. T. Williams. (1990). Diverse forms of a receptor for acidic and basic fibroblast growth factors. *Mol Cell Biol* 10 : 4728-36.

Johnson, R. L., and C. Tabin. (1995). The long and short of Hedgehog signaling. *Cell* 81 : 313-6.

Kappen, C. (1996). Theoretical approaches to the analysis of homeobox gene evolution. *Comput Chem* 20 : 49-59.

Kessel, M. (1992). Respecification of vertebral identities by retinoic acid. *Development* 115 : 487-501.

Kessel, M., and P. Gruss. (1991). Homeotic transformations of murine vertebrae and concomitant alteration of *Hox* codes by retinoic acid. *Cell* 67 : 89-104.

Kieny, M. (1971). Les phases d'activité morphogène du mésoderme somatopleural pendant le développement précoce du membre chez l'embryon de poulet. *Ann. Embryol. Morphol.* 4 : 281-298.

Kiortsis, V. (1953). Potentialités du territoire patte chez le Triton. *Rev Suisse Zool* : 301-410.

Klagsbrun, M., and A. Baird. (1991). A dual receptor system is required for basic fibroblast growth factor activity. *Cell* 67 : 229-231.

Koyama, E., T. Yamaai, S. Iseki, H. Ohuchi, T. Nohno, H. Yoshioka, Y. Hayashi, J. L. Leatherman, E. B. Golden, S. Noji, and M. Pacifici. (1996). Polarizing activity, Sonic hedgehog, and tooth development in embryonic and postnatal mouse. *Dev Dyn* 206 : 59-72.

Krumlauf, R. (1992). Evolution of the vertebrate Hox homeobox genes. *Bioessays* 14 : 245-52.

Krumlauf, R. (1994). *Hox* genes in vertebrate development. *Cell* 78 : 191-201.

Laufer, E., R. Dahn, O. E. Orozco, C. Y. Yeo, J. Pisenti, D. Henrique, U. K. Abbott, J. F. Fallon, and C. Tabin. (1997). Expression of *Radical fringe* in limb-bud ectoderm regulates apical ectodermal ridge formation. *Nature* 386 : 366-73.

Laufer, E., C. E. Nelson, R. L. Johnson, B. A. Morgan, and C. Tabin. (1994). Sonic hedgehog and Fgf-4 act through a signaling cascade and feedback loop to integrate growth and patterning of the developing limb bud. *Cell* 79 : 993-1003.

Lewis, E. (1978). A gene complex controlling segmentation in *Drosophila*. *Nature* 276 : 565-570.

Li, Q. Y., R. A. Newbury-Ecob, J. A. Terret, D. I. Wilson, A. R. Curtis, C. H. Yi, T. Gebuhr, P. J. Bullen, S. C. Robson, T. Strachan, D. Bonnet, S. Lyonnet, I. D. Young, J. A. Raeburn, A. J. Buckler, D. J. Law, and J. D. Brook. (1997). Holt-Oram syndrome is caused by mutations in TBX5, a member of the Brachyury (T) family. *Nature Genetics* 15 : 21-29.

Liem, K. F., G. Tremml, H. Roelink, and T. M. Jessell. (1995). Dorsal differentiation of neural plate cells induced by BMP-mediated signals from epidermal ectoderm. *Cell* 82 : 969-979.

Locatelli, P. (1924). Sulla formazione di arti sopranumerari. *Boll Soc Med-Chir Pavia* 36

Logan, C., A. Hornbruch, I. Campbell, and A. Lumsden. (1997). The role of *Engrailed* in establishing the dorsoventral axis of the chick limb. *Development* 124 : 2317-24.

Lohnes, D., P. Kastner, A. Dierich, M. Mark, M. LeMeur, and P. Chambon. (1993). Function of retinoic acid receptor γ in the mouse. *Cell* 73 : 643-658.

Lohnes, D., M. Mark, C. Mendelsohn, P. Dollé, A. Dierich, P. Gorry, A. Gansmuller, and P. Chambon. (1994). Function of the retinoic acid receptors (RARs) during development (I) Craniofacial and skeletal abnormalities in RAR double mutants. *Development* 120 : 2723-2748.

Loomis, C. A., E. Harris, J. Michaud, W. Wurst, M. Hanks, and A. Joiner. (1996). The mouse *Engrailed-1* gene and ventral limb patterning. *Nature* 382 : 360-363.

López-Martínez, A., D. T. Chang, C. Chiang, J. A. Porter, M. A. Ros, B. K. Simandl, P. A. Beachy, and J. F. Fallon. (1995). Limb-patterning activity and restricted posterior localization of the amino-terminal product of Sonic hedgehog cleavage. *Curr. Biol.* 5 : 791-796.

- Lu, H. C., J. P. Revelli, L. Goering, C. Thaller, and G. Eichele. (1997). Retinoid signaling is required for the establishment of a ZPA and for the expression of Hoxb-8, a mediator of ZPA formation. *Development* 124 : 1643-51.
- Lumsden, A., and R. Krumlauf. (1996). Patterning the vertebrate neuraxis. *Science* 274 : 1109-1115.
- Luo, G., C. Hofmann, A. L. J. J. Bronckers, M. Sohocki, A. Bradley, and G. Karsenty. (1995). BMP-7 is an inducer of nephrogenesis, and is also required for eye development and skeletal patterning. *Genes Dev.* 9 : 2808-2820.
- MacCabe, A. B., M. T. Gasseling, and Jw Jr Saunders. (1973). Spatiotemporal distribution of mechanisms that control outgrowth and anteroposterior polarization of the limb bud in the chick embryo. *Mech Ageing Dev* 2 : 1-12.
- MacCabe, J. A., J. Errick, and J. W. Saunders. (1974). Ectodermal control of the dorsoventral axis in the leg bud of the chick embryo. *Dev Biol* 39 : 69-82.
- MacCabe, J. A., and B. W. Parker. (1976). Polarizing activity in the developing limb of the Syrian hamster. *J Exp Zool* 195 : 311-7.
- Maden, M. (1993). The homeotic transformation of tails into limbs in *Rana temporaria* by retinoids. *Dev Biol* 159 : 379-91.
- Maden, M., D. E. Ong, D. Summerbell, and F. Chytil. (1988). Spatial distribution of cellular protein binding to retinoic acid in the chick limb bud. *Nature* 335 : 733-5.
- Mansukhani, A., D. Moscatelli, D. Talarico, V. Levytska, and C. Basilico. (1990). A murine fibroblast growth factor (FGF) receptor expressed in CHO cells is activated by basic FGF and Kaposi FGF. *Proc Natl Acad Sci U S A* 87 : 4378-82.
- Marcelle, C., A. Eichmann, O. Halevy, C. Breant, and N. Le Douarin. (1994). Distinct developmental expression of a new avian fibroblast growth factor receptor. *Development* 120 : 683-94.
- Marigo, V., R. A. Davey, Y. Zuo, J. M. Cunningham, and C. J. Tabin. (1996a). Biochemical evidence that patched is the Hedgehog receptor. *Nature* 384 : 176-9.
- Marigo, V., M. P. Scott, R. L. Johnson, L. V. Goodrich, and C. J. Tabin. (1996b). Conservation in hedgehog signaling: induction of a chicken patched homolog by Sonic hedgehog in the developing limb. *Development* 122 : 1225-33.
- Marti, E., D. A. Bumcrot, R. Takada, and A. P. McMahon. (1995a). Requirement of 19K form of Sonic hedgehog for induction of distinct ventral cell types in CNS explants. *Nature* 375 : 322-5.

- Marti, E., R. Takada, D. A. Bumcrot, H. Sasaki, and A. P. McMahon. (1995b). Distribution of Sonic hedgehog peptides in the developing chick and mouse embryo. *Development* 121 : 2537-47.
- Masuya, H., T. Sagai, K. Moriwaki, and T. Shiroishi. (1997). Multigenic control of the localization of the zone of polarizing activity in limb morphogenesis in the mouse. *Dev Biol* 182 : 42-51.
- Masuya, H., T. Sagai, S. Wakana, K. Moriwaki, and T. Shiroishi. (1995). A duplicated zone of polarizing activity in polydactylous mouse mutants. *Genes Dev* 9 : 1645-53.
- McNeil, P. L. (1993). Cellular and molecular adaptations to injurious mechanical stress. *Trends in Cell Biology* 3 : 302-307.
- Metscher, A. L., and D. Gospodarowicz. (1979). Mitogenic effect of a growth factor derived from myelin on denervated regenerates of newt forelimbs. *J Exp Zool* 207 : 497-503.
- Michaud, J. L., F. Lapointe, and N Le Douarin. (1997). The dorsoventral polarity of the presumptive limb is determined by signals produced by the somites and by the lateral somatopleure. *Development* 124 : 1453-63.
- Mignatti, P., and D. B. Rifkin. (1991). Release of basic fibroblast growth factor, an angiogenic factor devoid of secretory signal sequence: a trivial phenomenon or a novel secretion mechanism? *J Cell Biochem* 47 : 201-7.
- Miki, T., D. P. Bottaro, T. P. Fleming, C. L. Smith, W. H. Burgess, A. M. Chan, and S. A. Aaronson. (1992). Determination of ligand-binding specificity by alternative splicing: two distinct growth factor receptors encoded by a single gene. *Proc Natl Acad Sci U S A* 89 : 246-50.
- Mohanty-Hejmadi, P., S. K. Dutta, and P. Mahapatra. (1992). Limbs generated at site of tail amputation in marbled balloon frog after vitamin A treatment. *Nature* 355 : 352-3.
- Molven, A., C. V. E. Wright, R. BreMiller, E. De Robertis, and C. Kimmel. (1990). Expression of a homeobox gene product in normal and mutant zebrafish embryos: evolution of the tetrapod body plan. *Development* 109 : 279-288.
- Morgan, B. A., J. C. Izpisúa-Belmonte, D. Duboule, and C. J. Tabin. (1992). Targeted misexpression of Hox-4.6 in the avian limb bud causes apparent homeotic transformations. *Nature* 358 : 236-9.
- Morgan, B. A., and C. Tabin. (1994). Hox genes and growth: early and late roles in limb bud morphogenesis. *Development Supplement* : 181-6.
- Morrison, A., M. C. Moroni, McNaughton L. Ariza, R. Krumlauf, and F. Mavilio. (1996). In vitro and transgenic analysis of a human HOXD4 retinoid-responsive enhancer. *Development* 122 : 1895-907.
- Mullen, L. M., S. V. Bryant, M. A. Torok, B. Blumberg, and D. M. Gardiner.

(1996). Nerve dependency of regeneration: the role of Distal-less and FGF signaling in amphibian limb regeneration. *Development* 122 : 3487-97.

Muller, G. B., J. Streicher, and R. J. Muller. (1996). Homeotic duplication of the pelvic body segment in regenerating tadpole tails induced by retinoic acid. *Dev Genes Evol* 206 : 344-348.

Nelson, C. E., B. A. Morgan, A. C. Burke, E. Laufer, E. DiMambro, L. C. Murtaugh, E. Gonzales, L. Tessarollo, L. F. Parada, and C. Tabin. (1996). Analysis of Hox gene expression in the chick limb bud. *Development* 122 : 1449-66.

Niederreither, K., S. J. Ward, P. Dolle, and P. Chambon. (1996). Morphological and molecular characterization of retinoic acid-induced limb duplications in mice. *Dev Biol* 176 : 185-98.

Nieto, M. A., K. Patel, and D. G. Wilkinson. (1996). In situ hybridization analysis of chick embryos in whole-mount and tissue sections. In *Methods in Avian Embryology*. Edited by M. Bronner-Fraser. San Diego: Academic Press.

Niswander, L., S. Jeffrey, G. R. Martin, and C. Tickle. (1994). A positive feedback loop coordinates growth and patterning in the vertebrate limb. *Nature* 371 : 609-12.

Niswander, L., and G. R. Martin. (1992). Fgf-4 expression during gastrulation, myogenesis, limb and tooth development in the mouse. *Development* 114 : 755-68.

Niswander, L., and G. R. Martin. (1993). FGF-4 and BMP-2 have opposite effects on limb growth. *Nature* 361 : 68-71.

Niswander, L., C. Tickle, A. Vogel, I. Booth, and G. R. Martin. (1993). FGF-4 replaces the apical ectodermal ridge and directs outgrowth and patterning of the limb. *Cell* 75 : 579-87.

Nohno, T., Y. Kawakami, H. Ohuchi, A. Fujiwara, H. Yoshioka, and S. Noji. (1995). Involvement of the Sonic hedgehog gene in chick feather formation. *Biochem Biophys Res Commun* 206 : 33-9.

Noji, S., T. Nohno, E. Koyama, K. Muto, K. Ohyama, Y. Aoki, K. Tamura, K. Ohsugi, H. Ide, S. Taniguchi, and a. l. et. (1991). Retinoic acid induces polarizing activity but is unlikely to be a morphogen in the chick limb bud. *Nature* 350 : 83-6.

Noramly, S., J. Pisenti, U. Abbott, and B. Morgan. (1996). Gene expression in the limbless mutant: polarized gene expression in the absence of Shh and an AER. *Dev Biol* 179 : 339-46.

Ohuchi, H., T. Nakagawa, A. Yamamoto, A. Araga, T. Ohata, Y. Ishimaru, H. Yoshioka, T. Kuwana, T. Nohno, M. Yamasaki, N. Itoh, and S. Noji. (1997). The mesenchymal factor, FGF10, initiates and maintains the outgrowth of the chick limb bud through interaction with FGF8, an apical ectodermal factor.

Development 124 : 2235-44.

Ohuchi, H., H. Yoshioka, A. Tanaka, Y. Kawakami, T. Nohno, and S. Noji. (1994). Involvement of androgen-induced growth factor (FGF-8) gene in mouse embryogenesis and morphogenesis. Biochem Biophys Res Commun 204 : 882-8.

Oliver, G., C. V. Wright, J. Hardwicke, and E. M. De Robertis. (1988a). Differential antero-posterior expression of two proteins encoded by a homeobox gene in *Xenopus* and mouse embryos. Embo J 7 : 3199-209.

Oliver, G., C. V. Wright, J. Hardwicke, and E. M. De Robertis. (1988b). A gradient of homeodomain protein in developing forelimbs of *Xenopus* and mouse embryos. Cell 55 : 1017-24.

Ornitz, D. M., J. Xu, J. S. Colvin, D. G. McEwen, C. A. MacArthur, F. Coulier, G. Gao, and M. Goldfarb. (1996). Receptor specificity of the fibroblast growth factor family. J Biol Chem 271 : 15292-7.

Orr-Utreger, A., M. T. Bedford, T. Burakova, E. Arman, Y. Zimmer, A. Yayon, D. Givol, and P. Lonai. (1993). Developmental localization of the splicing alternatives of fibroblast growth factor receptor-2 (FGFR2). Dev Biol 158 : 475-86.

Orr-Utreger, A., D. Givol, A. Yayon, Y. Yarden, and P. Lonai. (1991). Developmental expression of two murine fibroblast growth factor receptors, flg and bek. Development 113 : 1419-34.

Panganiban, G., A. Sebring, L. Nagy, and S. Carroll. (1995). The development of crustacean limbs and the evolution of arthropods. Science 270 : 1363-6.

Parr, B. A., and A. P. McMahon. (1995). Dorsalizing signal Wnt-7a required for normal polarity of D-V and A-P axes of mouse limb. Nature 374 : 350-3.

Parr, B. A., M. J. Shea, G. Vassileva, and A. P. McMahon. (1993). Mouse Wnt genes exhibit discrete domains of expression in the early embryonic CNS and limb buds. Development 119 : 247-61.

Patel, K., R. Nittenberg, D. D'Souza, C. Irving, D. Burt, D. G. Wilkinson, and C. Tickle. (1996). Expression and regulation of Cek-8, a cell to cell signalling receptor in developing chick limb buds. Development 122 : 1147-55.

Pendleton, J. W., B. K. Nagai, M. T. Murtha, and F. H. Ruddle. (1993). Expansion of the Hox gene family and the evolution of chordates. Proc Natl Acad Sci U S A 90 : 6300-4.

Peters, K., S. Werner, X. Liao, S. Wert, J. Whitsett, and L. Williams. (1994). Targeted expression of a dominant negative FGF receptor blocks branching morphogenesis and epithelial differentiation of the mouse lung. Embo J 13 : 3296-301.

Peters, K. G., S. Werner, G. Chen, and L. T. Williams. (1992). Two FGF

receptor genes are differentially expressed in epithelial and mesenchymal tissues during limb formation and organogenesis in the mouse. *Development* 114 : 233-43.

Pollock, R. A., G. Jay, and C. J. Bieberich. (1992). Altering the boundaries of Hox-3.1: evidence for antipodal gene regulation. *Cell* 71 : 911-924.

Porter, J. A., K. E. Young, and P. A. Beachy. (1996). Cholesterol modification of hedgehog signaling proteins in animal development. *Science* 274 : 255-9.

Pownall, M. E., A. S. Tucker, J. M. Slack, and H. V. Isaacs. (1996). eFGF, Xcad3 and Hox genes form a molecular pathway that establishes the anteroposterior axis in Xenopus. *Development* 122 : 3881-92.

Prince, V. E., L. Joly, M. Ekker, and R. K. Ho. (1997). Zebrafish *Hox* genes: genomic organization and modified colinear expression of trunk genes. *Development* : In press.

Rahmani, T. M. Z. (1974). Morphogenesis of the rudimentary hind-limb of the glass snake (*Ophisaurus apodus* Pallas). *J. Embryol Exp Morphol* 32 : 431-443.

Rancourt, D. E., T. Tsuzuki, and M. R. Capecchi. (1995). Genetic interaction between *Hoxb-5* and *Hoxb-6* is revealed by nonallelic noncomplementation. *Genes Dev* 9 : 108-22.

Raynaud, A. (1977). Somites and early morphogenesis in reptile limbs. In *Vertebrate Limb and Somite Morphogenesis*. Edited by D. A. Ede, J. R. Hinchliffe and M. Balls. 373-386. Cambridge: Cambridge University Press.

Raynaud, A. (1985). Development of limbs and embryonic limb reduction. In *Biology of the Reptilia*. Edited by C. Gans. 60-147. New York: John Wiley and Sons.

Raynaud, A. (1990). Developmental mechanisms involved in the embryonic reduction of limbs in reptiles. *Int J Dev Biol* 34 : 233-243.

Raynaud, A., P. Kan, G. Bouche, and A. M. Duprat. (1995). Fibroblast growth factors (FGF-2) and delayed involution of the posterior limbs of the slow-worm embryo (*Anguis fragilis*, L.). *C R Acad Sci Iii* 318 : 573-8.

Riddle, R. D., M. Ensini, C. Nelson, T. Tsuchida, T. M. Jessell, and C. Tabin. (1995). Induction of LIM homeobox gene *Lmx-1* by *WNT7a* establishes dorsoventral pattern in the vertebrate limb. *Cell* 83 : 631-640.

Riddle, R. D., R. L. Johnson, E. Laufer, and C. Tabin. (1993). Sonic hedgehog mediates the polarizing activity of the ZPA. *Cell* 75 : 1401-16.

Rieppel, O. (1988). The Classification of the Squamata. In *The Phylogeny and Classification of the Tetrapods*. Edited by M. J. Benton. 261-294.

Rijli, F. M., and P. Chambon. (1997). Genetic interactions of *Hox* genes in limb development: learning from compound mutants. *Curr Opin Genet Dev* 7

: 481-487.

Roberts, D. J., R. L. Johnson, A. C. Burke, C. E. Nelson, B. A. Morgan, and C. Tabin. (1995). Sonic hedgehog is an endodermal signal inducing Bmp-4 and Hox genes during induction and regionalization of the chick hindgut. *Development* 121 : 3163-74.

Rodriguez-Esteban, C., J. W. R. Schwabe, J. De la Pena, B. Foys, B. Eshelman, and J. C. Izpisúa-Belmonte. (1997). *Radical fringe* positions the apical ectodermal ridge at the dorsoventral boundary of the vertebrate limb. *Nature* 386 : 360-366.

Romer, A. S. (1956). *Osteology of the Reptiles*. Chicago: University of Chicago Press.

Romer, A. S. (1966). *Vertebrate Paleontology*. Third ed. Chicago: University of Chicago Press.

Ros, M. A., A. Lopez-Martinez, B. K. Simandl, C. Rodriguez, J. C. Izpisúa-Belmonte, R. Dahn, and J. F. Fallon. (1996). The limb field mesoderm determines initial limb bud anteroposterior asymmetry and budding independent of sonic hedgehog or apical ectodermal gene expressions. *Development* 122 : 2319-30.

Ross, R. A. (1990). *The Reproductive Husbandry of Pythons and Boas*. Stanford: Institute for Herpetological Research.

Rudnick, D. (1945). Limb forming potencies of the chick blastoderm: Including notes on associated trunk structures. *Trans Conn Acad Sci* 36 : 353-377.

Ruiz i Altaba, A., and D. A. Melton. (1989). Interaction between peptide growth factors and homoeobox genes in the establishment of antero-posterior polarity in frog embryos. *Nature* 341 : 33-8.

Rutledge, J. C., A. G. Shourbaji, L. A. Hughes, J. E. Polifka, Y. P. Cruz, J. B. Bishop, and W. M. Generoso. (1994). Limb and lower-body duplications induced by retinoic acid in mice. *Proc Natl Acad Sci U S A* 91 : 5436-40.

Saunders, Jw Jr, and C. Reuss. (1974). Inductive and axial properties of prospective wing-bud mesoderm in the chick embryo. *Dev Biol* 38 : 41-50.

Saunders, J. W. (1948). The proximo-distal sequence of origin of the parts of the chick wing and the role of the ectoderm. *J. Exp. Zool.* 108 : 363-402.

Saunders, J. W., and M. T. Gasseling. (1968). Ectodermal-mesenchymal interactions in the origin of limb symmetry. In *Epithelial Mesenchymal Interactions*. Edited by R. Fleischmajer and R. Billingham. 78-97. Baltimore: Williams and Wilkins.

Savage, M. P., C. E. Hart, B. B. Riley, J. Sasse, B. B. Olwin, and J. F. Fallon. (1993). Distribution of FGF-2 suggests it has a role in chick limb bud growth. *Dev Dyn* 198 : 159-70.

- Schulte-Merker, S., and J. C. Smith. (1995). Mesoderm formation in response to Brachyury requires FGF signalling. *Curr Biol* 5 : 62-7.
- Scott, W. J. Jr, R. Walter, G. Tzimas, J. O. Sass, H. Nau, and M. D. Collins. (1994). Endogenous status of retinoids and their cytosolic binding proteins in limb buds of chick vs mouse embryos. *Dev Biol* 165 : 397-409.
- Searls, R. C., and M. Y. Janners. (1971). The initiation of limb bud outgrowth in the embryonic chick. *Dev. Biol.* 24 : 198-213.
- Sharman, A. C., and P. W. H. Holland. (1996). Conservation, duplication and divergence of developmental genes during chordate evolution. *Netherlands Journal of Zoology* 46 : 46-67.
- Shashikant, C. S., C. J. Bieberich, H. G. Belting, J. C. H. Wang, M. A. Borbély, and F. H. Ruddle. (1995). Regulation of *Hoxc-8* during mouse embryonic development: identification and characterization of critical elements involved in early neural tube expression. *Development* 121 : 4339-4347.
- Shubin, N., C. Tabin, and S. Carroll. (1997). Fossils, genes and the evolution of animal limbs. *Nature* 388 : 639-48.
- Simon, J. (1995). Locking in stable states of gene expression: transcriptional control during *Drosophila* development. *Curr. Opin. Cell biol.* 7 : 376-385.
- Singh, G., D. M. Supp, C. Schreiner, J. McNeish, H. J. Merker, N. G. Copeland, N. A. Jenkins, S. S. Potter, and W. J. Scott. (1991). *leg/ess* insertional mutation: morphological, molecular, and genetic characterization. *Genes Dev* 5 : 2245-2255.
- Slack, J. M. (1976). Determination of polarity in the amphibian limb. *Nature* 261 : 44-6.
- Slack, J. M. (1977a). Determination of anteroposterior polarity in the axolotl forelimb by an interaction between limb and flank rudiments. *J Embryol Exp Morphol* 39 : 151-68.
- Slack, J. M. W. (1977b). Control of anteroposterior pattern in the axolotl forelimb by a smoothly graded signal. *J Embryol Exp Morphol* 39 : 169-182.
- Slack, J. M. W. (1980). Regulation and potency in the forelimb rudiment of the axolotl embryo. *J Embryol Exp Morphol* 57 : 203-217.
- Smith, J. C. (1979). Evidence for a positional memory in the development of the chick wing bud. *J Embryol Exp Morphol* 52 : 105-13.
- Smith, J. C. (1980). The time required for the positional signalling in the chick wing bud. *J Embryol Exp Morphol* 60 : 321-328.
- Sordino, P., and D. Duboule. (1996). A molecular approach to the evolution of vertebrate paired appendages. *Trends Evol Ecol* 11 : 114-119.

- Sordino, P., F. van der Hoeven, and D. Duboule. (1995). Hox gene expression in teleost fins and the origin of vertebrate digits. *Nature* 375 : 678-81.
- Stephens, T. D., and T. R. McNulty. (1981). Evidence for a metamer pattern in the development of the chick humerus. *J Embryol Exp Morphol* 61 : 191-205.
- Stephens, T. D., R. Spall, W. C. Baker, S. R. Hiatt, D. E. Pugmire, M. R. Shaker, H. J. Willis, and K. P. Winger. (1991). Axial and paraxial influences on limb morphogenesis. *J Morph* 208 : 367-379.
- Stocum, D. L., and J. F. Fallon. (1984). Mechanisms of polarization and pattern formation in urodele limb ontogeny: a polarizing zone model. In *Pattern formation: a primer in developmental biology*. Edited by G. M. Malacinski and S. V. Bryant. London: MacMillan.
- Stratford, T., C. Horton, and M. Maden. (1996). Retinoic acid is required for the initiation of outgrowth in the chick limb bud. *Curr Biol* 6 : 1124-33.
- Stratford, T. H., K. Kostakopoulou, and M. Maden. (1997). Hoxb-8 has a role in establishing early anteroposterior polarity in chick forelimb but not hindlimb. *Development* in press
- Suemori, H., N. Takahashi, and S. Noguchi. (1995). *Hoxc-9* mutant mice show anterior transformation of the vertebrae and malformation of the sternum and ribs. *Mech Dev* 51 : 265-273.
- Summerbell, D. (1974). A quantitative analysis of the effect of excision of the AER from the chick limb-bud. *J Embryol Exp Morphol* 32 : 651-60.
- Summerbell, D., J. H. Lewis, and L. Wolpert. (1973). Positional information in chick limb morphogenesis. *Nature* 244 : 492-6.
- Tabin, C. J. (1992). Why we have (only) five fingers per hand: Hox genes and the evolution of paired hands. *Development* 116 : 289-296.
- Tanaka, M., K. Tamura, S. Noji, T. Nohno, and H. Ide. (1997). Induction of additional limb at the dorsal-ventral boundary of a chick embryo. *Dev Biol* 182 : 191-203.
- Thaller, C., and G. Eichele. (1987). Identification and spatial distribution of retinoids in the developing chick limb bud. *Nature* 327 : 625-8.
- Thesleff, I., A. Vahtokari, and A. -M. Partanen. (1995). Regulation of organogenesis: common molecular mechanisms regulating the development of teeth and other organs. *Int. J. Dev. Biol.* 39 : 39-50.
- Thisse, B., C. Thisse, and J. Weston. (1995). Novel FGF receptor (Z-FGFR4) is dynamically expressed in mesoderm and neurectoderm during early zebrafish embryogenesis. *Dev. Dyn.* 203 : 377-391.
- Thomas, K.H. (1993). Biochemistry and molecular biology of fibroblast

growth factors. In *Neurotrophic Factors*. Edited by S. E. Loughlin and J. H. Fallon. London: Academic Press.

Thorogood, P., and P. Ferretti. (1993). Hox genes, fin folds and symmetry. *Nature* 364 : 196.

Tickle, C. (1981). The number of polarizing region cells required to specify additional digits in the developing chick wing. *Nature* 289 : 295-8.

Tickle, C., B. Alberts, L. Wolpert, and J. Lee. (1982). Local application of retinoic acid to the limb bond mimics the action of the polarizing region. *Nature* 296 : 564-6.

Tickle, C., J. Lee, and G. Eichele. (1985). A quantitative analysis of the effect of all-trans-retinoic acid on the pattern of chick wing development. *Dev Biol* 109 : 82-95.

Tickle, C., G. Shellswell, A. Crawley, and L. Wolpert. (1976). Positional signalling by mouse limb polarising region in the chick wing bud. *Nature* 259 : 396-7.

Tickle, C., D. Summerbell, and L. Wolpert. (1975). Positional signalling and specification of digits in chick limb morphogenesis. *Nature* 254 : 199-202.

Vachon, G., B. Cohen, C. Pfeifle, M. E. McGuffin, J. Botas, and S. M. Cohen. (1992). Homeotic genes of the Bithorax complex repress limb development in the abdomen of the *Drosophila* embryo through the target gene Distal-less. *Cell* 71 : 437-50.

van der Hoeven, F., P. Sordino, N. Fraudeau, J. C. Izpisúa-Belmonte, and D. Duboule. (1996). Teleost HoxD and HoxA genes: comparison with tetrapods and functional evolution of the HOXD complex. *Mech Dev* 54 : 9-21.

Vargesson, N., J. D. Clarke, K. Vincent, C. Coles, L. Wolpert, and C. Tickle. (1997). Cell fate in the chick limb bud and relationship to gene expression. *Development* 124 : 1909-18.

Vogel, A., Clarke D. Roberts, and L. Niswander. (1995). Effect of FGF on gene expression in chick limb bud cells in vivo and in vitro. *Dev Biol* 171 : 507-20.

Vogel, A., C. Rodriguez, and J. C. Izpisúa-Belmonte. (1996). Involvement of FGF-8 in initiation, outgrowth and patterning of the vertebrate limb. *Development* 122 : 1737-50.

Vogel, A., C. Rodriguez, W. Warnken, and J. C. Izpisúa-Belmonte. (1995). Dorsal cell fate specified by chick Lmx1 during vertebrate limb development. *Nature* 378 : 716-20.

Vogel, A., and C. Tickle. (1993). FGF-4 maintains polarizing activity of posterior limb bud cells in vivo and in vitro. *Development* 119 : 199-206.

Wagner, M., C. Thaller, T. Jessell, and G. Eichele. (1990). Polarizing activity

and retinoid synthesis in the floor plate of the neural tube. *Nature* 345 : 819-22.

Wall, N. A., and B. L. M. Hogan. (1995). Expression of bone morphogenetic protein-4 (BMP-4), bone morphogenetic protein-7 (BMP-7), fibroblast growth factor-8 (FGF-8) and sonic hedgehog (SHH) during branchial arch development in the chick. *Mech. Dev.* 53 : 383-392.

Wall, N. A., C. M. Jones, B. L. Hogan, and C. V. Wright. (1992). Expression and modification of Hox 2.1 protein in mouse embryos. *Mech Dev* 37 : 111-20.

Warren, R. W., L. Nagy, J. Selegue, J. Gates, and S. Carroll. (1994). Evolution of homeotic gene regulation and function in flies and butterflies. *Nature* 372 : 458-461.

Werner, S., D. S. R. Duan, C. De Vries, K. P. Peters, D. Johnson, and L. T. Williams. (1992). Differential splicing in the extracellular region of fibroblast growth factor receptor 1 generates receptor variants with different ligand-binding affinities. *Mol Cell Biol* 12 : 82-88.

Wilde, S. M., S. E. Wedden, and C. Tickle. (1987). Retinoids reprogramme pre-bud mesenchyme to give changes in limb pattern. *Development* 100 : 723-733.

Wilkinson, D. G., S. Bhatt, and A. P. McMahon. (1989). Expression pattern of the FGF-related proto-oncogene int-2 suggests multiple roles in fetal development. *Development* 105 : 131-6.

Wolpert, L. (1969). Positional information and the spatial pattern of cellular differentiation. *J Theor Biol* 25 : 1-47.

Wolpert, L. (1996). One hundred years of positional information. *Trends Genet* 12 : 359-64.

Yang, Y., G. Drossopoulou, P. T. Chuang, D. Duprez, E. Marti, D. Bumcrot, N. Vargesson, J. Clarke, L. Niswander, A. McMahon, and C. Tickle. (1997). Relationship between dose, distance and time in *Sonic Hedgehog*-mediated regulation of anteroposterior polarity in the chick limb. *Development* 124 : 4393-4404.

Yang, Y., and L. Niswander. (1995). Interaction between the signaling molecules WNT7a and SHH during vertebrate limb development: dorsal signals regulate anteroposterior patterning. *Cell* 80 : 939-47.

Yayon, A., M. Klagsbrun, J. D. Esko, P. Leder, and D. M. Ornitz. (1991). Cell surface, heparin-like molecules are required for binding of basic fibroblast growth factor to its high affinity receptor. *Cell* 64 : 841-8.

Yokouchi, Y., S. Nakazato, M. Yamamoto, Y. Goto, T. Kameda, H. Iba, and A. Kuroiwa. (1995). Misexpression of Hoxa-13 induces cartilage homeotic transformation and changes cell adhesiveness in chick limb buds. *Genes Dev* 9 : 2509-22.

Yonei, S., K. Tamura, K. Ohsugi, and H. Ide. (1995). MRC-5 cells induce the AER prior to the duplicated pattern formation in chick limb bud. Dev Biol 170 : 542-52.

Yu, B. D., J. L. Hess, S. E. Horning, G. A. J. Brown, and S.J. Korsmeyer. (1995). Altered *Hox* expression and segmental identity in *Mll*-mutant mice. Nature 378 : 505-508.

Zeltser, L., C. Desplan, and N. Heintz. (1996). *Hoxb-13*: a new *Hox* gene in a distant region of the HOXB cluster maintains colinearity. Development 122 : 2475-84.

Zwilling, E. (1956a). Interaction between limb bud ectoderm and mesoderm in the chick embryo. II. Experimental limb duplication. J Exp Zool 132 : 173-188.

Zwilling, E. (1956b). Interaction between limb bud ectoderm and mesoderm in the chick embryo. IV. Experiments with a wingless mutant. J Exp Zool 132 : 241-253.